

AD-A082 424

WEIZMANN INST OF SCIENCE REHOVOTH (ISRAEL) DEPT OF --ETC F/6 1/3
RESEARCH IN ADVANCED FLIGHT CONTROL DESIGN. (U)

JAN 80 I HOROWITZ, B GOLUBEV, T KOPELMAN

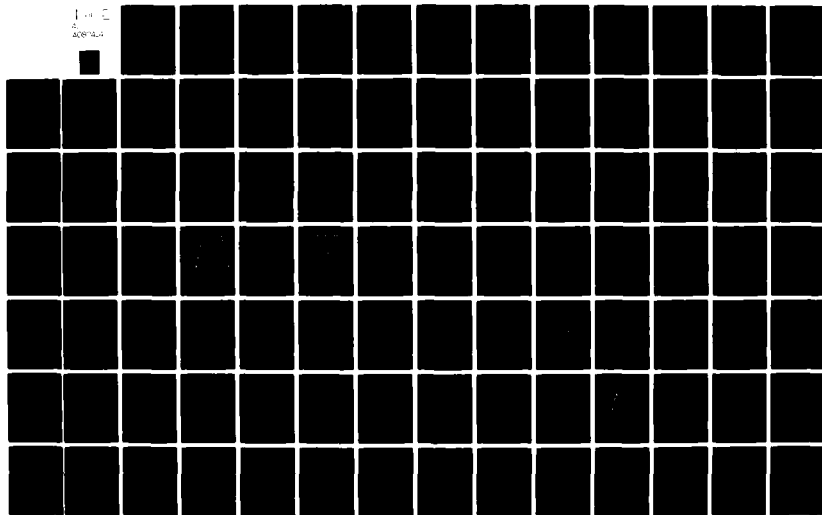
AFOSR-77-3355

UNCLASSIFIED

AFDL-TR-79-3120

NL

1-1-0
A
A082424



AD A 082424

AFFDL-TR-79-3120

(2)
NW

LEVEL 4

RESEARCH IN ADVANCED FLIGHT CONTROL DESIGN

ISAAC HOROWITZ

B. GOLUBEV

T. KOPELMAN

S. BRITMAN

DEPARTMENT OF APPLIED MATHEMATICS
THE WEIZMANN INSTITUTE OF SCIENCE
REHOVOT, ISRAEL

JANUARY 1980

TECHNICAL REPORT AFFDL-TR-79-3120

Final Report: 1 June 1977 - 31 May 1979

Approved for public release; distribution unlimited.

DTIC
ELECTE
S MAR 3 1 1980 D
A

AIR FORCE FLIGHT DYNAMICS LABORATORY
AIR FORCE WRIGHT AERONAUTICAL LABORATORIES
AIR FORCE SYSTEM COMMAND
WRIGHT-PATTERSON AIR FORCE BASE, OHIO 45433

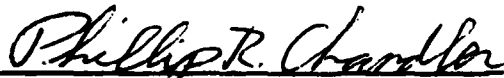
80 3 28 010

NOTICE

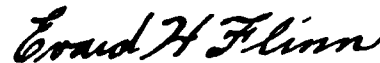
When Government drawings, specifications, or other data are used for any purpose other than in connection with a definitely related Government procurement operation, the United States Government thereby incurs no responsibility nor any obligation whatsoever; and the fact that the government may have formulated, furnished, or in any way supplied the said drawings, specifications, or other data, is not to be regarded by implication or otherwise as in any manner licensing the holder or any other person or corporation, or conveying any rights or permission to manufacture, use, or sell any patented invention that may in any way be related thereto.

This report has been reviewed by the Information Office (OI) and is releasable to the National Technical Information Service (NTIS). At NTIS, it will be available to the general public, including foreign nations.

This technical report has been reviewed and is approved for publication.



PHILLIP CHANDLER
Project Manager



EVARD H. FLINN, Chief
Control Systems Development Branch
Flight Control Division

FOR THE COMMANDER



MORRIS A. OSTGAARD
Acting Chief
Flight Control Division

"If your address has changed, if you wish to be removed from our mailing list, or if the addressee is no longer employed by your organization please notify AFFDL/FGLA, W-PAFB, OH 45433 to help us maintain a current mailing list".

Copies of this report should not be returned unless return is required by security considerations, contractual obligations, or notice on a specific document.

⑨ Final Scientific Rpt. 1 Jun 77-31 May 79

SECURITY CLASSIFICATION OF THIS PAGE (When Data Entered)

REPORT DOCUMENTATION PAGE		READ INSTRUCTIONS BEFORE COMPLETING FORM	
1. REPORT NUMBER	2. GOVT ACCESSION NO.	3. RECIPIENT'S CATALOG NUMBER	
18 AFFDL TR-79-3126			
4. TITLE (and Subtitle)		5. TYPE OF REPORT & PERIOD COVERED	
6 RESEARCH IN ADVANCED FLIGHT CONTROL DESIGN		Final Scientific Report June 1, 1977 - May 31, 1979	
7. AUTHOR(s)		6. PERFORMING ORG. REPORT NUMBER	
10 I. S. Horowitz, B. Golubev, T. Kopelman, S. Britman		N/A	
9. PERFORMING ORGANIZATION NAME AND ADDRESS		8. CONTRACT OR GRANT NUMBER(s)	
The Weizmann Institute of Science Department of Applied Mathematics Rehovot, Israel		15 AFOSR-77-3355 new	
11. CONTROLLING OFFICE NAME AND ADDRESS		10. PROGRAM ELEMENT, PROJECT, TASK AREA & WORK UNIT NUMBERS	
Air Force Flight Dynamics Laboratory Wright-Patterson AFB OH 45433		61102F 2307/03 23070307	
14. MONITORING AGENCY NAME & ADDRESS (if different from Controlling Office)		12. REPORT DATE	
EOARD (Box 14) FPO New York 09510		11 Jan 1980	
16. DISTRIBUTION STATEMENT (of this Report)		13. NUMBER OF PAGES	
Approved for public release; distribution unlimited.		113	
17. DISTRIBUTION STATEMENT (of the abstract entered in Block 20, if different from Report)		15. SECURITY CLASS. (of this Report)	
18. SUPPLEMENTARY NOTES		15a. DECLASSIFICATION/DOWNGRADING SCHEDULE	
19. KEY WORDS (Continue on reverse side if necessary and identify by block number)			
Flight Control, C. Star, Nonlinear system, Adaptive, Parameter uncertainty, Multivariable systems.			
20. ABSTRACT (Continue on reverse side if necessary and identify by block number)			
The flight control problem is one of regulation and control of a nonlinear, highly uncertain multiple input-output system, to achieve desired performance bounds. Feedback control theory has not been able to cope with even its approximate linear time-invariant version, because of its neglect of synthesis techniques in which uncertainty and performance bounds appear quantitatively. However, there have been two recent breakthroughs, giving precise, rigorous, quantitative synthesis techniques for both linear and nonlinear time-varying, single and multiple input-output systems containing plants with large (over)			

DD FORM 1 JAN 73 1473 EDITION OF 1 NOV 65 IS OBSOLETE

SECURITY CLASSIFICATION OF THIS PAGE (When Data Entered)

440763

JCB

uncertainties. In these techniques, quantitative performance bounds can be assigned in the time and/or frequency domain. For a large problem class, it is guaranteed that the design satisfies the specifications over the entire range of plant uncertainty.

One of the breakthroughs was applied to a significantly nonlinear model of the short-period, longitudinal flight control problem. Uncertainty was included in the model by allowing for a large range in velocity and air-density, without any provision for their measurement. The output $c^*(t)$, was to lie within specified bounds in response to a range of step commands. The design was simulated with excellent results.

FOREWORD

This report was prepared by the Weizmann Institute of Science, Rehovot, Israel, under Air Force Office Scientific Research Grant AFOSR-77-3355, "Research in Advanced Flight Control Design." The effort was performed under the direction of Air Force Wright Aeronautical Laboratories, Air Force Flight Dynamics Laboratory, Flight Control Division, Control Systems Development Branch, Control Techniques Group, Wright-Patterson Air Force Base, Ohio 45433. Phillip R. Chandler was the project engineer/manager on the project. Isaac Horowitz, Cohen Professor of Applied Mathematics, was Principal Investigator of this effort with contributing authors, B. Golubev, T. Kopelman and S. Britman. The work covered by this report was performed between June 1977 and May 1979.

[illegible]

TABLE OF CONTENTS

	PAGE
CHAPTER 1. THE NEGLECT OF QUANTITATIVE SYNTHESIS IN FEEDBACK CONTROL THEORY	
1.1 Introduction	1
1.2 A Quantitative Problem	2
CHAPTER 2. QUANTITATIVE FEEDBACK SYNTHESIS THEORY FOR LINEAR TIME INVARIANT SINGLE INPUT-OUTPUT SYSTEMS	
2.1 Origin and Tools	5
2.2 Frequency Somain vs. State Domain	6
2.3 Translation of Time Domain into Frequency Domain Specifications	9
2.4 The Single-Loop-Two-Degree-of-Freedom System	13
2.4.1 A 2-degree-of-freedom structure with 2-loop implementation	14
2.4.2 Review of two-degree-of-freedom quantitative design theory	15
2.4.3 Bounds on $L_0(j\omega)$ in Nichols chart	17
2.4.4 Nature of the bounds on $L_0(j\omega)$	18
2.4.5 Universal high-frequency (UHF) boundary	20
2.4.6 The optimum $L(j\omega)$	22
2.4.7 Numerical example	23
2.5 Cost of Feedback and Effect of Sensor Noise	25
2.5.1 Reduction in cost of feedback by means of linear time-varying compensation and nonlinear compensation	26
2.6 Multiple-Loop Feedback	27
2.7 More Complex Multiple-Loop Structures Including Plant Modification	31
2.8 Summary	35
CHAPTER 3. A BREAKTHROUGH IN QUANTITATIVE FEEDBACK SYNTHESIS	
3.1 Introduction	36
3.2 Concept of the Linear Time Invariant Equivalent Set (LTIE)	36

	PAGE
3.3 Outline of Synthesis Procedure for Nonlinear Uncertain Plants	39
3.3.1 Problem statement	39
3.3.2 Design procedure	40
3.3.3 A condition for guaranteed solvability of the linear time invariant (LTIE) problem	41
3.3.4 System response to other inputs	42
3.4 Extensions of the Nonlinear Design Technique	43
3.5 Comparisons with Other Synthesis Techniques	45
CHAPTER 4. FLIGHT CONTROL DESIGN BASED ON NONLINEAR MODEL WITH UNCERTAIN PARAMETERS	
4.1 Statement of the Problem	47
4.2 Design Execution	49
4.2.1 The linear time invariant (lti) equivalent set P	49
4.2.2 Design of $G(s)$, $F(s)$	51
4.2.3 Design simulation	57
4.3 Discussion	71
CHAPTER 5. A SECOND BREAKTHROUGH IN QUANTITATIVE FEEDBACK SYNTHESIS	
5.1 The Multiple Input-Output (mio) Problem	73
5.2 Extension to Nonlinear Uncertain Multiple Input-Output Plants	75
5.3 Application of Nonlinear and Multivariable Synthesis Techniques to Flight Control	76
REFERENCES	77
APPENDIX. QUANTITATIVE SYNTHESIS OF UNCERTAIN MULTIPLE INPUT-OUTPUT FEEDBACK SYSTEMS	79

LIST OF ILLUSTRATIONS

	PAGE
<u>Chapter 1</u>	
Fig. 1-1 Two sets of bounds on step response	4
<u>Chapter 2</u>	
2-1a Time domain step response specification	10
2-1b Frequency domain specification	11
2-1c Time domain bounds and design results for various plant parameter combinations	12
2-1d Equivalent frequency domain bounds	12
2-2a,b Structures of two-degree-of-freedom (D.O.F.) system	13
2-3 Two loop, 2-D.O.F. structure	14
2-4 Derivation of bounds on $L_0(j\omega)$ in Nichols chart	17
2-5 Typical bounds on L_0 in Nichols chart	19
2-6a Typical bounds on $L_0(j\omega)$ in complex plane	20
2-6b Bounds on $L_0(j\omega)$ in Nichols chart	21
2-7 Bounds on L_0 and optimum L_0 in Nichols chart	23
2-8 Single loop L_{S0} and outer loop L_{10} of design example in Sec. 2.4.7	24
2-9 Enormous sensor noise amplification in the single loop design for Sec. 2.4.7 example	26
2-10a The general cascaded feedback structure. (Constrained plant and sensors in heavy lines)	28
2-10b Sec. 2.4.7 2-loop design. $L_{10} = G_{1a}P_{10}P_{2eqa}$, $P_{2eqa} = L_{2a}/(1+L_{2a})$, $L_{2a} = G_{2a}P_{20}$	28
2-10c Sec. 2.4.7 3-loop design. $L_{10} = G_{1b}P_{10}P_{2eqb}$, $P_{2eqb} = L_{2b}/(1+L_{2b})$, $L_{2b} = G_{2b}P_{20}P_{3eqb}$, $P_{3eqb} = L_{3b}/(1+L_{3b})$, $L_{3b} = G_{3b}P_{30}$	28
2-11 Various loop designs for Sec. 2.4.7. Exact (solid lines) and Approximate (dashed) obtained by Design Perspective	29

	PAGE
2-12 Sensor noise effects for various designs for design problem of Sec. 2.4.7	30
2-13a,b The Triangular and Parallel-Cascade feedback structures	32
2-14 Some feedback structures with Plant Modification	34
<u>Chapter 3</u>	
3-1a Single loop feedback system with nonlinear uncertain plant $w \in W$	37
3-1b Tolerances on response to 2-unit step command	37
3-2 Acceptable output sets of a nonlinear system nature, for response to steps of 1, 2, 4	43
<u>Chapter 4</u>	
4-1 System structure	48
4-2 Aerodynamic coefficients $C_{ij}(\alpha)$ are strongly nonlinear functions of α	48
4-3 Frequency domain bounds on $ T(j\omega) $ derived from time-domain bounds. Bode plots of $ F(j\omega) $, $ G(j\omega) $ used in design.	50
4-4 Loci of typical $ t_i $ $P(j\omega)$. Cases e, f are open-loop unstable	52
4-5a-f Templates of equivalent plant	53-5
4-6 Bounds $B(\omega)$ on $G(j\omega)$ and $G(j\omega)$ chosen	56
4-7a-h Simulation results. Response to step command of c^* , magnitude K	58-61
4-8a,b Responses of $\alpha(t)$, $\dot{\theta}$, δ , c^*	62-3
4-9a,b Responses for input causing hard δ saturation	65-6
4-10a Responses to gust and simultaneous c^* step command	67
4-10b,c Responses to gust	68
4-11a-d Responses to stochastic gaussian gusts; (a,b with simultaneous c^* step command).	69
4-12a-c Response to a single square wave c^* command	70

	PAGE
<u>Appendix</u>	
1 Multiple input-output feedback structure	108
2 Single-loop structure equivalent, for synthesis of t_{uv}	108
3a,b To reach A, a zero must cross $j\omega$ axis above $j\omega_H$	108
4a,b Bounds on $t_{11}, t_{22}(j\omega)$ and experimental results	109-110
5 Equivalent frequency domain bounds and experimental results	111
6 Templates of P_{22}^{-1}, P_{11}^{-1}	112
7 Bounds on $\ell_{110}(j\omega)$	113

LIST OF ABBREVIATIONS AND SYMBOLS

$B(\omega)$	bounds on $G(j\omega)$
C	mean aerodynamic chord
$C_{ij}(\alpha)$	various aerodynamic coefficients
c^*	output variable = a handling qualities criterion
$c^*(s)$	$\chi c^*(t)$
db	decibels ($20 \log_{10}$)
d.o.f.	degrees of freedom
e_G	excess of poles over zeros of $G(s)$
$F(s)$	prefilter transfer function
g	gravity acceleration 9.8 m/sec^2
$G(s)$	loop compensation function
I_y	moment of inertia in pitch, kgm-m^2
j	$\sqrt{-1}$
lti	linear time-invariant
$L(s)$	$G(s)P(s)$, loop transfer function
$L_0(s)$	nominal $L(s)$
χ	Laplace transform
LTIE	linear time invariant equivalent
m	mass of vehicle, kgm
mio	multiple input-output
mp	minimum-phase
nmp	non minimum-phase
$P(s)$	plant transfer function
P	set $\{P(s)\}$
$q = \dot{\theta}$	pitch angular velocity
$r(t)$	system command input

$R(s)$	$\mathcal{L}r(t)$
R	set $\{r(t)\}$ or $\{R(s)\}$
s	complex variable
S	wing surface area, m^2
$T(s)$	closed loop transfer function
T_N	sensor noise amplification at plant input
T	set of acceptable $\{T(s)\}$
T_p	template of $P = P(j\omega)$
u	vertical velocity, m/sec
v_0	horizontal velocity a constant, m/sec
w	nonlinear plant function, $y = w(x)$
w^{-1}	inverse of w , $x = w^{-1}(y)$
W	set $\{w\}$
x	input to plant
$X(s)$	$\mathcal{L}x(t)$
y	acceptable output of plant
$Y(s)$	$\mathcal{L}y(t)$
\mathcal{Y}	set $\{y\}$
α	angle of attack
δ	elevator deflection
$\Delta(s)$	$\mathcal{L}\delta(t)$
ζ	parameter in model of $T(s)$
θ	pitch angle
ρ	air density, kgm/m^3
ω	frequency, rpm
ω_n	design parameter

CHAPTER I

THE NEGLECT OF QUANTITATIVE SYNTHESIS IN FEEDBACK CONTROL THEORY

1.1 Introduction

The flight control problem is one of regulation and control despite parameter uncertainty and disturbances. The pilot has a number of control variables (elevator, aileron angles, etc.) available. The mathematical relations between these control inputs and the output variables he wishes to control, are highly nonlinear. The parameters are functions of Mach (M) and dynamic pressure (N) and are not precisely known even if M and N are accurately measured. In addition, his objectives are not always the same. For example, in the longitudinal mode he is primarily interested in acceleration when violently maneuvering, and in pitch angle when aiming at a target. Wind gusts are external disturbances whose effects must be controlled.

There is no complete synthesis theory as yet for this problem. Classical linear time-invariant feedback theory (Nyquist and Bode plots, root locus, etc.) has been a useful tool based, of course, on the highly approximate linear time-invariant model. Describing function theory has been helpful for the stability problem. But these tools are obviously far from satisfactory. They must be accompanied by extensive simulation and cut and try modifications. They have worked because of the ingenuity of practical designers and the inherent power of feedback, but a great deal of cut and try design is essential. Certainly, in this field, theory has lagged far behind practice.

1.2 A Quantitative Problem

A primary reason for this sad state is due to the almost total neglect of a quantitative feedback synthesis theory. After all, feedback is used to achieve desired outputs despite uncertainty. Should not the extent of the uncertainty enter into the design? For example, suppose the plant (constrained part of the system) has the transfer function

$$P_1(s) = \frac{k_1}{s^2 + A_1s + B_1}, \quad (1.1)$$

with uncertainties in k, A, B given by

$$k_1 \in [1,10], \quad A_1 \in [-2,4], \quad B_1 \in [2,8]. \quad (1.2)$$

Suppose that in a completely different problem, the plant $P_2(s)$ has exactly the same form but with $k_2 \in [8,10]$, $A_2 \in [2,3]$, $B_2 \in [4,6]$. Suppose also that the output performance tolerances are the same for both, e.g., the system step response must lie within the solid line bounds shown in Fig. 1-1, for all plant parameter values in the above intervals. Common sense suggests that the two designs should be significantly different. There is much more uncertainty in the first plant. The "amount of feedback" it needs should certainly be much more than in the second problem. But classical design theory ignores this problem. One presumably emerges with the same design for both problems. It is as if the mere use of feedback suffices to scare both plants into the desired behavior.

Consider a variation of the above problem. Suppose the uncertainties of the two plants are the same, but the output tolerances are different, e.g., for one (a) they are the dashed-line bounds in Fig. 1, and the solid ones for the other (b). Common sense suggests that design (a) should need

less feedback and therefore be more economical in some sense than design (b). However, again classical feedback theory cannot cope directly with this problem except by cut and try, because it has no quantitative design techniques. Modern state-variable design theory also ignores this quantitative problem. It too has concentrated on design to achieve a desired output for a fixed, known plant transfer function. It offers no design technique for the above problem of Fig. 1, and this includes the recent work on robust design. It too must resort to cut and try.

This is indeed a very sad situation. Feedback is used primarily to achieve desired output tolerances despite uncertainty. But the extent of the uncertainty and of the tolerances do not appear at all as design parameters in the vast majority of the synthesis theories. Thousands of papers and hundreds of books have been written on the subject, but one hardly finds anywhere a quantitative problem statement. By this is meant a quantitative statement of the uncertainty as in Eq. (2), and a quantitative output tolerance statement as in Fig. 1. This makes it practically impossible to compare design techniques, especially the so-called adaptive techniques which claim to be superior to "conventional" techniques.

However, as described in Chapter 2, quantitative design techniques have been developed in the last eight years which can cope directly with the quantitative problem given by Fig. 1 and Eqs. (1,2). Hence, if one comes forth with claims for "superior" design techniques, he should be challenged to prove his claims quantitatively. He can do this only by applying his technique to a quantitative problem, and comparing it to a design based on the methods of Chapter 2. In fact, the references noted there contain many design examples, which can be used for this purpose. It is scandalous that

the proponents of "adaptive" design and of "modern" design theories have failed to provide such quantitative proofs of their claims.

The quantitative techniques described in Chapter 2 are devoted to single input-output linear time invariant (lti) uncertain plants. This constitutes a significant improvement over conventional nonquantitative techniques, classical or modern. But the flight control problem is a multiple input-output nonlinear problem with large uncertainty, so the methods of Chapter 2 are also inadequate. However, there have recently appeared two breakthroughs. The first extends quantitative synthesis rigorously (no approximations) to nonlinear uncertain single input-output systems. The method is outlined in Chapter 3, and is applied in Chapter 4 to a single-axis flight control problem. The second breakthrough extends quantitative synthesis to lti multiple input-output systems with large uncertainty. It may be combined with the first breakthrough, to permit quantitative synthesis of highly uncertain nonlinear multiple input-output feedback systems (Chapter 5 and Appendix 1). The result is a powerful synthesis tool, ideally suited to the multi-axes nonlinear flight control problem.

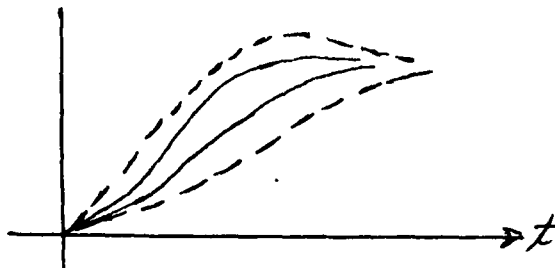


Figure 1-1. Two sets of bounds on step response

CHAPTER 2

QUANTITATIVE FEEDBACK SYNTHESIS THEORY FOR LINEAR TIME INVARIANT SINGLE INPUT-OUTPUT SYSTEMS

2.1 Origin and Tools

Modern quantitative synthesis theory is based to a significant extent on the work of Bode [1] in single-loop amplifier systems. Bode emphasized that the reason for using feedback was to control the plant sensitivity function. There is only one in the single-loop system, and it controls the effect of parameter uncertainty and external disturbances. Bode showed the central role of the loop transmission function $L(s)$ and intensively studied the properties of $L(s)$ on the frequency axis, $s = j\omega$. Unfortunately, classical feedback control theory and modern control theory even more so, have neglected the work of Bode. His contributions are still not appreciated by most control specialists, especially that the essential price of feedback is in the bandwidth of the loop. The loop bandwidth may have to be hundreds of times greater than the control bandwidth, depending on the extent of uncertainty and the tolerances on the output (recall Chapter 1). In one extreme (no uncertainty) the loop bandwidth can be zero, i.e. feedback is not needed at all. In fact, this is a good test of a feedback synthesis technique: What is the bandwidth of the loop transmission when there is no uncertainty? If it is not zero, then the design is not "tuned" to the specifications and is therefore wasteful in loop bandwidth. It is noteworthy how the relation of loop bandwidth to sensitivity is neglected in classical control and even more so in modern state-variable design theory. Bode showed that loop bandwidth reduction is a central challenge in feedback theory, and is the proper motivation for nonlinear feedback compensation. Thus, an

adaptive technique should justify itself by achieving the same quantitative tolerances for the same quantitative uncertainty, by means of a slower (smaller bandwidth) loop transmission.

2.2 Frequency Domain vs. State-Domain

It follows from the above that frequency response is a natural tool in linear time-invariant feedback synthesis. There are several reasons. Numbers 1, 2, 6 apply to system theory as a whole.

(1) The transfer function of a cascade of two blocks $P_1(s)$, $P_2(s)$ is the product $P_1P_2(s)$, with their parameters thus remaining separate. But the differential equation for their cascade connection is a complicated mixture of the individual ones, with their respective parameters all mixed up. If one wants the product $P_1P_2(s)$ to have the properties of some desired function $G(s)$, and if P_1 is fixed P_2 free, then obviously $P_2(s) = G/P_1(s)$ is easy to determine. This is not so if the cascade combination is expressed in differential equation form. Similar properties apply to other kinds of interconnections.

(2) Desired system properties are relatively easily stated in the frequency domain, which is also insensitive to the order of the system. They are much less easily formulated as coefficients of a differential equation, whose number and properties are furthermore very sensitive to system order.

(3) In feedback theory, loop bandwidth is the price paid for sensitivity reduction, which is a frequency domain parameter. The equivalent in the time domain is the speed of the impulse response of the loop transmission and this is very opaque in a state-variable formulation. Integral equations would be a much more logical time-domain formulation for feedback purposes, but for the next reason.

(4) In the problem posed in Fig. 1-1, one wants to control the response at every t . The response at $t = t_1$ is a function of all $t < t_1$, the convolution of (uncertain) functions for all $t < t_1$. The problem would not be so bad if one were interested in only a few t_1 values, but as noted it is for all t_1 values. In the frequency domain the analogous problem is to control the response to be within certain bounds (see Section 2.3, Figs. 2-1a,b) for all ω , so frequency ω replaces time t in the above. However, the behavior of the function at ω_1 is very loosely linked with its behavior at all other ω values. The constraint of analyticity of the s -domain function is much, much easier to bear than the convolution constraint in the t -domain.

(5) The nonminimum-phase property, as noted by Bode, is crucial in feedback design. It is explicit and obvious in the ω -domain, but opaque and hidden in the t -domain, whether in state-variables or in integral equation form.

(6) System theory differs basically from physics, chemistry and the specialized engineering disciplines in that it deals with the interconnection of devices and the overall system properties as functions of the input-output properties of the devices. Its great pride and boast is that it can do precisely this (i.e., control the system's input-output relations), with no need for study or even understanding of the equations and natural laws governing the mechanisms of these individual devices. The device can have a thousand internal states but if its connection to the overall system is via only a single input and a single output, then the system theorist needs only the single equation relating these two variables. What is the point of cluttering up the formulation with the thousand internal variables? The essence of good engineering is simplicity and economy of representation, in

order that one may see the forest from the trees. The problems are usually difficult enough without this unnecessary clutter.

(7) It has been argued that the state-variable description is more accurate and fundamental. Obviously, it is more detailed, but why does this make it more fundamental? The latter is a subjective concept related to one's objectives. As George Zames has noted, that in pursuing this argument a quantum mechanical description is far more accurate and "fundamental" than state-variable.

(8) Much has been made of the concepts of "controllability and observability" as a justification for the state-variable description and methodology. But it has been shown [2] that a system can be controllable and observable, and yet is totally inadequate for proper control. Thus, these concepts can be highly misleading. Also, it has been shown they are not at all needed even for what they purport to do, if one formulated the problem with the concept of uncertainty.

(9) Much has been made of the fact that the Laplace transform is unavailable in linear time-varying and in nonlinear systems, whereas the state-variable formulation is universal. To this the answer is, "So what?" The objective is synthesis, not mere formulation. Quantitative techniques with deep insight, for the synthesis of uncertain systems to satisfy quantitative performance specifications, are available in the transform domain, for linear time-invariant systems. They are not available by state-variable methods. Of what value is a universal formulation if it cannot cope with the quantitative uncertainty problem even in its simplest category -- the linear, time-invariant one.

Ironically, transform concepts have led to precise quantitative design techniques for both time-varying and nonlinear systems [3-5]. The application of such a technique to the flight control problem is, in fact, the main theme of this report.

It should be emphasized that there are areas in system theory where the state-variable formulation is the natural one, e.g. in optimal control if the realistic cost function is indeed a function of all the states. It is not our purpose to derogate state-variables, but rather to present honestly the role of frequency response in quantitative feedback theory. In such a presentation one naturally contrasts it with state variable theory. At least our presentation gives detailed arguments, whereas frequency-response is generally cast aside by state-variable enthusiasts, with hardly any detailed, reasoned discussion. Also, our argument is not against state-variable formulation per se, but to the synthesis technique that is used thereafter.

2.3 Translation of Time Domain into Frequency Domain Specifications

In the synthesis techniques listed next, there is always a constrained Plant which is described by a system of differential equations whose parameters are uncertain, giving a set of plant functions $P = \{P\}$. Thus in Eqs. (1.1, 2), each parameter combination gives a different $P \in P$. The same design philosophy can be used for sampled-data systems [6].

The objective is to achieve certain apriori specified performance objectives $\forall P \in P$. If the overall system is to be linear time-invariant (lti) even if the plant itself is nonlinear, it can be characterized by its response to any input, and the step response is very popular because it combines within it both the fastest kind of input (an abrupt change) and the slowest (no change). Time domain specifications are reasonable in many cases,

as in Figure 2-1a, where the step response is to be inside the bounds $b_1, b_2 \forall P \in P$, with additional bounds of similar nature on the first and

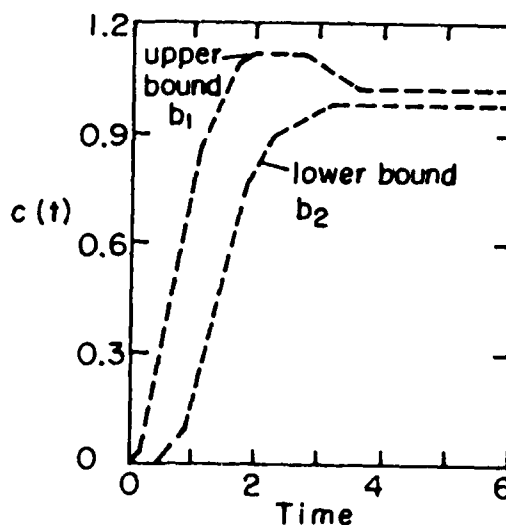


Figure 2-1a. Time domain step response specification.

perhaps higher derivatives. Our design technique is in the frequency-domain, so we must translate such t-domain bounds into "equivalent" ω -domain bounds on the system frequency response $T(j\omega)$. If the system is minimum-phase [6], $|T(j\omega)|$ suffices and we restrict ourselves here to such systems. This translation is, as of this date, an engineering art rather than a science. Advice on how to translate is scattered in the literature [7-9]. Very good results have been obtained with only moderate effort. We shall assume in this work that the translation has already been done. It is worth noting that it has been shown [4] that for minimum-phase systems, time-domain specifications on the step response and on its derivatives of the following nature

$$b_2^{(i)}(t) \leq c^{(i)}(t) \leq b_1^{(i)}(t), \quad i = 0, 1, \dots, n, \quad t \in [0, \infty) \quad (2.1)$$

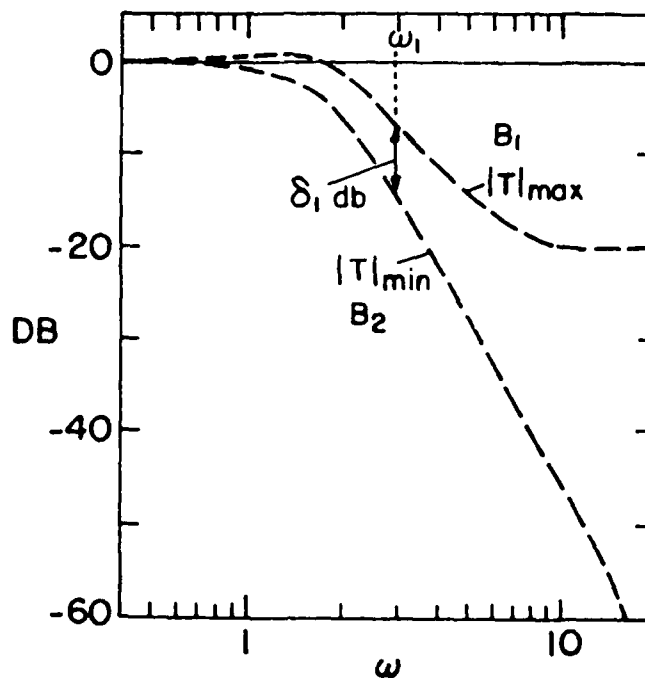


Figure 2-1b. Frequency domain specification.

can always be satisfied by means of ω -domain bounds of the following nature

$$B_2(\omega) \leq |T(j\omega)| \leq B_1(\omega) . \quad (2.2)$$

Hence, it is guaranteed that there exist ω -domain bounds of the form of Fig. 2-1b, which satisfy time-domain bounds of the form Eq. (2.1).

An example of time-domain bounds and their equivalent ω -domain bounds is shown in Figs. 2-1c,d. Fig. 2-1c also shows the simulation results obtained from the design, which was incidentally a multiple-loop one (see Section 2.7), for the structure of Fig 2-13b. Such good correlation between t and ω domain bounds are not atypical.

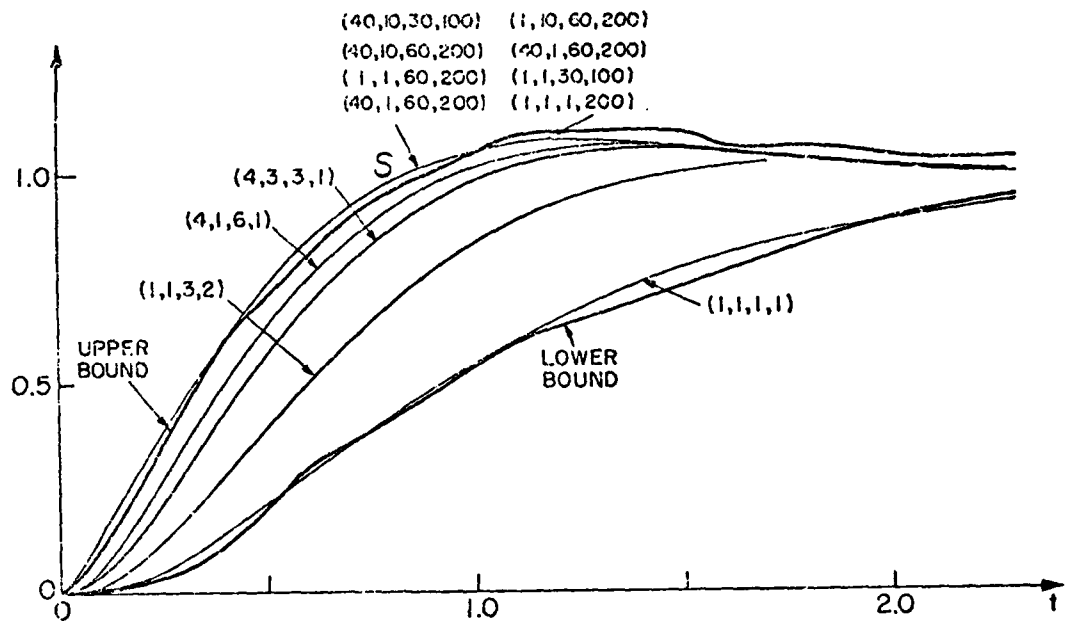


Figure 2-1c. Time domain bounds and design results for various plant parameter combinations.

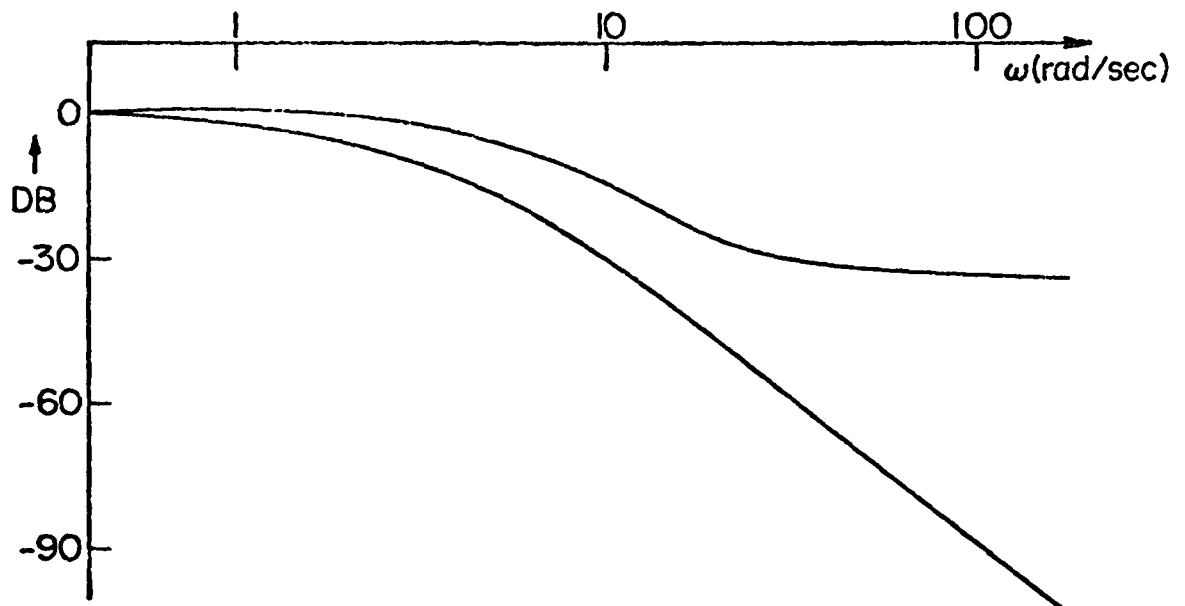


Figure 2-1d. "Equivalent" frequency-domain bounds.

2.4. The single-loop two-degree-of-freedom system [7]. (Fig. 2-2)

Here the plant output $c(t)$ is assumed measurable and available for feedback and so is the command input $r(t)$. The processing of these two signals provides two independent compensation functions to the designer. An infinitude of canonical two-degree-of-freedom structure may be used [6]. The design procedure developed in [7] used Figure 2-2a, but suppose the

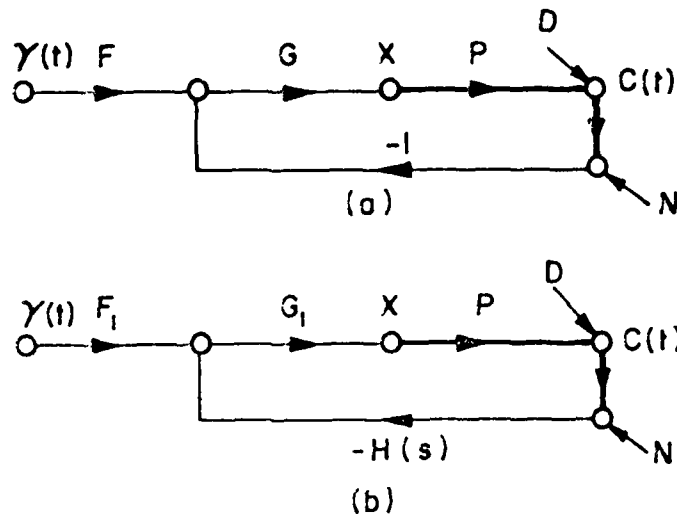


Figure 2-2. Structures of 2 - D.O.F. system.

sensor transfer function is $H(s)$, then one can use Figure 2-2b; letting $G_1 H$ (of Figure 2-2b) = G (of Figure 2-2a), in order to have the same loop transmission function $L(s) = GP = G_1 PH$, and $F_1 G_1 = FG$ in order to have the same system transfer function

$$\frac{C(s)}{R(s)} = T(s) = \frac{FGP}{1 + GP} = \frac{F_1 G_1 P}{1 + G_1 PH} \quad (2.3)$$

2.4.1 A 2-degree-of-freedom structure with 2-loop implementation

Suppose large loop feedback bandwidth is needed and it is found that an independent sensor measuring $\dot{c}(t)$ (e.g., a tachometer in a position servo) gives less noise than the differentiation of a position sensor, so both sensors are used, as in Figure 2-3, with the two sensor transfer functions H_1, H_2 , and say the structure in Figure 2-3 is used. This is a two-loop

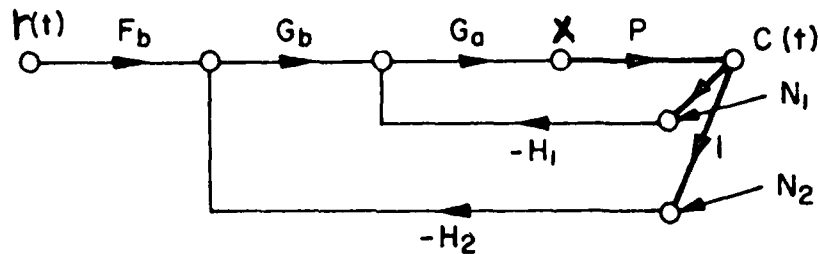


Figure 2-3. 2-loop, 2-D.O.F. structure.

structure physically, but in terms of fundamental feedback design it is a two-degree-of-freedom system, so the quantitative design theory of Figure 2-2a is used, giving G and F . It is required that the loop transmission around P , be the same in both cases, i.e.,

$$L = PG \text{ (Fig. 2-2a)} = P[G_a(H_1 + G_b H_2)] \quad (2.4a)$$

and

$$T = F \frac{GP}{1 + GP} \text{ (Fig. 2.2a)} = F_b \frac{G_b G_a P}{1 + P[G_a(H_1 + G_b H_2)]} \quad (2.4b)$$

so

$$G = G_a(H_1 + G_b H_2), \quad FG = F_b G_b G_a. \quad (2.4c)$$

H_1, H_2 are known, so one must decide how to split $G = G_a(H_1 + G_b H_2)$ between G_a and G_b . This is done by considering the effect of sensor noise N_1, N_2 at the plant input,

$$-X_N(j\omega) = \frac{G_a(H_1 N_1 + H_2 G_b N_2)}{1 + P[G_a(H_1 + G_b H_2)]} \quad (2.5)$$

given that

$$G = \frac{L}{P}(j\omega) = G_a(H_1 + H_2 G_b) \quad (2.6)$$

is fixed by the quantitative design technique of [7].

The objective is to minimize $\int_0^\infty |X_N|^2 d\omega$, subject to the above constraint. This is a straightforward optimization problem which can be solved outside the realm of quantitative feedback synthesis. The latter only provides the design with the feedback loop transmission (L) needed around the plant, and the prefilter (F) needed to process the command input $r(t)$. The state-of-the-art in sensors and in filter synthesis determines how L and F are to be realized. In fact, in the above context one might consider use of an accelerometer in a 3-loop feedback structure. But from our point of view the structure remains that of a two-degree-of-freedom system and we shall continue to associate the latter with a single-loop system. The single-loop design technique is the basic building block for all the other more complex structures, so it is next reviewed.

2.4.2 Review of Two-Degree-of-Freedom Quantitative Design Theory

Figure 2-2a is used with $T = F \frac{GP}{1+GP}$. It is assumed that the compensation networks, whose power levels can be very low (as the plant contains the power elements), can be constructed with negligible uncertainty in their transfer functions. Hence, due to the uncertainty in P,

$$\Delta \ln T = \Delta \ln \frac{LP}{1+GP} = \Delta \ln \frac{L}{1+L}, \quad L = GP \quad (2.7)$$

and

$$\Delta \ln |T(j\omega)| = \Delta \ln \left| \frac{L(j\omega)}{1+L(j\omega)} \right|. \quad (2.8)$$

Given that the specifications require that $\Delta \ln |T(j\omega)| \leq \delta_1 \text{ db}$ at ω_1 in Figure 2-1b, what are the resulting constraints on $L(j\omega_1)$? It is convenient to pick a "nominal" plant $P_0(s)$, and derive the bounds on the resulting "nominal" loop function $L_0 = P_0 G$. These bounds can be found by means of a digital computer, but it is very useful for insight to see it done on the Nichols chart (logarithmic complex plane with abscissa in degrees, ordinate in decibels = $20 \log_{10}$). The procedure is illustrated for the case

$$P(s) = \frac{ka}{s(s+a)}; \quad k \in [1, 10], \quad a \in [1, 10], \quad (2.9)$$

and say $k = 1$, $a = 10$ are chosen as nominal, giving $P_0 = 10/(s(s+10))$. At $\omega = 2$ rps, $F(j2)$ lies within the boundaries given by ABCD in Figure 2-4. Since $\ln L = \ln G + \ln P$, the pattern outlined by ABCD may be translated, but not rotated, on the Nichols' chart, the amount of translation being given by the value of $\ln G(j2)$. For example, if a trial design of $L(j2)$ corresponds to the template $P(j2)$ at A'B'C'D' in Figure 2-4, then

$$\begin{aligned} G(j2)_{\text{db}} &= |L(j2)|_{\text{db}} - |P(j2)|_{\text{db}} \\ &= (-2.0) - (-13.0) = 11.0 \text{ db} \end{aligned} \quad (2.10)$$

$$\begin{aligned} \text{Arg } G(j2) &= \text{Arg } L(j2) - \text{Arg } P(j2) \\ &= (-60^\circ) - (-153.4^\circ) = 93.4^\circ. \end{aligned} \quad (2.11)$$

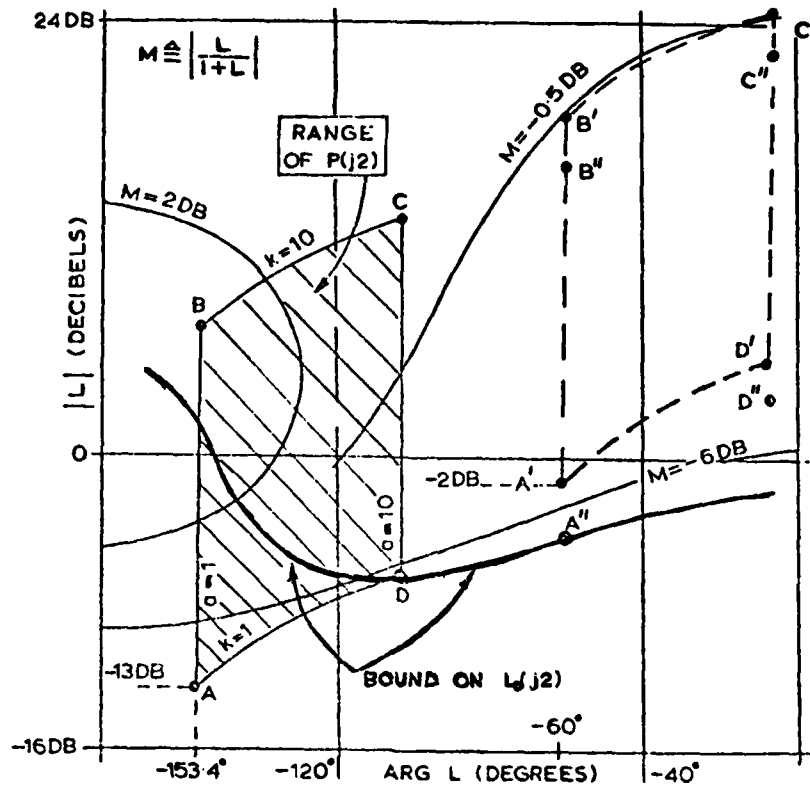


Figure 2-4. Derivation of bounds on $L_0(j\omega)$ on Nichols chart.

2.4.3 Bounds on $L_0(j\omega)$ in the Nichols chart

The templates of $P(j\omega)$ are manipulated to find the position of $L_0(j\omega)$ which results in the specifications of Figure 2-1b on $\ln |T(j\omega)|$ being satisfied. Taking the $\omega = 2$ template, one tries, for example, positioning it, as shown in Figure 2-4, at $A'B'C'D'$. Contours of constant $\ln |L/(1+L)|$ are available on the Nichols' chart. Using these contours, it is seen that the maximum change in $\ln |T|$ is, in this case, very closely $(-0.49) - (-5.7) = 5.2$ db, the maximum being at point C' , the minimum at point A' . Suppose that the specifications tolerate a change of 6.5 db

at $\omega = 2$, so the above trial position of $|L_0(j2)|$ is in this case more than satisfactory. The template is lowered on the Nichols' chart to A''B''C''D'', where the extreme values of $\ln|L/(1+L)|$ are at C'' (-0.7 db), A'' (-7.2 db). Thus, if $\text{Arg } L_0(j2) = -60^\circ$, then -4.2 db is the smallest magnitude of $L_0(j2)$ which satisfies the 6.5 db specification for $\Delta \ln |T|$. Any larger magnitude is satisfactory but represents over-design at that frequency. The manipulation of the $\omega = 2$ template is repeated along a new vertical line, and a corresponding new minimum of $|L_0(j2)|$ found. Sufficient points are obtained in this manner to permit drawing a continuous curve of the bound on $L_0(j2)$, as shown in Figure 2-4. The above is repeated at other frequencies, resulting in a family of boundaries of permissible $L_0(j\omega)$.

2.4.4 Nature of the bounds on $L_0(j\omega)$

A typical set of bounds is shown in Figure 2-5. The bounds tend to move down in the Nichols chart (become less onerous), obviously because as ω increases, greater change in $|T(j\omega)|$ is permitted, as in Figure 2-1b. However, they may cross and even temporarily move up higher with increase of ω . It is in fact essential that at large enough ω , the uncertainty in $|T(j\omega)|$ (i.e., the bounds on $|T(j\omega)|$) be greater than the uncertainty in $P(j\omega)$, because the net sensitivity reduction is always zero in any practical system as was long ago [1] shown by Bode,

$$\int_0^\infty \ln |S_P^T(j\omega)| d\omega = - \int_0^\infty \ln |1+L(j\omega)| d\omega = 0 \quad (2.12)$$

where $S_P^T = \frac{\partial T/T}{\partial P/P}$ is the sensitivity function.

In the above examples as $\omega \rightarrow \infty$, $P \rightarrow \frac{ka}{s^2}$, so $\Delta \ln |P| \rightarrow \Delta \ln(ka) = 40 \text{ db}$.

Note in Figure 2-1b that the permitted $\Delta \ln |T(j\omega)| \gg 40 \text{ db}$ as $\omega > 50$.

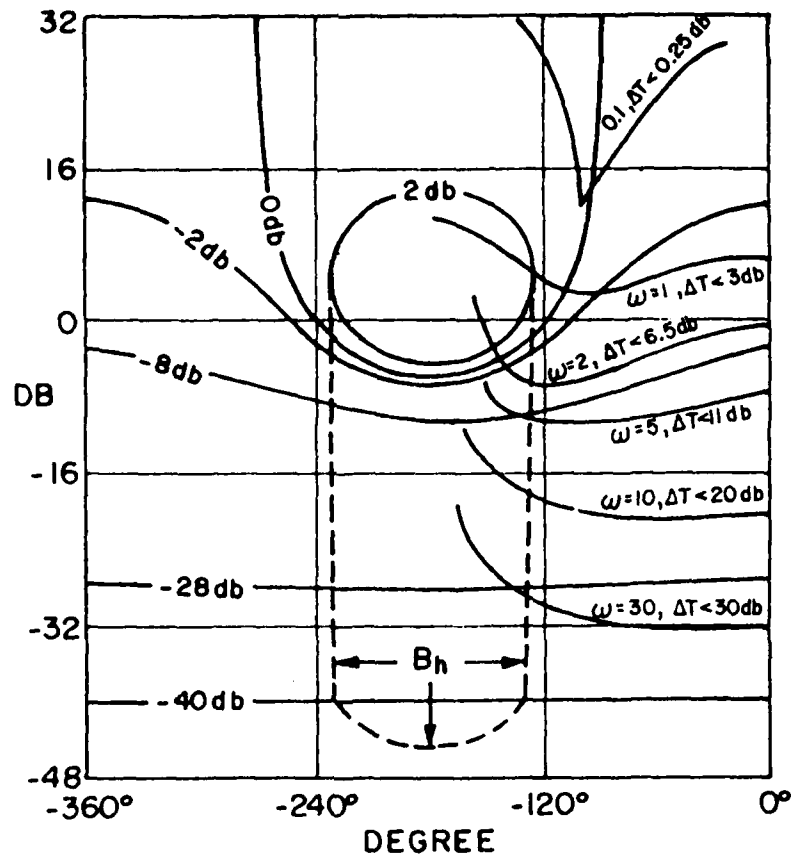


Figure 2-5. Typical bounds on L_0 in Nichols chart.

Such large tolerances on $|T(j\omega)|$ at large ω are tolerable because $|T(j\omega)|$ is negligible at large ω , e.g., if $|P(j\omega)|$ can change at most by 40 db at large ω but $|T(j\omega)|$ changes by 52 db, who cares if this 52 db change is from $|T|_{\min} = 10^{-6}$ to $|T|_{\max} = 400 \times 10^{-6}$. In return, one can concentrate the sensitivity reduction over the bandwidth of $T(j\omega)$. Thus, although $|P(j\omega)|$ in this region varies by say 40 db, $|T(j\omega)|$ may be controlled to vary by only 4 db, or 0.04 db if desired.

2.4.5 Universal high-frequency (UHF) boundary

As noted, in the high-frequency range $\Delta \ln|T(j\omega)|$ must realistically be allowed to be $\gg \Delta \ln|P(j\omega)|$, and this is reflected in the bounds on $L_0(j\omega)$ tending to a very narrow pencil B_V^P in the arithmetic complex plane (if $P_0 \rightarrow \frac{k_{\min}}{s^e}$ as $s \rightarrow \infty$) as in Figure 2-6a and as in 2-6b in the Nichols' chart. In Figure 2-6b, the boundary B_V^P is drawn for the case

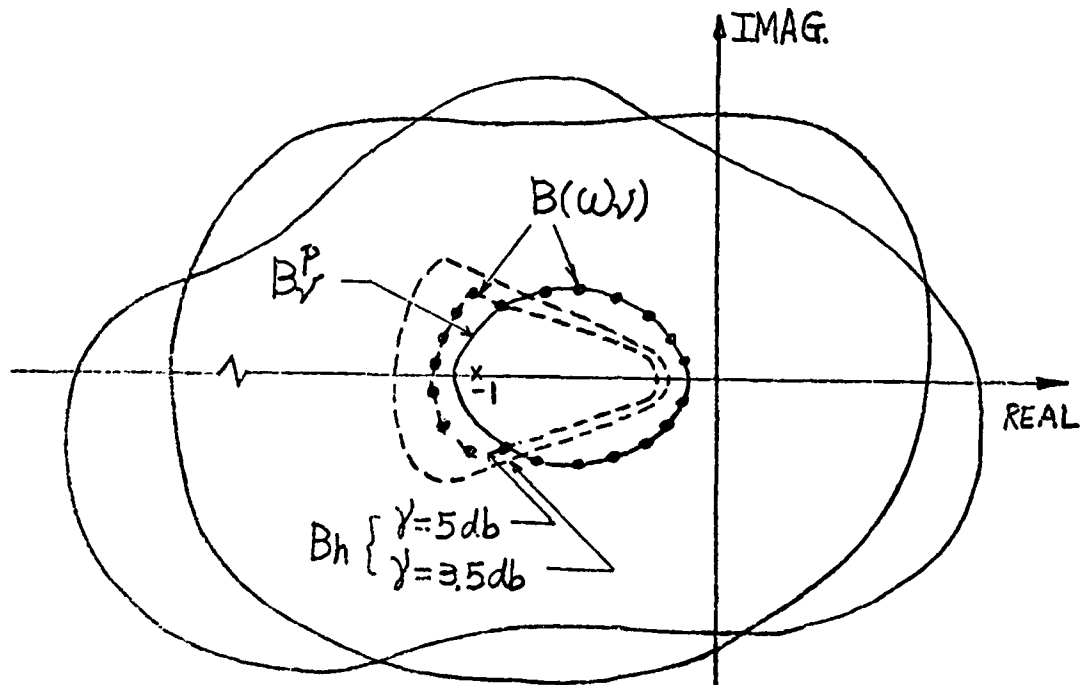


Figure 2.6a. Typical bounds on $L_0(j\omega)$ in complex plane.

$$\Delta \ln L = \Delta \ln k = 20 \text{ db}, \quad \Delta \ln|T(j\omega)| = \Delta \ln|L/(1+L)| \leq 23 \text{ db at } \omega_V.$$

However, the resulting peak value of $|L/(1+L)|$ is 23 db = 14.1 arithmetic at $k = k_{\max}$, indicating a highly under-damped pole pair at the corresponding

frequency with damping ratio $\xi = 0.034$, when $k = k_{\max}$. This tremendous peaking does not appear in the system response to the command inputs R , because it is filtered out by the pre-filter F in Figure 2-2a. But the system response to a disturbance D in Figure 2-2a, is given by $T_d = \frac{C}{D} = (1+L)^{-1}$. Disturbance attenuation generates its own requirements on L , which may lead to more stringent bounds on L than those due to $T(j)$. The final contours used in the design [7] must be the most stringent

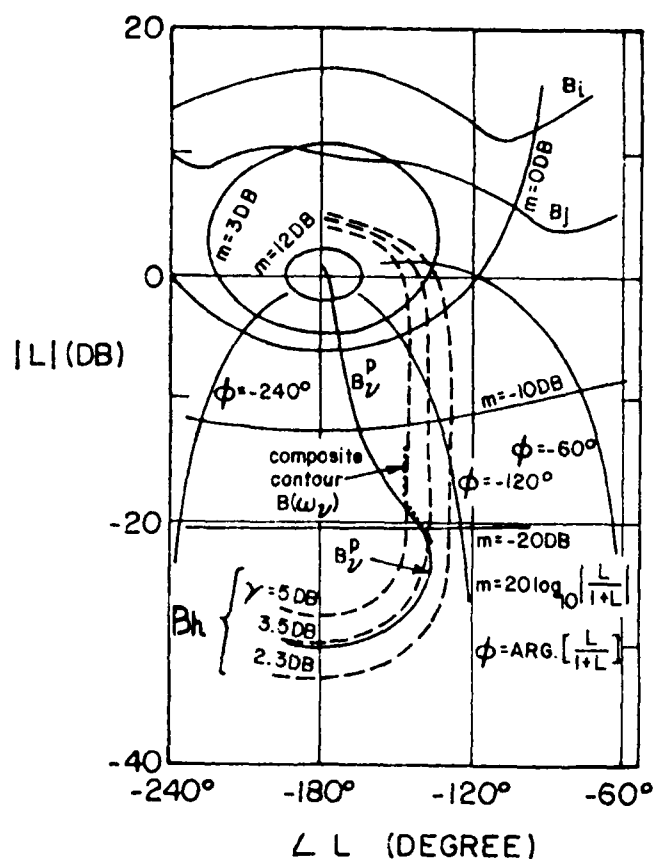


Figure 2-6b. Bounds on $L_0(j\omega)$ on Nichols' chart

composite of the two. However, even if D is very small, it is usually certain that a peak $|T_d|$ of 14.1 is intolerable. It is reasonable to add a requirement $\left| \frac{L}{1+L} \right| \leq \gamma$ a constant, for all ω and over the whole range of P parameter values. The resulting constraining contours denoted by B_h are shown in Figure 2-6b for the case $\Delta \ln k = 20$ db, and for $\gamma = 2.3, 3.5, 5$ db (all those contours are symmetrical with respect to the vertical $\text{Arg } L = -180^\circ$ on the Nichols' chart). If $\gamma = 5$ db is used, then $B(\omega_\gamma)$ indicates the composite contour shown in Figure 2-6b. For $\omega > \omega_\gamma$, $|\Delta T(j\omega)|$ increases while γ remains the same, so that sooner or later there is reached a frequency $\omega_\gamma \ni B(\omega) = B_h(\gamma)$, $\forall \omega \geq \omega_\gamma$. This boundary B_h is called the "universal high frequency" (UHF) boundary.

2.4.6 The optimum $L(j\omega)$

It has been shown [10,11] that a realistic definition of optimum in the lti system is the minimization of k , defined by $\lim_{s \rightarrow \infty} L(s) = ks^{-e}$, where e is the excess of poles over zeros assigned to $L(s)$.

It has been proven [10,11] that the optimum L lies on its boundary B_i at each ω_i and that such an optimum exists and is unique. Most important for the present purpose, is that in significant plant ignorance problems the ideal optimal L has the properties shown in Figure 2-7, i.e., over a significant range it follows B_h along UV up to the point J at which it abruptly jumps to infinity along $WW'W''$ and returns on the vertical line YZ , whose phase is $(-90^\circ)e$. Such an ideal $L(j\omega)$ is, of course, impractical. A practical suboptimum L is shown in Figure 2-7.

Some results of a numerical design example are shown in Figure 2-8. They were derived for the following problem.

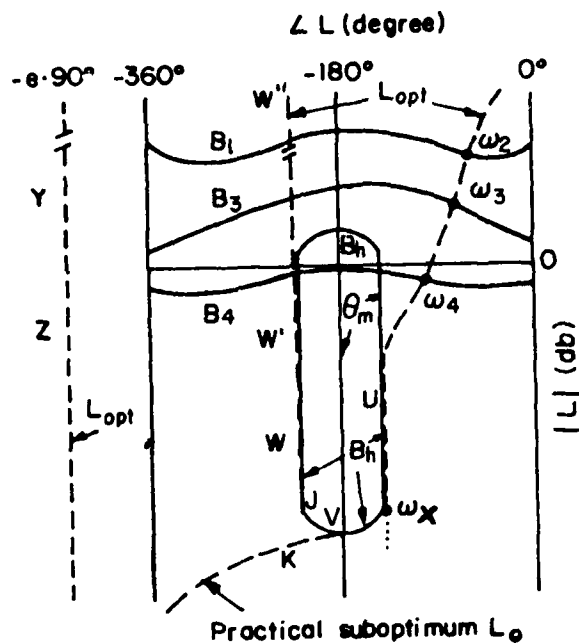


Figure 2-7. Bounds on L_0 and Optimum L_0 on Nichols' Chart.

2.4.7. Numerical example. (Figures 2-2a, 2-8, Section 2.6)

Plant: $P = P_1 P_2 = P_1 (P_2' P_3')$

Plant uncertainty: $P_1 = \frac{K_1}{s^2 + 2\xi\omega_n s + \omega_n^2}$, $-3 \leq \xi\omega_n \leq 5$

$$2 \leq \omega_n \sqrt{1 - \xi^2} \leq 10, \quad 4 \leq K_1 \leq 1250$$

$$P_2' = \frac{AK_2'}{s+A}, \quad 1 \leq A \leq 3, \quad 10 \leq K_2' \leq 33.3$$

$$P_3' = \frac{BK_3'}{s+B}, \quad 10 \leq B \leq 20, \quad 100 \leq K_3' \leq 158$$

Performance Specification: Shown in Figure 2-1b, were originally derived from time domain bounds [9].

Disturbance response: $Y \leq 3.0 \text{ db}$

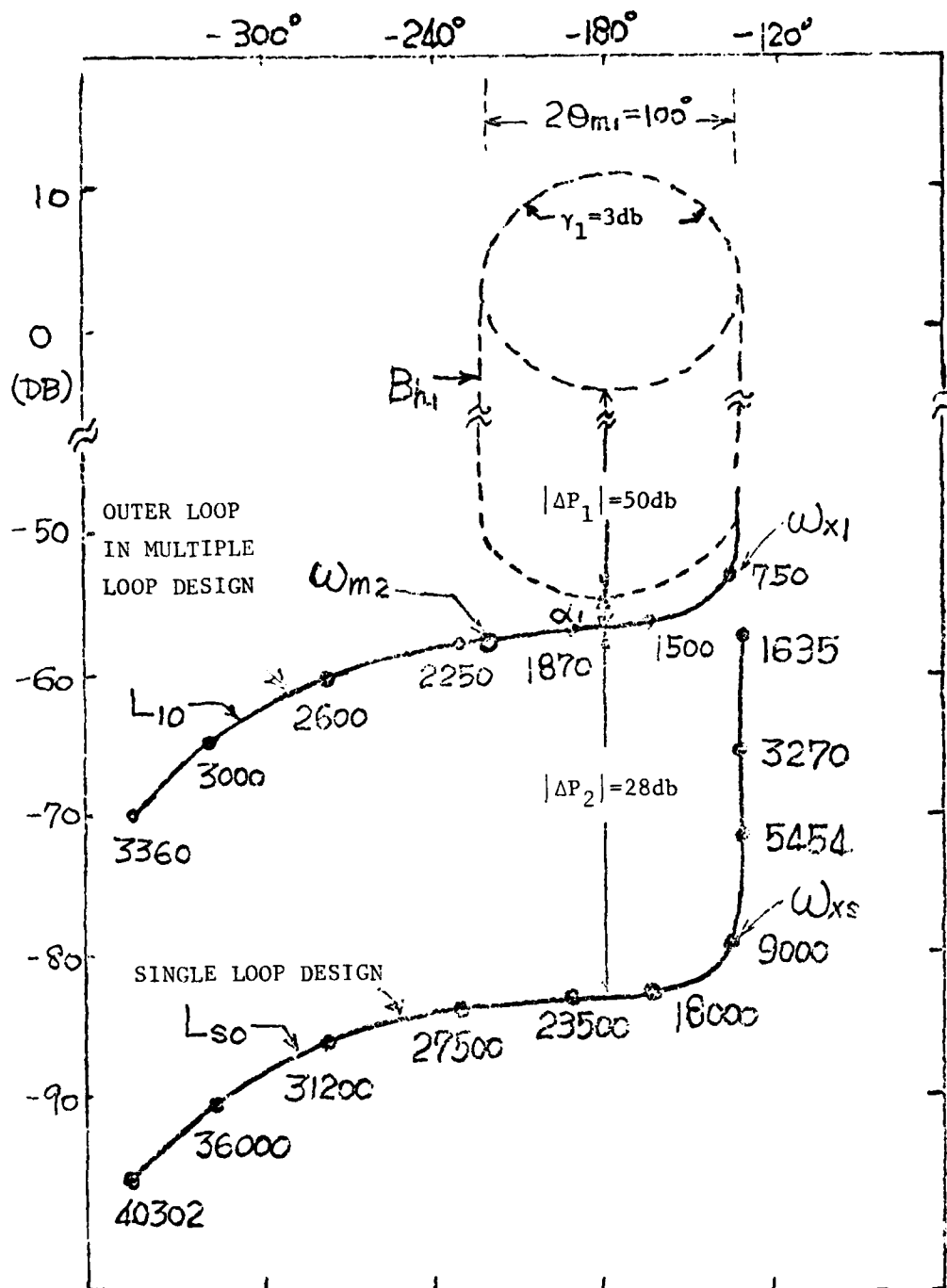


Figure 2-8. Single loop L_{so} and outer loop L_{10} of the numerical example in Section 2.4.7.

This example is used in Section 2.6 in a demonstration of the advantages of multiple-loop design.

2.5 Cost of Feedback and Effect of Sensor Noise

In significant plant ignorance problems, there is a strong tendency for the design to be such that N , in Figure 2-2a, is so highly amplified as to saturate the plant input at X . The noise response function is (see Figure 2-2a)

$$T_N \triangleq \frac{X}{N} = \frac{-G}{1+GP} = \frac{-L/P}{1+L}$$

$$\approx -L/P \text{ in h.f. range where } |L| \ll 1. \quad (2.13)$$

N represents the square root of the noise power spectrum. The noise response of the numerical design example of the last section is shown in Figure 2-9. Notice that the noise component at x , in Figure 2-2a, is most important in the high-frequency range where the useful command and disturbance components, due to R and D are relatively small, rather than in the low frequency range where the latter are relatively large. Hence, it is desirable to decrease $|L|$ vs. ω , as fast as possible in the high frequency range. Even a saving which is small in the logarithmic scale can be significant in rms sensor noise effect. Reduction in this 'cost of feedback' is the primary motivation for turning to multiple-loop design.

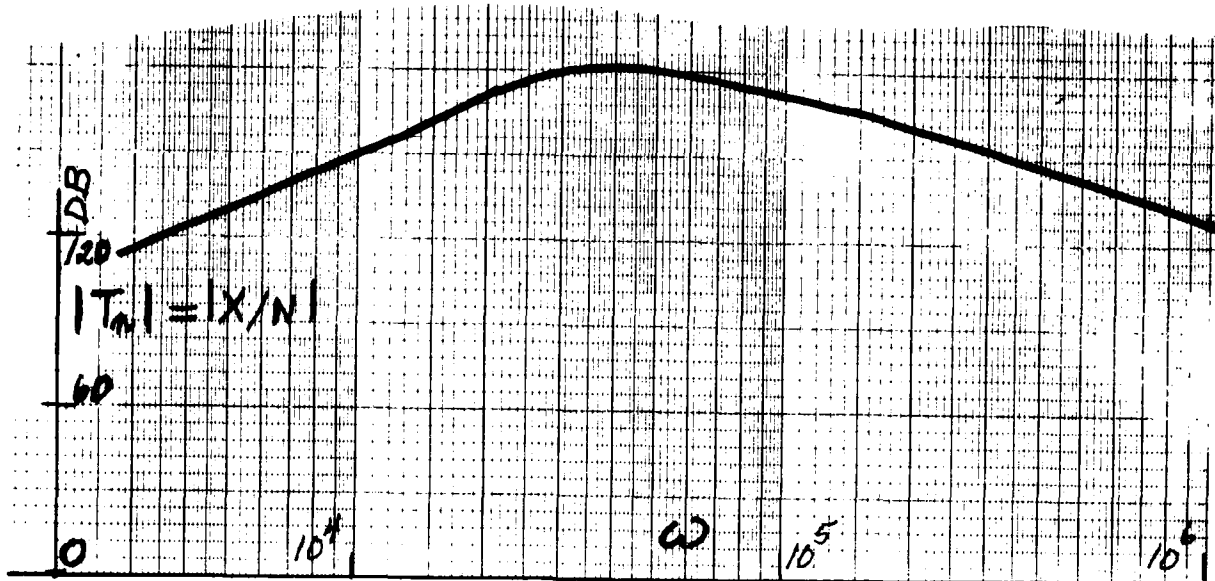


Figure 2-9. Enormous sensor noise amplification in the single-loop design for Section 2.4.7 example.

2.5.1. Reduction in Cost of Feedback by means of linear time-varying compensation and nonlinear compensation.

To reduce the hf sensor noise effect, one way is by linear time-varying compensation if the problem has time-varying features [12]. Another is by nonlinear compensation. Actually the so-called "adaptive" system is in the category of nonlinear compensation. They may or may not be better than lti compensation in reducing the 'cost of feedback'. It is noteworthy and scandalous that in the vast literature on adaptive systems, there is hardly ever any quantitative comparison between the adaptive design promoted and a proper lti design accomplishing the same design objectives. One could excuse this not being done in a general manner, because there is hardly any 'adaptive' method permitting quantitative design in the sense here defined.

However, it could at least be done experimentally. Occasionally one sees a comparison, with an 'ordinary' or so-called 'classical' design. But the comparison is usually greatly biased, because generally some very naive lti design is used, and there is no statement of specifications -- even made up after the fact. There is not recalled a single comparison, on the part of the proponents of adaptive systems, with the lti quantitative design technique [7] discussed here. Some nonlinear compensation techniques for which a quantitative design theory exists to a greater or lesser extent have appeared in the literature [13-17] for which such comparisons are possible. It is noteworthy that these were expressly motivated by the desire to reduce the 'cost of feedback', so that such comparisons were a natural by-product.

2.6 Multiple-loop feedback.

Another method of 'cost of feedback' reduction, in the context of lti design, is by means of multiple-loop feedback, restricted to those cases where an additional plant variable (besides the plant output) are available for feedback purposes. Such a multiple loop design technique was first developed [18] for the cascaded structure of Figure 2-10a.

The design example of Section 2.4.7 was done by means of a two-loop design ($n = 2$ in Fig. 2-10). The resulting new outer loop (L_{10}) is shown in Figures 2-8, 2-11 and is considerably more economical in bandwidth than the single-loop design (L_{50}) for the same problem. The effects of the outer sensor noise N_1 at the plant input are compared in Fig. 2-12. Note the tremendous improvement. However, there is now a second sensor with noise source N_2 in Fig. 2-10b. Its effect is shown in Fig. 2-12. It can be reduced by using 3 loops ($n = 3$ in Fig. 2-10). Compare X/N_2 for 2 and 3 loop designs in Fig. 2-12. But now there is N_3 to consider and X/N_3 is shown in Fig. 2-12.

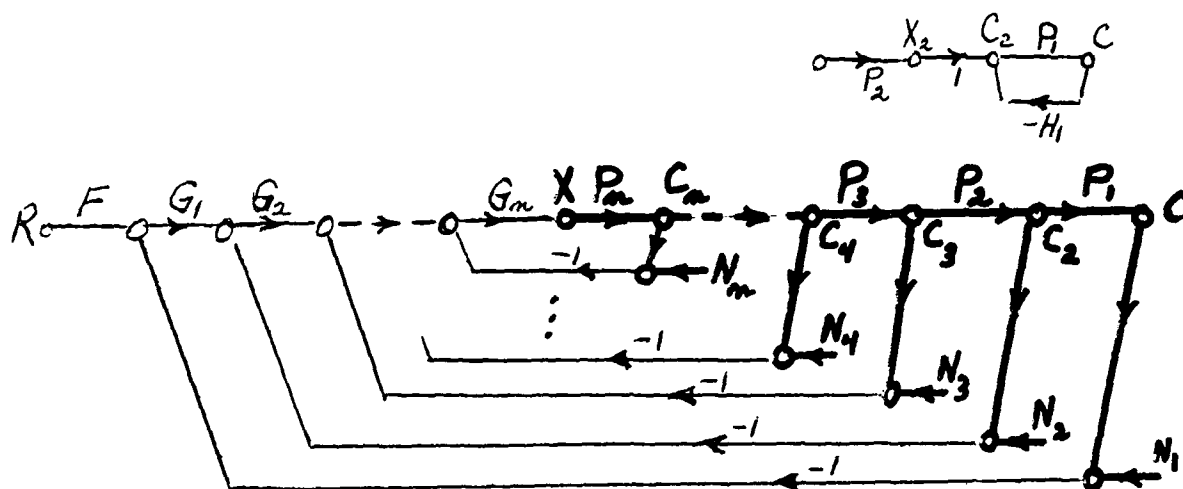


Figure 2-10a. The general cascaded feedback structure.
(Constrained plant and sensors in heavy lines.)

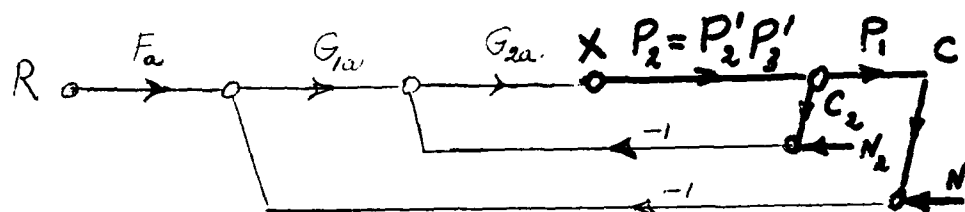


Figure 2-10b. Sec. 2.4.7 2-loop design. $L_{10} = G_{1a}P_{10}P_{2eqa}$,
 $P_{2eqa} = L_{2a}/(1 + L_{2a})$, $L_{2a} = G_{2a}P_{20}$.

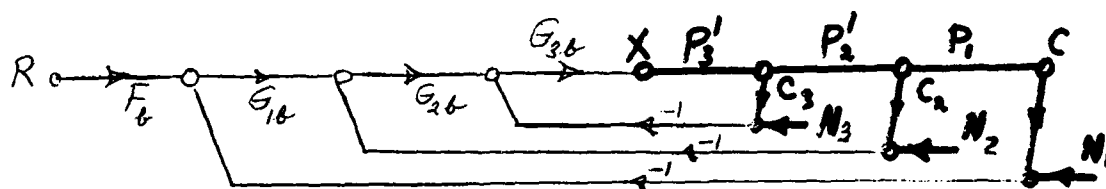
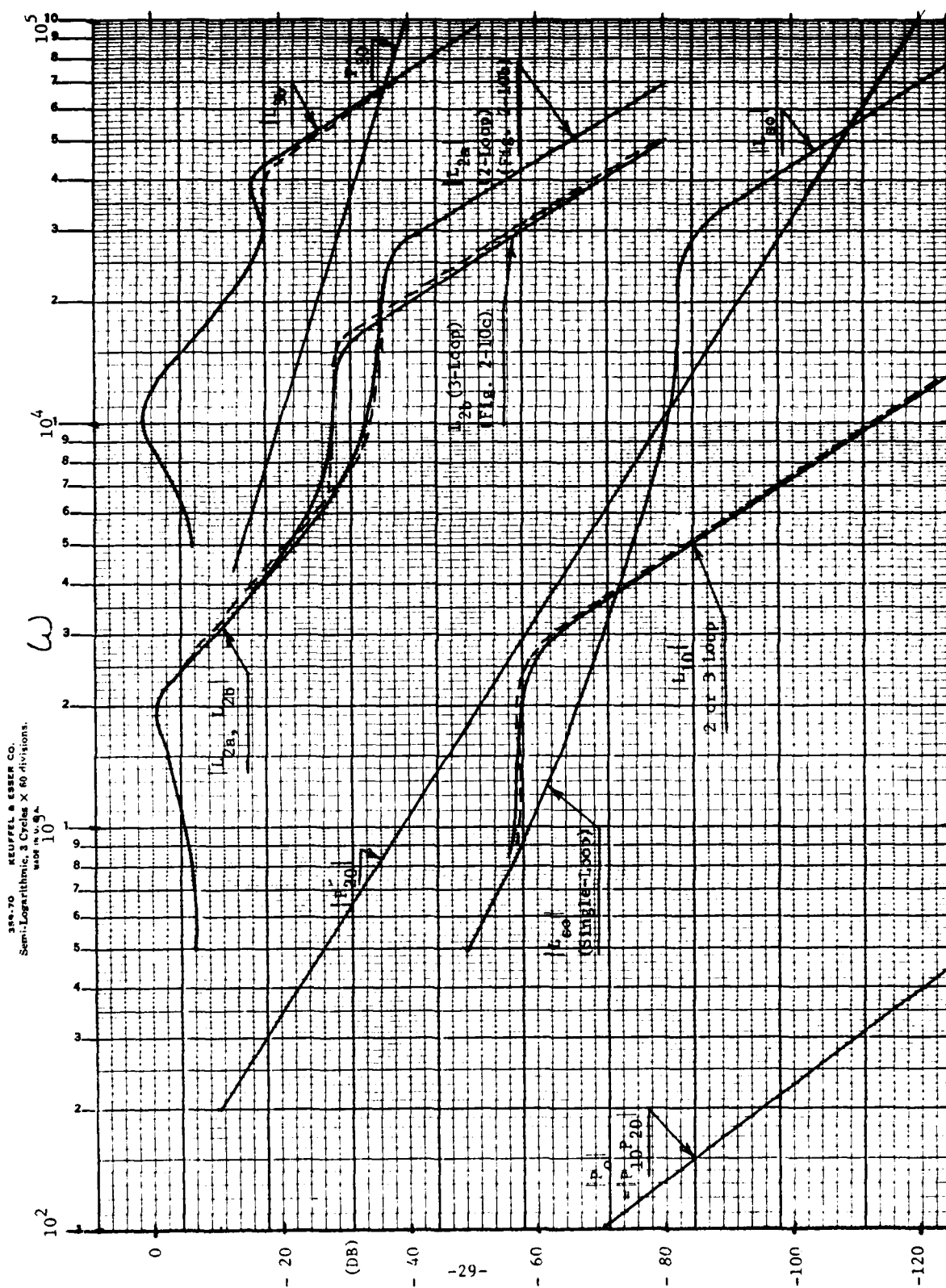


Figure 2-10c. Sec. 2.4.7 3-loop design. $L_{10} = G_{1b}P_{10}P_{2eqb}$,
 $P_{2eqb} = L_{2b}/(1 + L_{2b})$, $L_{2b} = G_{2b}P_{20}P_{3eqb}$,
 $P_{3eqb} = L_{3b}/(1 + L_{3b})$, $L_{3b} = G_{3b}P_{30}$.



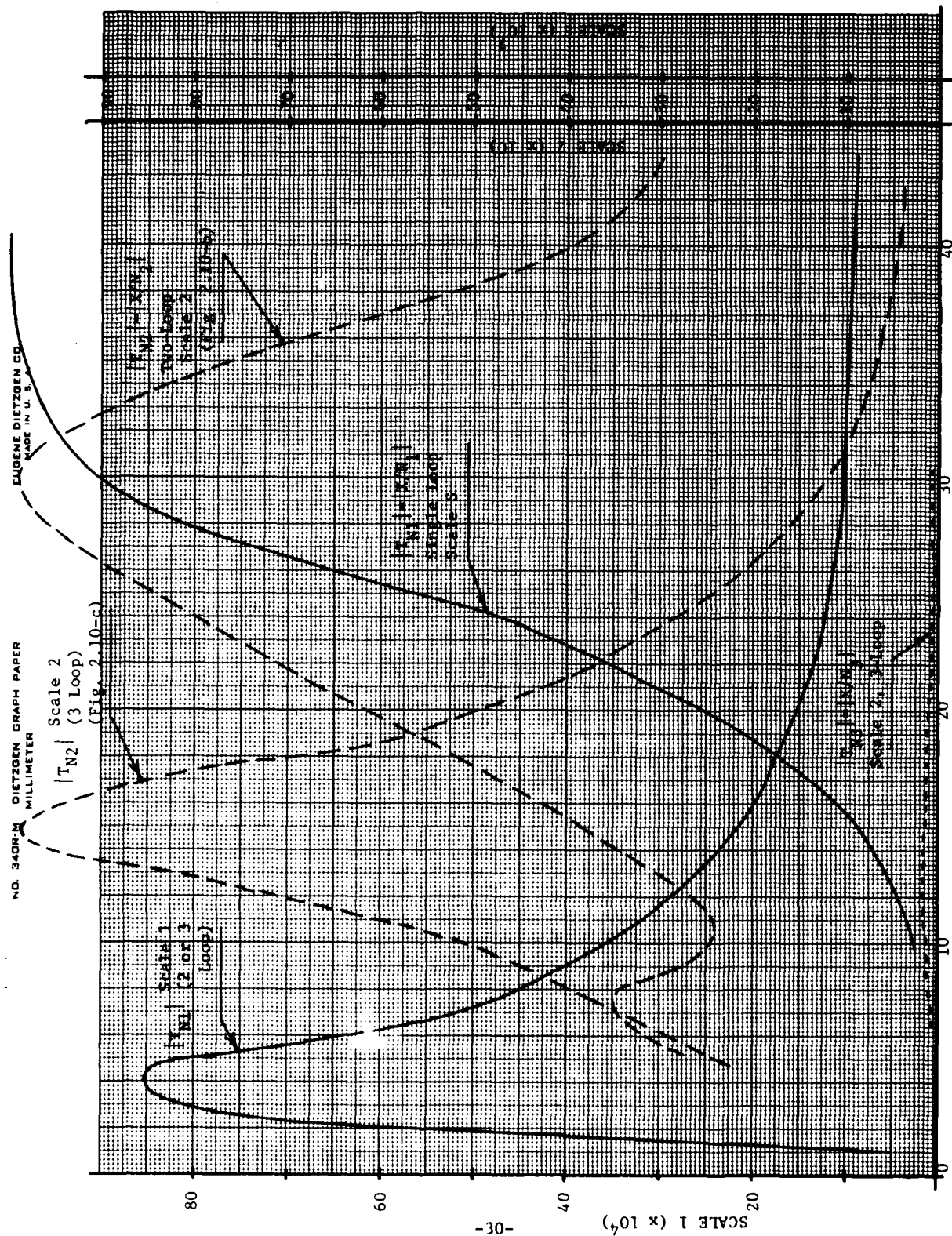


Figure 2-12. Sensor Noise Effects for various designs for Design Problem of Section 2.4.7.

2.6.1. Design perspective

The above results are very impressive. But what is even more impressive is that a very good approximation to the final multiple-loop designs and the sensor noise effects, can be gotten very quickly by means of a technique called "Design Perspective" [19,20]. The application of Design Perspective to the above example is shown in Fig. 2-11. A detailed design was required only for the single-loop L_{50} . The dashed lines show the results using Design Perspective for L_{10} - outer loop in 2 or 3-loop design, L_{2a} - first inner loop in a 2-loop design, L_{2b} - first inner loop in a 3-loop design, L_{3b} - second inner loop in a 3-loop design. Note the excellent agreement between the approximate Design Perspective results and the final detailed designs. Design Perspective enables the designer to obtain a good understanding and perspective of the important design trade-offs quite early in the game, without the need of a detailed design.

2.7 More Complex Multiple-Loop Structures Including Plant Modification

Systematic quantitative design techniques have also been developed [19,20] for the more complex multiple-loop structures of Figures 2-13a,b denoted as the Triangular and Parallel-Cascade structures respectively. The results shown in Figures 2-1c,d were obtained for a design example based on Figure 2-13b with two parallel sections ($m = 2$) $n_1 = 3$, $n_2 = 1$ and $P_{1i} = k_{1i}/s$ for $i = 1, 2, 3$, $P_{21} = k_2/s^3$, and very large uncertainties $k_{11} \in [50, 500]$, $k_{12} \in [20, 800]$, $k_{13} \in [1, 60]$, $k_2 \in [1000, 200,000]$. The parameter values in the brackets in Fig. 2-1c have been normalized and are given in the order k_{12} , k_{11} , k_{13} , k_2 . Design Perspective has also been developed for these structures [19,20].

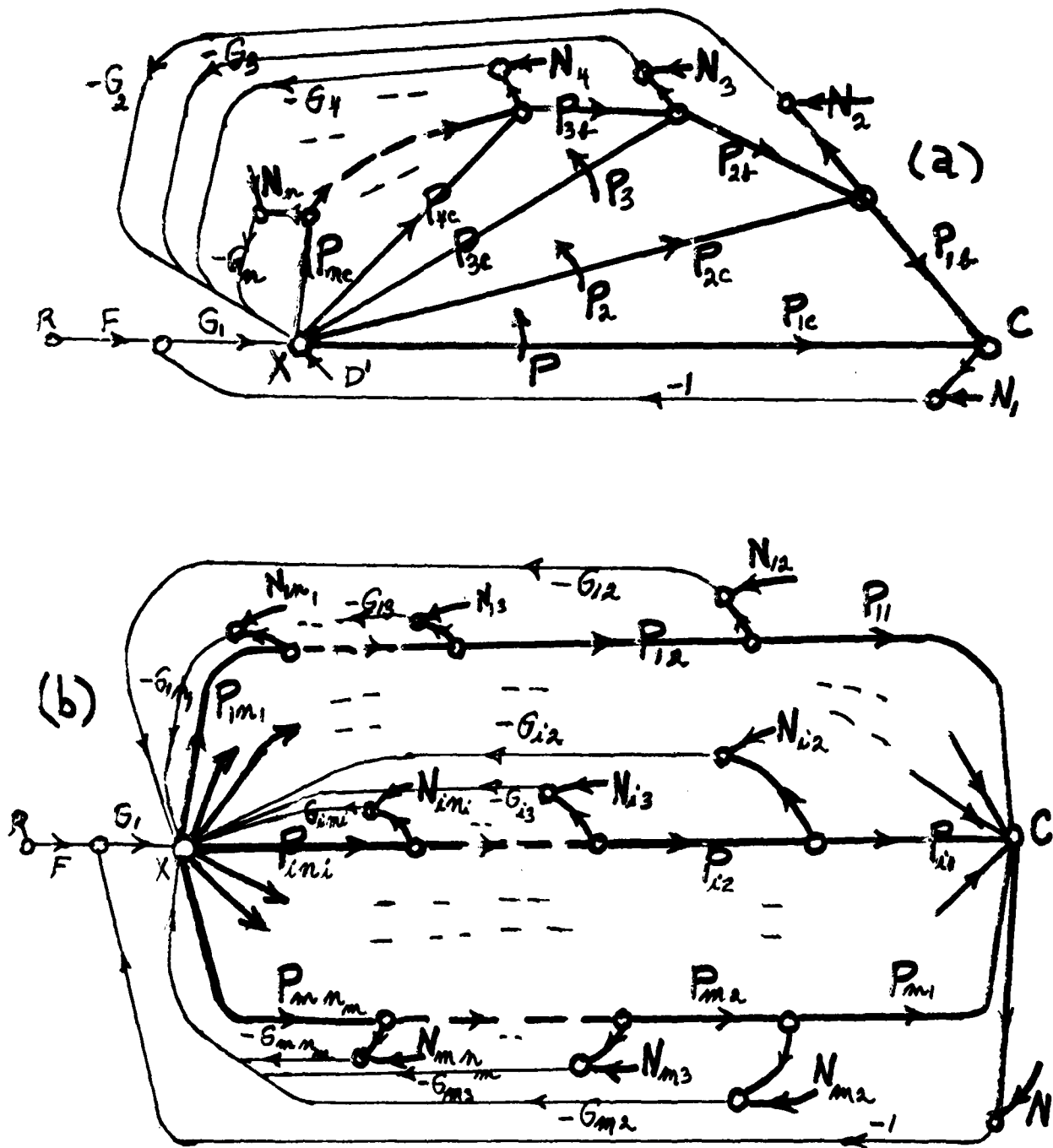


Figure 2.13 a,b. The Triangular and Parallel-Cascade Feedback Structures.

Plant Modification

It is noted that in Figures 2-10, 13a,b, each feedback loop is returned to the plant input X . No feedback is allowed to any internal plant variables e.g. from C to C_2 or more generally from any C_i to C_j , $j > i$ and $j = 2, 3, \dots, n-1$. The reason is that any such internal feedback constitutes "plant modification". The plant has been assembled by its specialists to deliver some maximum output C and the permissible levels of $C_2 = C/P_1$, $C_3 = C/P_1 P_2, \dots, C_i = C/P_1 \dots P_{i-1}$ are thereby determined. Suppose there is feedback from C vis H_1 to C_2 , as shown in the insert in Figure 2-10a. Now $X_2 = \frac{C}{P_1} (1 + P_1 H_1)$ with signal level possibly much greater than the previous C/P_1 , which the plant may perhaps not be able to handle.

We thus assume that the "feedback specialist" is called in to design the feedback network around the plant, after the latter has been built by the "plant specialist". This is the situation very often in practice. If the feedback specialist does his job properly, i.e. achieves the system response function $T(s)$ within its tolerances $\forall P \in P$, then the signal levels inside the plant will be within the values allowed by the plant specialist, so long as the command input functions $r(t)$ are in the set for which the system was designed.

Recently, quantitative design has been extended for the first time [21-2], specifically to the single branch cascade plant, with plant modification allowed. Some of the resulting structures are shown in Figure 2-14. The degree of modification, in a rms sense, of the internal plant variables was added as one more design specification, in addition to those listed here. It was shown that the loop bandwidths can thereby be significantly decreased,

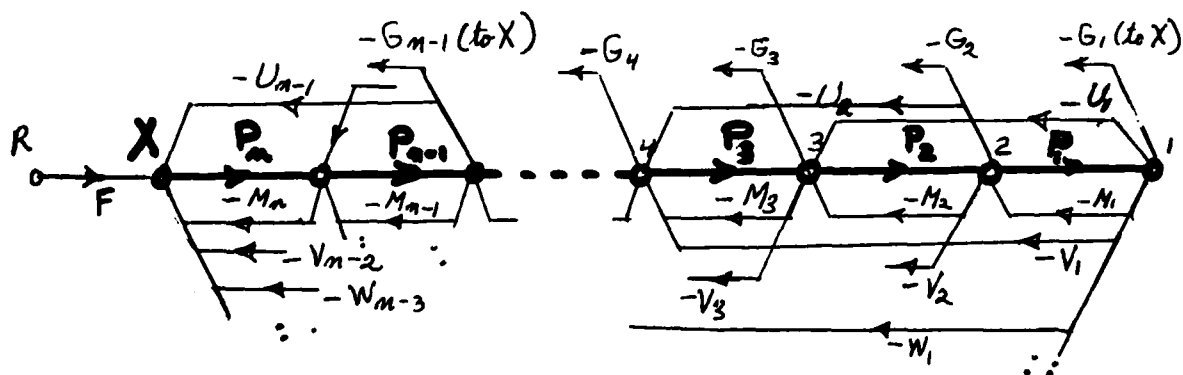
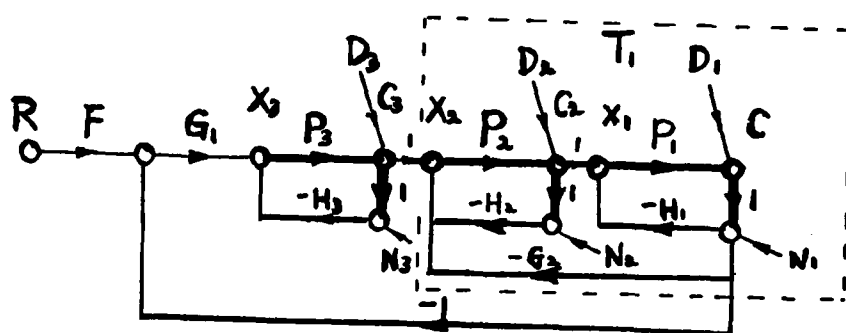
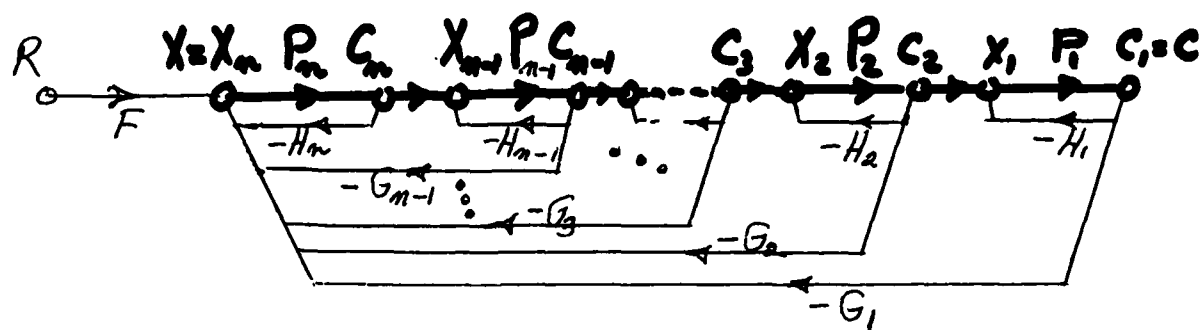


Figure 2-14. Some feedback structures with Plant Modification.

beyond that possible in "no plant modification" designs. This indicates that in significant plant uncertainty problems, it is definitely advantageous to have the "feedback specialist" participate with the "plant specialist" in the design of the plant.

2.8 Summary

Some of the principal features of single input-output linear time invariant (lti) quantitative synthesis theory for highly uncertain plants, have been presented briefly in this chapter. It should be clear that a respectable, mature synthesis theory exists for this class, although much remains to be done. Numerous quantitative design examples have been executed together with computer simulations, which have corroborated the design techniques. The existence of these design examples serve as benchmarks against which any "adaptive" design with claims of superiority can be checked. These design techniques can, of course, be applied to the lti flight control problem. But what is of much greater importance is the startling fact that most of these techniques are applicable exactly (no approximations) to linear time-varying, nonlinear and even nonlinear time-varying highly uncertain plant problems. This is treated in the next chapter.

CHAPTER 3

A BREAKTHROUGH IN QUANTITATIVE FEEDBACK SYNTHESIS

3.1 Introduction

Quantitative feedback synthesis in the frequency domain has clearly shown its value in the single input-output multiple-loop design techniques for lti systems, which were briefly outlined in Chapter 2. However, a fantastic, hitherto considered impossible achievement has recently been made [3-5]. It has been rigorously proven that these techniques can be applied exactly to a large class of nonlinear, highly uncertain plants, even nonlinear time-varying plants. The interesting point is that factors like uncertainty, synthesis, quantitative design to specifications are generally considered to make the design problem much more difficult. But it was precisely the precision and discipline involved in such strict requirements, which led to the development of the rigorous nonlinear synthesis technique. This claim of precise design of nonlinear, uncertain systems seems so unbelievable that it is worth repeating that there are no approximations involved, no linearizations, no describing function type of approximations, etc.

3.2 Concept of the Linear Time Invariant Equivalent Set (LTIE)

The simple single-loop structure of Figure 3-1a is first treated, for the case of a single system command input $r_1(t)$. The nonlinear plant w , with $y(t) = w(x(t))$, has uncertain parameters, e.g. w is given by

$$\ddot{y} + A\dot{y}^3 + By^m \text{sign } y = Ex \quad (3.1)$$

with A, B, m, E uncertain in that it is only known that $A \in [-1, 3]$,

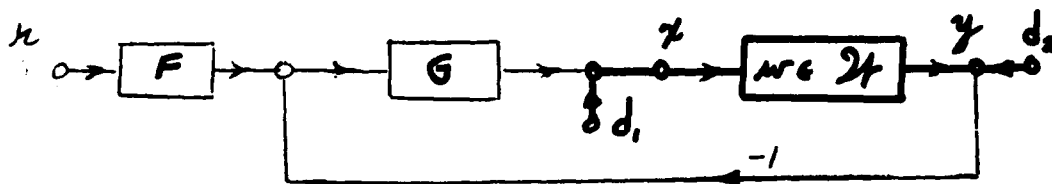


Figure 3-1a. Single loop feedback system with nonlinear uncertain plant $w \in W$.

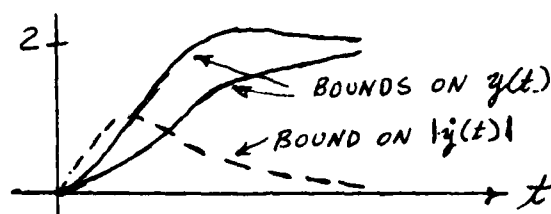


Figure 3-1b. Tolerances on response to 2-unit step command.

$B \in [2,8]$, $E \in [1,2]$, $m \in [.3,1.2]$. Each combination of possible values of A, \dots, m give a different w , thus generating a set $W = \{w\}$ of nonlinear plant functions. It is required that in response to command input $r_1(t)$, the system output $y(t)$ should be a member of a specified acceptable set A . For example, if $r_1(t)$ is a step function of 2 units magnitude, the tolerances on the output and its derivative may be as shown in Fig. 3-1b. Any $y(t)$ which satisfies these tolerances is a member of the acceptable set $A = \{a(t)\}$.

The next step is to find a linear time-invariant plant set P , which is precisely equivalent to the nonlinear plant set W , for the purpose of the synthesis problem. To do this, take any $a_i \in A$ and any plant $w^j \in W$. Find the input to w^j which gives the output a_i , i.e. solve Eq. (3.1) for

x given y , which in this case is a relatively easy operation.* Denote the resulting x by x_i^j . Now find a linear time-invariant plant P_i^j , which is equivalent to w^j for this special case i.e. the output of P_i^j is $a_i(t)$, when its input is $x_i^j(t)$. An easy way to do this is to let

$$P_i^j(s) = \frac{\int a_i(t)}{\int x_i^j(t)} \quad (3.2)$$

This implies that both $a_i(t)$ and $x_i^j(t)$ have Laplace transforms, a condition that is difficult to violate.

The lti $P_i^j(s)$ is precisely equivalent to the nonlinear w^j (from the input-output viewpoint), only when the input is x_i^j (or the output is $y = a_i$). Thus, imagine each is put inside separate, externally identical black boxes. The only measurement you are allowed is to inject an input signal $x_i^j(t)$. It will be impossible to say which black box contains the nonlinear w^j and which one the linear P_i^j .

Repeat this operation over all the $w \in W$, for the same a_i . Then repeat it for all the $a \in A$, generating a set of $\{P_i^j\} \triangleq P$. For example, if the set A had 10 elements and W had 20, then the set P would have 200 members. In practice both A and W are uncountable sets and so is P . The set P is equivalent to W only with respect to the set A . Thus, for any pair $a_m \in A$, $w^n \in W$, there exists a $P_m^n \in P$ which is equivalent to w^n , in the sense that some signal $x_m^n(t)$ must be applied to w^n to

* Implicit in this is the assumption that the plant has a unique inverse, excluding for example hard saturation. In practice, in such cases, one can model the hard saturation by a very small gain. Actually, the theory can be expanded to the case where there is no unique inverse but there is a set of possible inputs giving the same output, providing this set satisfies certain reasonable conditions.

give a_m , and if this same signal is applied to P_m^n , its output is also a_m . P is the linear time-invariant equivalent (LTIE) of W , with respect to A .

In Fig. 3-1a, suppose w (which can be any member of the nonlinear set W) is replaced by $P(s)$, any member at all of P . Consider the problem of choosing F, G so as to guarantee that the system output lies in the OK set A , no matter which $P \in P$ happens to be the plant. This is purely a quantitative lti design problem for which the techniques of Chapter 2 may be applicable. Suppose they are, which means that F, G are found such that the output is in A , no matter which $P \in P$ is chosen. Then, under very general conditions this same F, G compensation pair works for the nonlinear set W . This means that no matter which nonlinear plant $w \in W$ is used, the output is guaranteed to be in the OK set A . Functional analysis techniques are used [3,4] to prove the above, but the design execution involves simple, direct frequency response techniques, which can be performed by any reasonably competent feedback design engineer. A brief outline of the procedure is next presented.

3.3 Outline of Synthesis Procedure for Nonlinear Uncertain Plants

3.3.1 Problem Statement

To simplify the presentation, take an example where the nonlinear plant is given by the first order equation

$$\dot{y} + Ay^2 = Bx; \quad A \in [-1,5], \quad B \in [1,10] \quad (3.3)$$

Thus, the nonlinear plant is clearly "unstable" for a subset of plant parameter values. Suppose the typical command inputs are steps from $k_1 = 1$ to 5 magnitude, and other inputs of the form $k_2 te^{-\alpha t}$ with $k_2 \in [1,4]$,

$\alpha \in [.2, 3]$. It is desired that the closed-loop system behave like a lti system with transfer function

$$T(s) = \frac{E}{s^2 + Ks + E}, \quad E \in [16, 20], \quad K \in [9, 11] \quad (3.4)$$

3.3.2 Design Procedure

Take any command input $r(t)$ in the set $\{k_1 u(t), k_2 t e^{-\alpha t}\}$ and any acceptable $T(s)$. Their transform product is $R(s)T(s)$ whose inverse transform gives a possible output $y(t)$. For example, if $R(s) = 2/s$, then

$$y(t) = \mathcal{L}^{-1} R(s)T(s) \triangleq 2 + \frac{2[ae^{-bt} - (-be^{-at})]}{b-a} = 2 + \mu(t) \quad (3.5)$$

$$a+b = K, \quad ab = E .$$

Substitute $y(t)$ into Eq. (3.3) and solve for

$$Bx(t) = \frac{ab(e^{-at} - e^{-bt})}{b-a} + A[4 + 4\mu(t) + \mu^2(t)] . \quad (3.6)$$

Next find $P(s) = \frac{Y(s)}{X(s)}$. Actually, it is easier to find $\frac{1}{P(s)} = \frac{X(s)}{Y(s)}$ with $Y(s) = 2E/s(s^2 + Fs + E)$,

$$BX(s) = \frac{ab}{(s+a)(s+b)} + A \left[\frac{4}{s} - \frac{4(s+a+b)}{(s+a)(s+b)} + \frac{s^2 + 3s(a+b) + 2(a^2 + 3ab + b^2)}{(s+2a)(s+2b)(s+a+b)} \right] \quad (3.7)$$

The above gives a set $\{P(s)\}$, by letting a, b, A, B, k_1 , etc. range over their permissible values. The process is repeated by taking $r(t) = k_2 t e^{-\alpha t}$, giving in the same manner another set of $P(s)$. The union of the two sets gives the total P set. Thereafter, the design procedure is entirely the same as for an uncertain linear time-invariant P set--as briefly described in Section 2.4 and in much more detail in [7]. The objective is to find $F(s), G(s)$ in Fig. 3-1a, such that the system transfer function satisfies the frequency-domain tolerances given by (3.4), for all

$P(s) \in P$. This is completely a linear time invariant design problem. If it is solvable, then the same $F(s)$, $G(s)$ are guaranteed to work for the original uncertain nonlinear plant problem. In this case it is certainly solvable.

3.3.3 A Condition for Guaranteed Solvability of the Linear Time Invariant Equivalent (LTIE) Problem

If the LTIE set $P = \{P(s)\}$ is minimum-phase then the LTIE problem is solvable. Now $P(s) = Y(s)/X(s)$ with $x(t) = w^{-1}[y(t)]$ in the notation of Section 3.1. Zeros of $P(s)$ are the zeros of $Y(s)$ (those uncanceled by $X(s)$) and poles (uncanceled) of $X(s)$. If the command input is minimum-phase, then the OK output set A can be prescribed minimum-phase, so $Y(s)$ has no right half-plane zeros. The condition then is that $X(s)$ has no right half-plane poles, i.e. the plant input is "stable."

Consider a nonlinear plant described by a differential equation of the form $N_1 y = N_2 x$ with N_1, N_2 nonlinear differential operators. It is assumed $y(t)$ is "stable" and so is $N_1 y$. For example all $N_1 y$ of the form $\sum f_i(y) \frac{d^i y}{dt^i}$ with $f_i(y)$ bounded will give "stable" $N_1 y$. So the problem is the stability of x in $N_2 x = \psi(t)$ with $\psi(t) = N_1 y$ known and "stable". For example, if $N_2 x = \dot{x} - x$ (linear in this case), then the plant is nonminimum-phase, as it would be even if $N_1 y$ was linear time-invariant. The above gives a relatively simple means for determining whether the LTIE plant set is minimum-phase, a concept which is now also meaningful in nonlinear feedback design.

3.3.4 System Response to Other Inputs

It is important to emphasize that the desired performance can be guaranteed only for those system inputs which were explicitly listed and considered in the design. Thus, in the example of this section, what can be said of an input $r(t) = 5t$? Apriori not very much, because it was not in the list for which the ELTI plant set was found. We could however, check if the closed-loop system will behave like a $T(s)$ satisfying (3.4) to such an input, as follows.

Let $Y(s) = R(s)T(s)$, with $R(s) = 5/s^2$ in this case and $T(s)$ of (3.4). Solve (3.3) for $x(t)$ and find $P(s) = Y(s)/X(s)$. If $P(s) \in P$ the set previously obtained, then indeed the system behaves like $T(s)$ to this input too. However, if ramps of a certain size are indeed typical inputs, then it would be a good idea to include them at the outset in the set of $r(t)$, for which the design is explicitly made. In any significant problem (such as the flight control one described in Chapter 4), one must prepare a computer program for solving the nonlinear plant equation backwards for the input $x(t)$, given the output $y(t)$. A computer program is also prepared for finding $Y(s) = T(s)R(s)$. It is then a simple matter to err on the safe side and let the set $\{r(t)\}$ include all conceivable realistic inputs.

In the preceding, only system command inputs $r(t)$ in Figure 3-1a were considered. But disturbance inputs d_1 and/or d_2 in Figure 3-1a are similarly treated. One must assign acceptable output sets in response to the disturbances, in the same manner as the set $\{r(t)\}$. This gives a set of acceptable outputs $\{y_d(t)\}$, due to the disturbances. The corresponding plant inputs and LTIE plant set are found in the same manner. An example

in which both command and disturbance inputs were thus considered is given in [12]. Incidentally, it has been shown [4] that the design is not sensitive to the inputs, i.e., significant deviations from the $r(t)$ for which the design was made, will have small effect on the $T(s)$ presented by the system. The design can be executed such that noninfinitesimal changes in each $r(t)$ give a $T(s)$ within the acceptable set. This has been verified in all our design examples.

3.4 Extensions of the Nonlinear Design Technique.

There are quite a few significant extensions, briefly noted here. One is to nonlinear closed-loop synthesis, i.e. the closed-loop system can be designed to be nonlinear and quantitatively so. For example, it may be desirable to have the plant operate close to its saturated value nearly all the time, in order to have fastest possible response, say to step functions. The OK response sets may then be as shown in Fig. 3-2. Note that in a linear

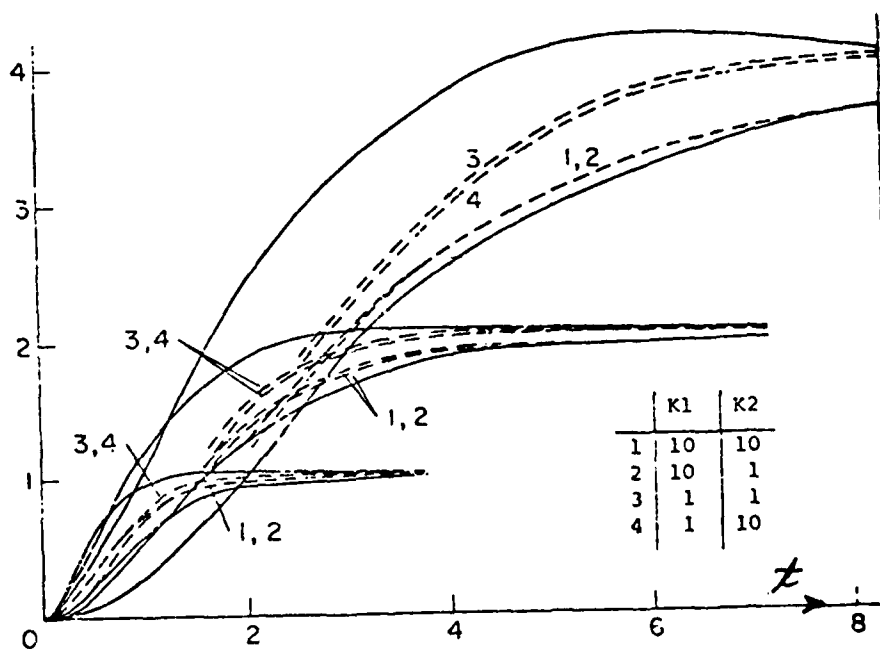


Figure 3-2. Acceptable output sets of a nonlinear system nature, for responses to steps of 1, 2, 4.

system the OK response set for a step input of magnitude 2 must be twice that for a step input of 1. This is not so in Fig. 3-2. For any step input in a specified range, the output is required to climb at the same (saturated) rate until it is close to the final commanded value. F in Figure 3-1 then emerges nonlinear. A design example of this kind is described in detail in [12]. Another such nonlinear closed-loop design philosophy may be applicable to flight control. In a fast maneuvering situation, the command inputs are fast and large, and it is desired to command acceleration while in a tracking mode, the command inputs are slow, and it is desired to command pitch. One could pose typical inputs of the first kind and define the desired acceptable set and repeat for inputs of the second kind. The design technique can handle this kind of situation -- even with the plant nonlinear and uncertain, of course.

The plant can be linear or nonlinear time-varying and uncertain, e.g.

$$\ddot{y} + \left(\frac{A + Be^{-\alpha t}}{E + Gt} \right) \dot{y} + Qy^{(H+je^{-\beta t})} = K\dot{x} + Me^{-\mu \sin vt} x^3 \quad (3.8)$$

with say uncertainties $E \in [1,5]$, $G \in [2,4]$, $\alpha \in [1,2]$, etc. The closed-loop system can be designed to be linear time invariant, linear time-varying, nonlinear time invariant or nonlinear time-varying. If linear time-varying then F, G in Figure 3-1 emerge linear time-varying. If nonlinear time-varying, F is nonlinear time-varying, G linear time-varying. One example of a highly uncertain nonlinear, time-varying plant but with linear time invariant closed loop specifications, is given in [4]. Another example with a linear time-varying uncertain plant and lti closed-loop specifications is given in [3].

Another extension is to single input-output multiple-loop systems of the kind described in Chapter 2, but excluding the plant modification structure.

Consider Figure 2-10, with nonlinear w_1, w_2, \dots replacing P_1, P_2, \dots . If $c(t)$ is known (a member of the OK set), one can solve the nonlinear equations backwards to find $c_2(t)$, $c_3(t)$, etc. Then $C(s)/C_2(s) = P_1$ the lti equivalent of w_1 , $C_2(s)/C_3(s) = P_2$ the equivalent of w_2 etc. A set of each is generated and the result is a multiple-loop lti problem solvable by the methods of [19]. The resulting lti design works for the nonlinear uncertain plant set.

Another extension being currently researched is for the case of non-minimum-phase system inputs. Nonminimum-phase OK output sets must then be postulated, leading to lti plant equivalents which may have both zeros and poles in the right half-plane. It appears that in the resulting lti design, there can be zeros of $1+L(s)$ in the right half-plane, where $L(s)$ is the lti equivalent loop transmission. In a real lti system this would give an unstable system, but it need not be so in a lti equivalent system. This research has not as yet been completed.

3.5 Comparison with Other Synthesis Techniques

There are no other techniques which cope directly with the quantitative synthesis problem described here, i.e. which guarantee outputs in the time or frequency domain, for apriori given uncertainty ranges of plant parameters, even for linear time invariant plants. Optimal control theory is mostly concerned with perfectly known plants. If parameter uncertainty is considered, it is usually done in a qualitative manner. And system performance is always formulated by a scalar functional--a single real number which is usually a quadratic function of the state and control variables. In most control problems, one is vitally interested in transient response, which is a function of time, not a scalar functional. Often systems which are optimal for the

quadratically based functional, have very poor (large overshoot) in their time response.

In the last decade, modern control theory has concentrated on state-variable feedback, use of observers, etc. for realizing desired system eigenvalues. Again, plant uncertainty has until recently, been completely neglected. Lately there has been a great deal of work on "robustness", mainly with the problem of stability for small enough parameter variations, or for disastrous failures of some components. This is a very welcome improvement in the realism of modern control theory. However, it has very far to go as yet. The role of loop bandwidth, or its time-domain equivalent of speed of loop response, is still not appreciated. The system performance is still judged by a scalar functional. This laudable attempt at realism in control of uncertain systems, is being handicapped by the mathematical formulations and techniques used. These were natural and sensible in optimal control of perfectly known plants, which is basically an open-loop problem. They are unnatural and opaque for quantitative synthesis of highly uncertain systems.

At the present time, any other synthesis technique applied to the quantitative problem formulated here, must proceed by cut and try. It is not even possible for any of them to declare apriori whether a specific quantitative performance specification set can be satisfied or not, even for lti problems. It is possible to do so with the techniques presented here, even for nonlinear time-varying problems. The next chapter presents a detailed application of the nonlinear technique to the longitudinal flight control problem, based on a simplified but highly nonlinear plant model.

CHAPTER 4

FLIGHT CONTROL DESIGN BASED ON NONLINEAR MODEL WITH UNCERTAIN PARAMETERS

4.1 Statement of Problem

In this chapter, the breakthrough of Chapter 3 is applied to a significantly nonlinear model of the short-period longitudinal flight control problem.

Nonlinear plant model (see Table of Symbols)

$$\dot{u} = qV_0 + g \cos \theta - \frac{\rho V_0^2 S}{2m} [C_{N\alpha}(\alpha) + C_{N\delta}(\alpha)\delta] \quad (4.1)$$

$$\ddot{\theta} = \dot{q} = \frac{\rho V_0^2 S C}{2I_y} [C_{m\delta}(\alpha)\delta + C_{m\alpha}(\alpha) + \frac{C}{2V_0} C_{mq}(\alpha)q],$$

$$\alpha = \tan^{-1} \frac{u}{V_0}. \quad (4.2, 3)$$

The control input is the elevator angle δ , and the output variable to be controlled is $[24]$,

$$c^* = 12.4 \ddot{\theta} + \frac{1}{9.8} (\dot{u} - V_0 \dot{\theta} + \ddot{\theta}) \quad (4.4)$$

The feedback structure used is shown in Fig. 4-1 with $c^* = w(\delta)$. The numbers used in Equations (4.1-4) are [25,26] $I_y = 207,000 \text{ kg m}^2$, $m = 17,000 \text{ kg}$, $C = 4.89 \text{ meters}$, $S = 49.2 \text{ m}^2$. The $C_{ij}(\alpha)$ are nonlinear functions of α , see Fig. 2-2. Since α (Fig. 4-8) ranges in $[0, 35^\circ]$, there is strong nonlinear operation. The horizontal velocity v was taken as V_0 fixed, which is incorrect for some low-velocity cases, but the objective here is to demonstrate the validity of the design technique in a strongly nonlinear situation, which is achieved sufficiently by means of the nonlinear $C_{ij}(\alpha)$.

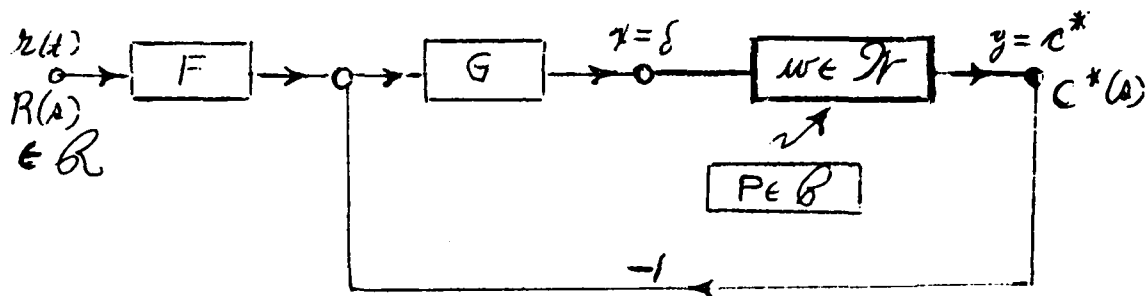


Figure 4-1. System structure

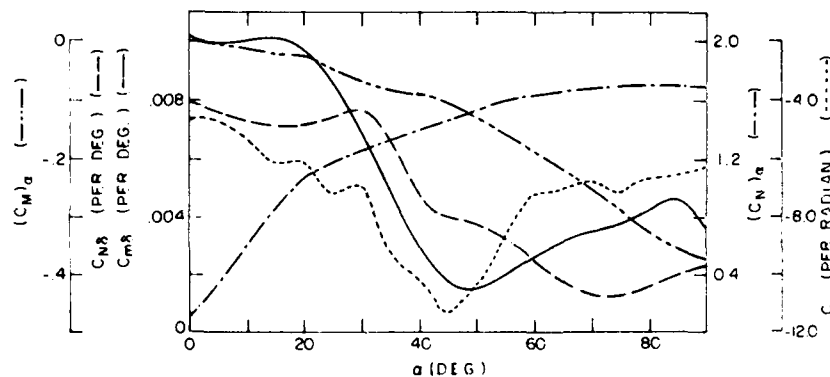


Figure 4-2. Aerodynamic coefficients $C_{ij}(\alpha)$ are strongly nonlinear functions of α .

The bounds on the acceptable $c^*(t)$ in response to a unit step command are included in Fig. 4-7, which also include design simulation results. The set of command inputs R consists of steps 1 to 5 in magnitude. Parameter uncertainty is due to ρ ranging in $[.3, 1.22]$ and V_0 in $[75, 206]$. Initial conditions are $\dot{w}(0) = \dot{q}(0) = q(0) = 0$, $\alpha(0) = \theta(0)$, giving initial values for δ (as well as u , θ , α) which is subtracted out so that the change in δ is used to find the lti equivalent P set. The detailed steps in the design implementation are next presented, with comments postposed to the end.

4.2 Design Execution

4.2.1 The linear time invariant (lti) equivalent set P

Let $\mathcal{L}c^*(t) \triangleq C^*(s) = T(s)R(s)$, where $T(s)$ is the equivalent system transfer function presented by the closed-loop system of Fig. 4-1. Here $R(s) = k/s$ with $k \in [1, 5]$, while it is required that $T(s) \in T$, a set derived from the bounds in Fig. 4-7. A simple means for generating T , taken from [25], is to let $T(s) = a^2(s+2.9)/2.9(s^2 + 2\zeta as + a^2)$, ζ ranging in $[3.7, 1.5]$, a in $[3.14, 7.6]$, giving the bounds on $|T(j\omega)|$ in Fig. 4-3. Such bounds suffice [7] for mp (and obviously stable) $T(s)$. Any $T(s), R(s)$ pair thus generates an acceptable $c^*(t)$. A computer program solved Eqs. (4.1-4) backwards for $\delta(t)$ and then checked the result by solving Eqs. (4.1-4) forwards for $c^*(t)$ from $\delta(t)$. The program was considered adequate only when excellent agreement was obtained over the entire range considered. $C^*(s)$ was a priori available and $\Delta(j\omega) \triangleq \{\delta(t)\}_{j\omega}$ was obtained by numerical integration. As c^* is a short-period criterion and for all the acceptable cases has definitely reached steady-state in 4 seconds (see Figs. 4-7), Eqs. (4.1-4) were solved only for $t \in [0, 4 \text{ seconds}]$, and the constant $\delta(4)$ was used for $t > 4$.

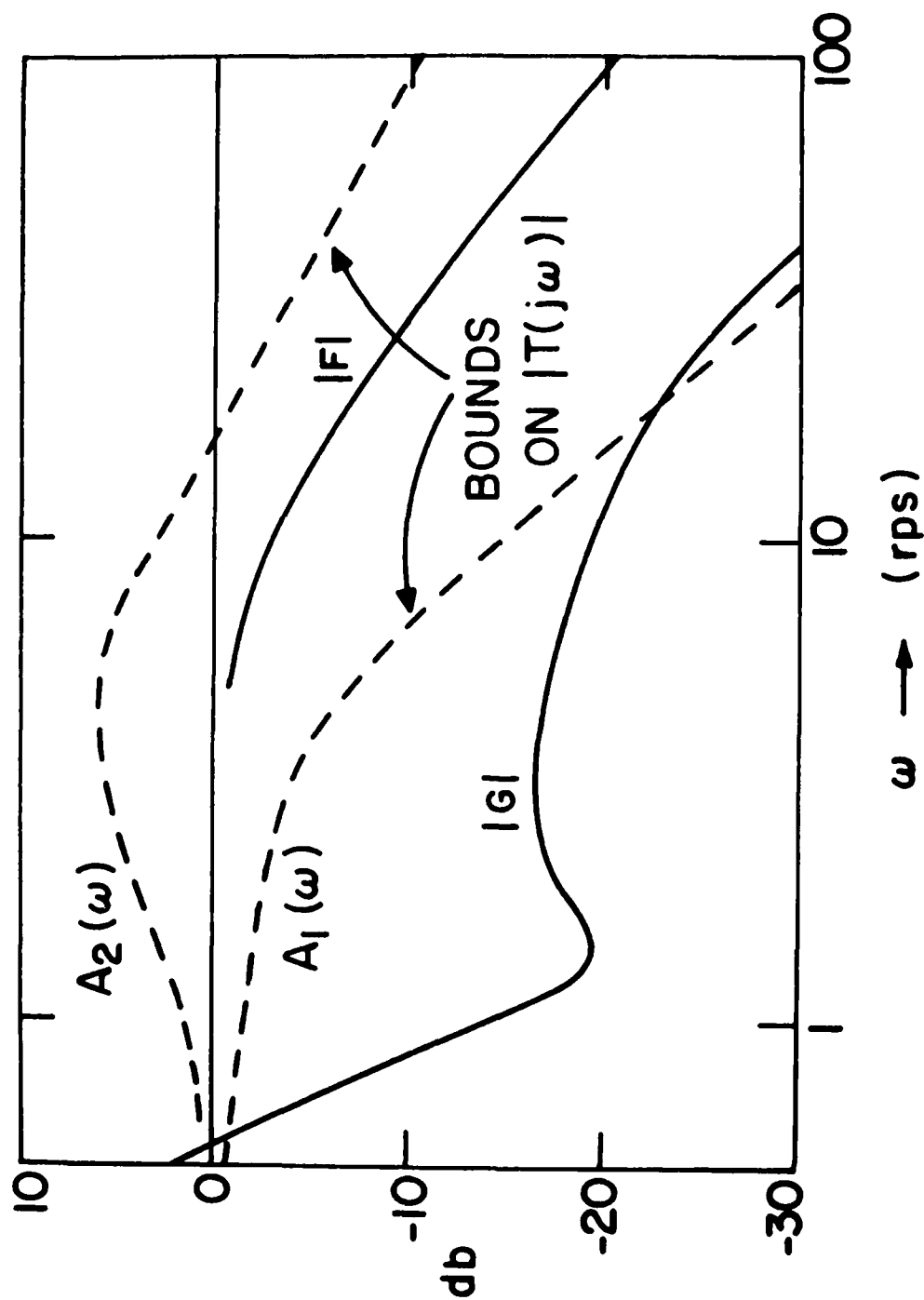


Figure 4-3. Frequency domain bounds on $|T(j\omega)|$ derived from time-domain bounds. Bode plots of $|F(j\omega)|$, $|G(j\omega)|$ used in design.

Loci of six $P(j\omega)$ are shown in Fig. 4-4, two of them (e,f) unstable with a pair of right half-plane poles, which are zeros of $\Delta(s)$. The set includes a large number of such unstable $P(s)$, which the design technique can easily handle.

Plant templates. At any ω say $\omega = \omega_1$, the set $\{P(j\omega)\}$, $P \in P$ consists of a region in the logarithmic complex plane (Nichols chart) denoted as the ω_1 -plant template $T_p(\omega_1)$. A number of $T_p(\omega)$ are shown in Figs. 4-5a to f. At very small ω there are two almost constant angle sub-templates 360° apart. This is due to the presence of both stable and unstable $P \in P$, and the fact that $\text{Arg } P$ near $\omega = 0$ is either 0 or $n\pi/2$ for some integer n . As ω increases, the two groups merge together and approach a single vertical line at large ω well beyond the plant "dynamics" ($\omega = 12$ is large enough in this case, see Fig. 4-5f). Note how this frequency response approach is indifferent to system order.

4.2.2 Design of $G(s)$, $F(s)$

Given the set $P = \{P\}$, the problem is to find $F(s)$, $G(s)$ in Fig. 4-1 such that the system transfer function $T(j\omega) = FGP/(1+GP) \in T$, for all $P \in P$. One may program the computer to find the (unique) bounds $B(\omega)$ on $G(j\omega)$, so that as P ranges over P , $\Delta \ln|T(j\omega)| =$

$\Delta \ln \left| \frac{GP}{1+GP} \right| \leq [A_2(\omega) - A_1(\omega)] \text{ db}$ of Fig. 4-3. Alternatively, this may be done by hand, giving useful insight as explained in Section 2.4.3, Figure 2-4.

Fig. 4-6 shows the bounds so obtained on $G(j\omega)$, and the $G(j\omega)$ chosen to satisfy these bounds. Let e_G be the excess of poles over zeros assigned to $G(s)$, so that as $s \rightarrow \infty$, $G \rightarrow k_G/s^{e_G}$. It is reasonable to define the optimum G as that which satisfies its bounds with minimum k_G .

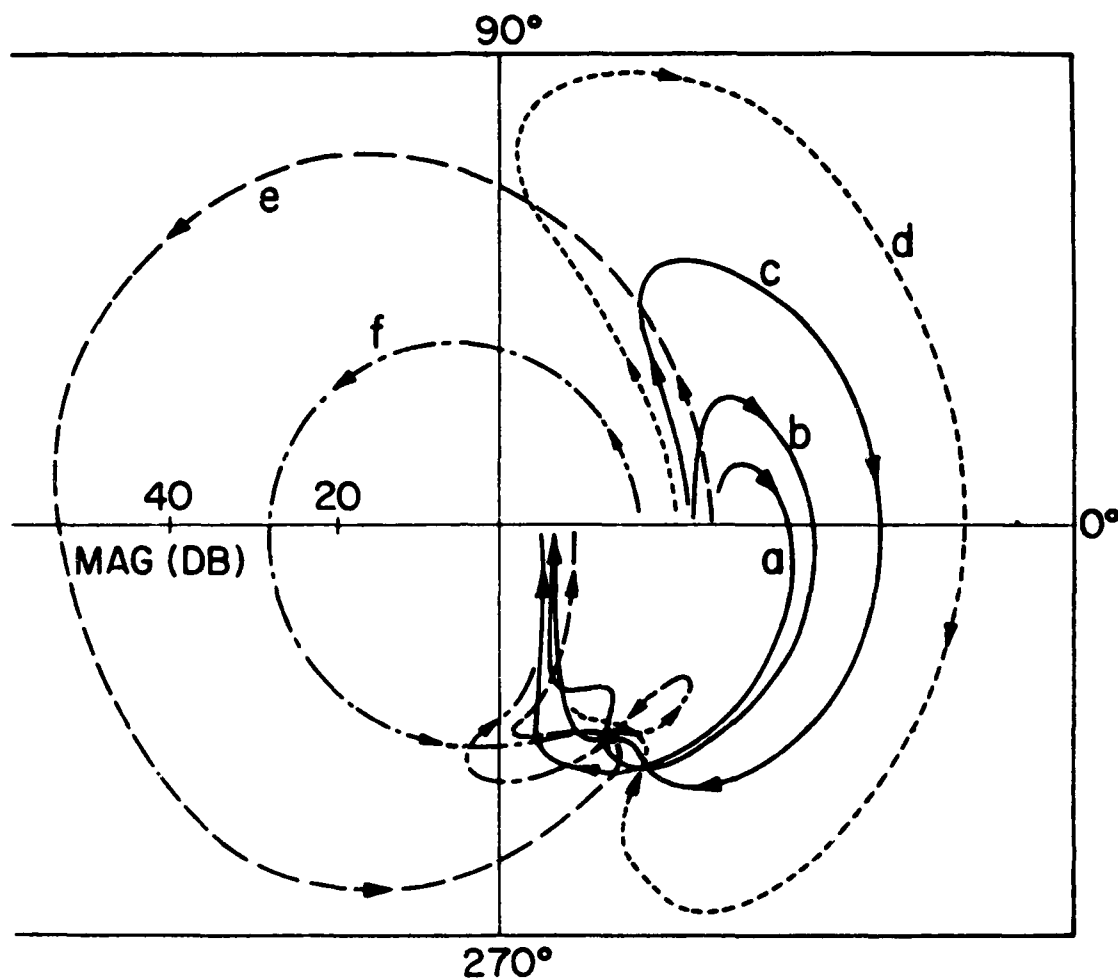
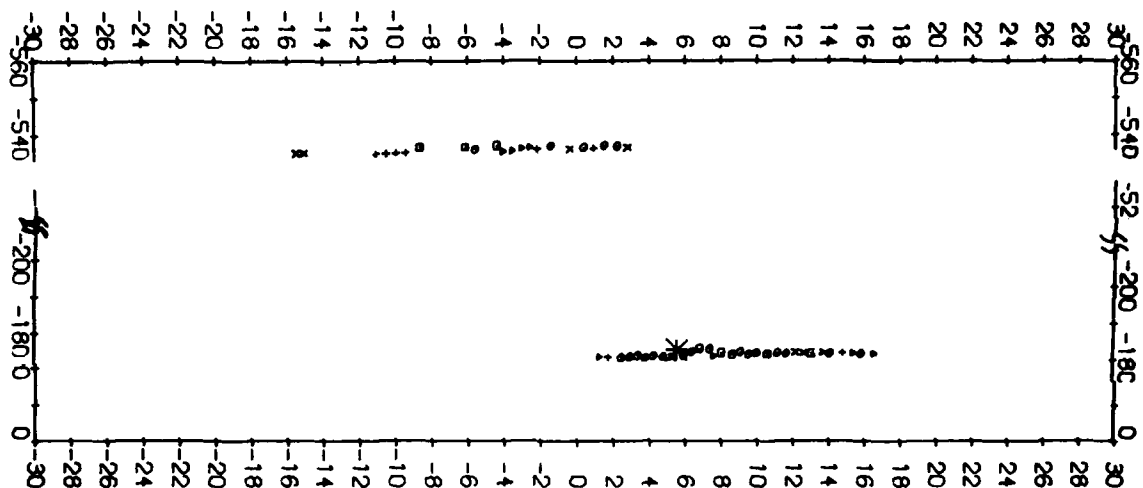


Figure 4-4. Loci of typical lti $P(j\omega)$. Cases e, f are open-loop unstable.

	k	ζ	ω_n	v_0	ρ	δ_{\max}	α_{\max}
(a)	1	1.0	3.77	180	.36	6.3	16.4
(b)	2	1.0	3.77	100	1.05	11.0	23.5
(c)	4	.45	5.66	120	1.05	18.6	29.3
(d)	4	.45	5.66	117	1.05	22.4	31.3
(e)	4	1.0	3.77	230	.36	13.8	27.0
(f)	3	.92	7.54	180	.36	27.4	34.2



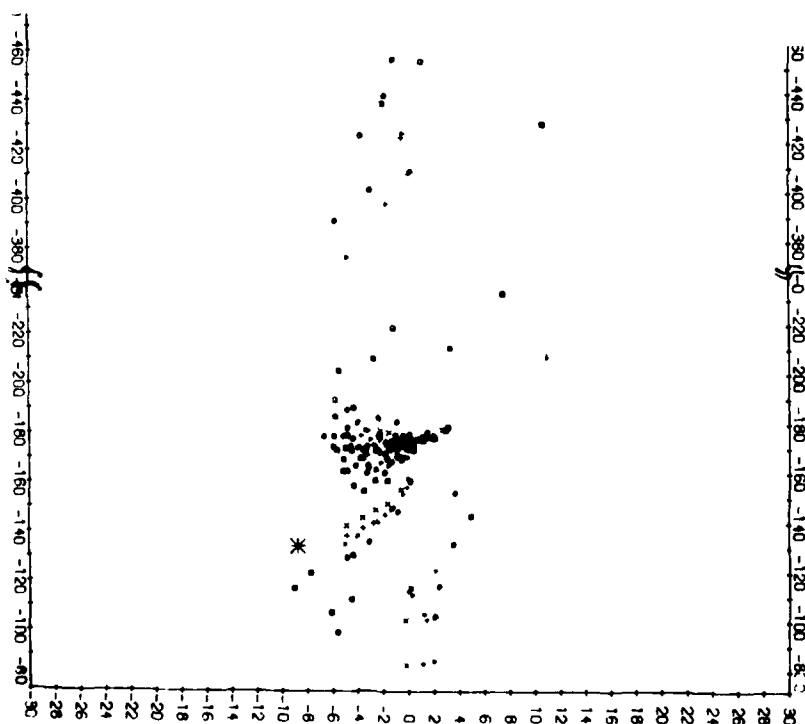
TEMPLATE OF EQUIVALENT PLANT

FREQUENCY $W=0.04$

SHIFT=21 DB

NUMBER OF POINTS = 562

POINT OF NOMINAL PLANT (5.6 DB, -180°)



TEMPLATE OF EQUIVALENT PLANT

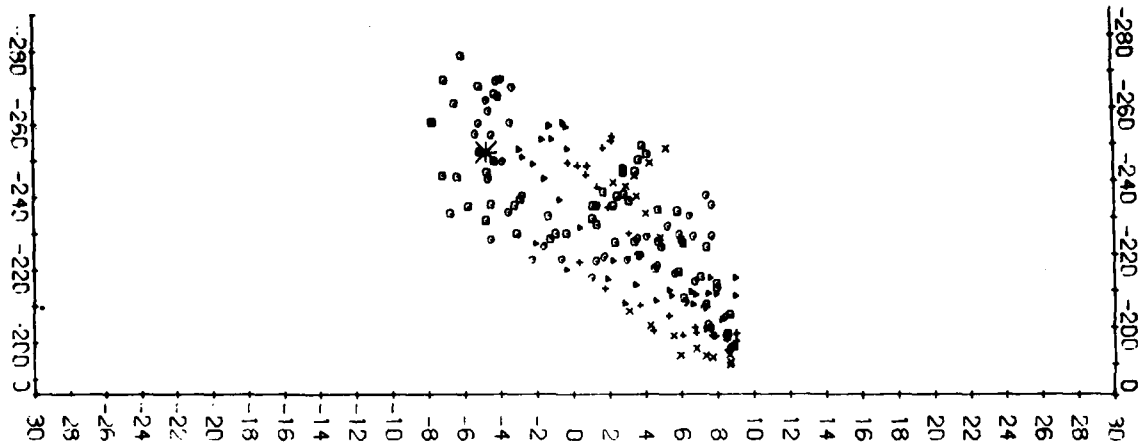
FREQUENCY $W=0.75$

SHIFT=35 DB

NUMBER OF POINTS = 179

POINT OF NOMINAL PLANT (-8.7 DB, -133°)

Figures 4-5 a, b.



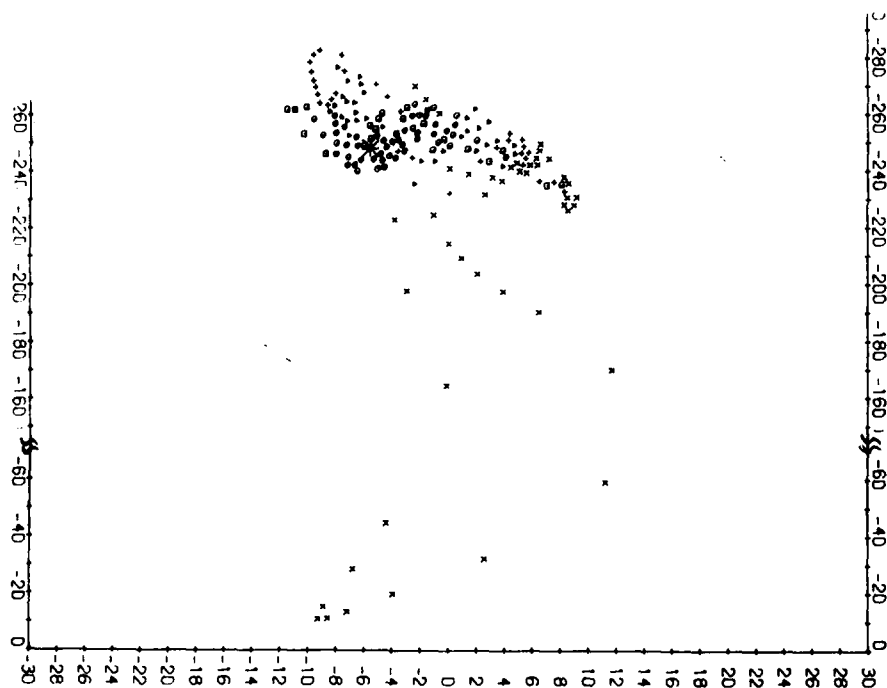
TEMPLATE OF EQUIVALENT PLANT

FREQUENCY $W=1.90$

SHIFT=32 DB

NUMBER OF POINTS = 179

POINT OF NOMINAL PLANT (-4.8 DB, -250°)



TEMPLATE OF EQUIVALENT PLANT

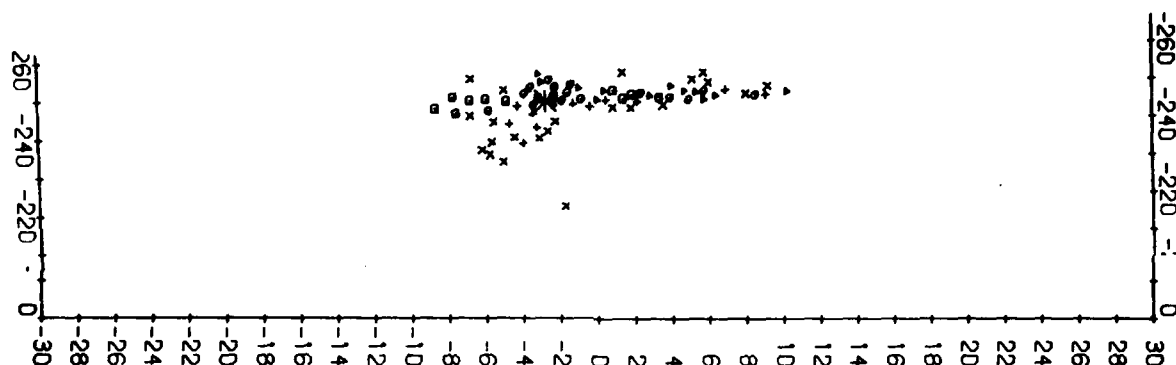
FREQUENCY $W=3.00$

SHIFT=31 DB

NUMBER OF POINTS = 562

POINT OF NOMINAL PLANT (-5.6 DB, -248°)

Figures 4-5 c, d.



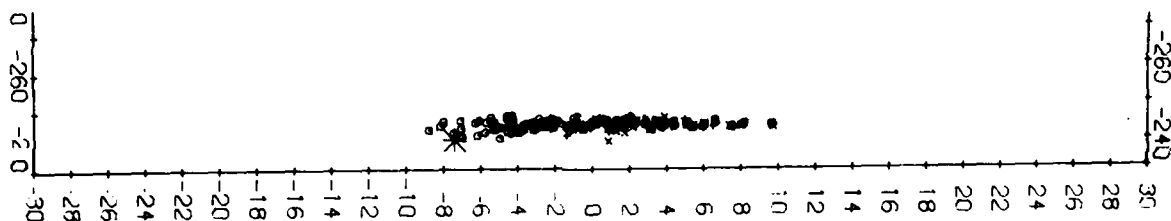
TEMPLATE OF EQUIVALENT PLANT

FREQUENCY W=10.00

SHIFT=17 DB

NUMBER OF POINTS = 562

POINT OF NOMINAL PLANT (-2.8 DB, -247°)



TEMPLATE OF EQUIVALENT PLANT

FREQUENCY W=12.00

SHIFT=16 DB

NUMBER OF POINTS = 179

POINT OF NOMINAL PLANT (-7.5 DB, -241°)

Figures 4-5 e, f.

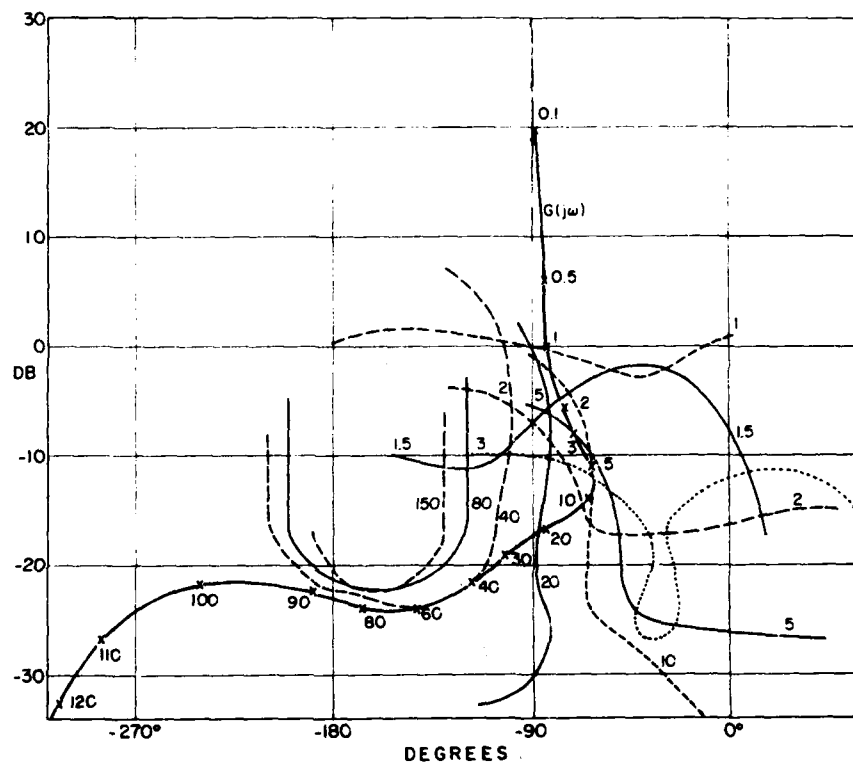


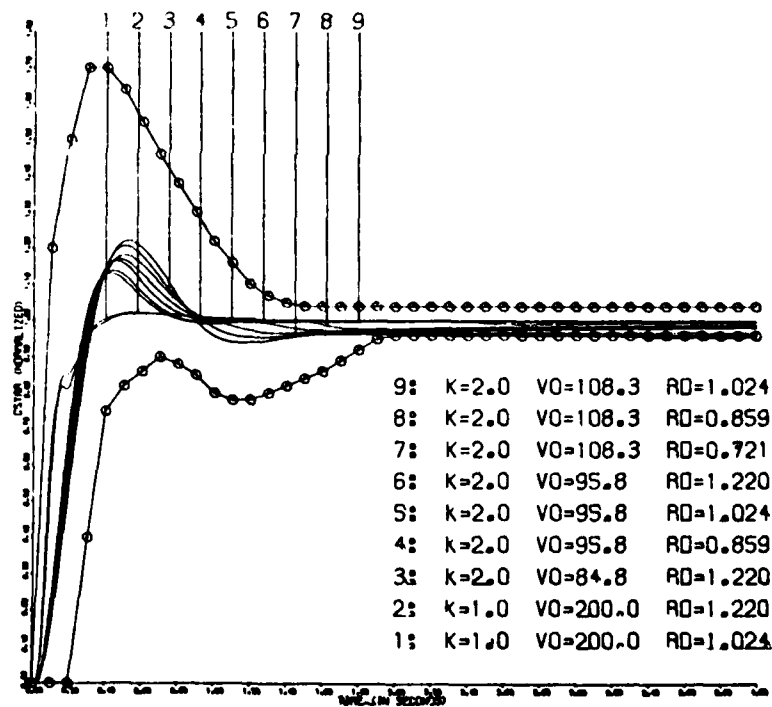
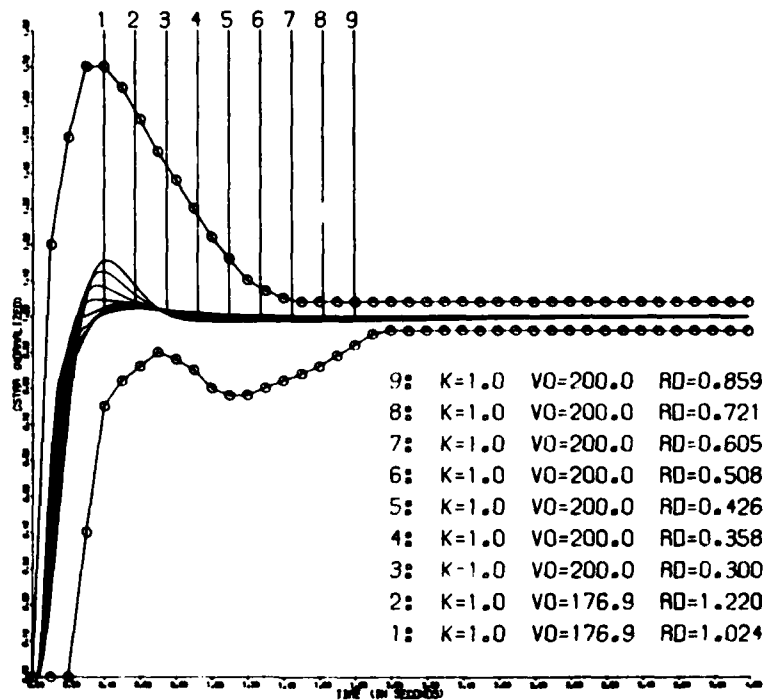
Figure 4-6. Bounds $B(\omega)$ on $G(j\omega)$ and $G(j\omega)$ chosen.

It has been shown [11] that G_{opt} lies on $B(\omega)$ at all ω and that G_{opt} exists and is unique. The design of a practical $G(s)$ to satisfy the bounds is somewhat of an art [7]. For a given skill in the art, the greater the number of poles and zeros of G , the closer one can get to the optimum, so there is trade-off between complexity and bandwidth. Here, we chose simply by cut and try $G(s) = (1 + .2s)/s(1 + .033s^2)(1 + .002s + 10^{-4}s^2)$ with very modest bandwidth, Figs. 4-3, 6. A much simpler $G(s)$ could have been chosen with larger bandwidth. The designer must make his own trade-off. Ref. 7 offers some advice on the shaping of a function to satisfy a set $\{B(\omega)\}$ in the Nichols chart.

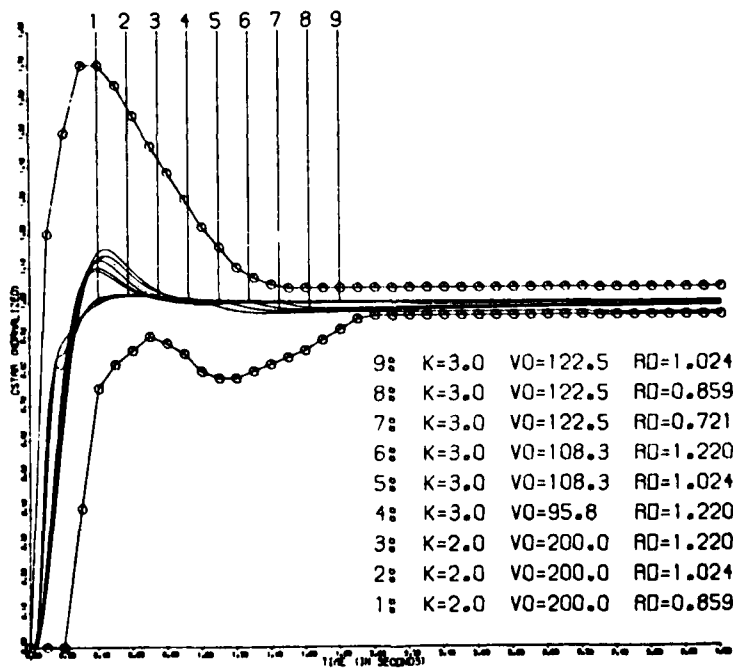
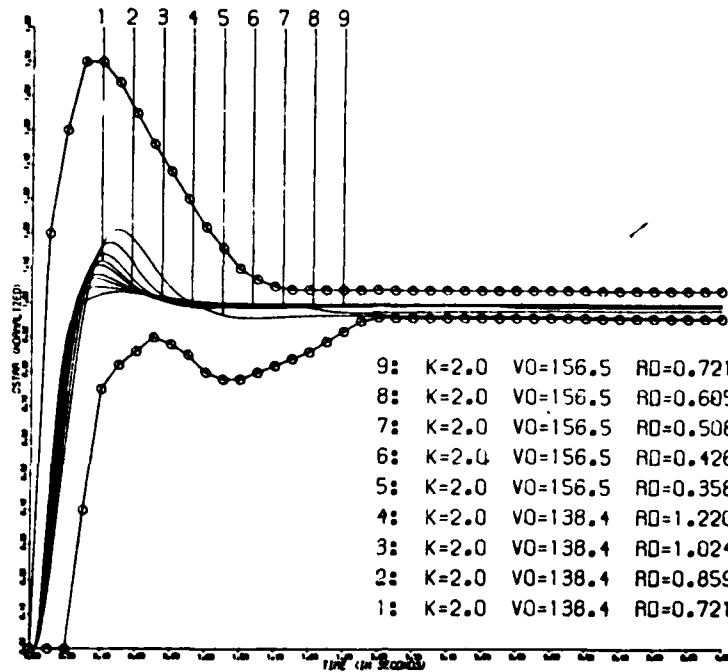
Design of $F(s)$. $G(s)$ only guarantees that $\Delta|T(j\omega)| \leq A_2(\omega) - A_1(\omega)$ of Fig. 4-3, e.g., at $\omega = 10$, the actual change in $|L(j10)/(1 + L(j10))|$ is from -7 db to 4 db, while from Fig. 4-3, the permitted change in $|T(j10)| = |FL/(1 + L)|$ is from -15 to 2.8 db. Hence, any value of $|F(j10)| \in [-8, -1.2 \text{ db}]$ is acceptable. In this way, upper and lower bounds on $|F(j\omega)|$ are obtained and $F(s)$ is chosen to satisfy them, which is also somewhat of an art. In this example, a satisfactory $F(s) = (1 + .33s)(1 + .05s)/(1 + .25s)(1 + .2s)(1 + .0125s)^2$, see Fig. 4-3.

4.2.3 Design Simulation

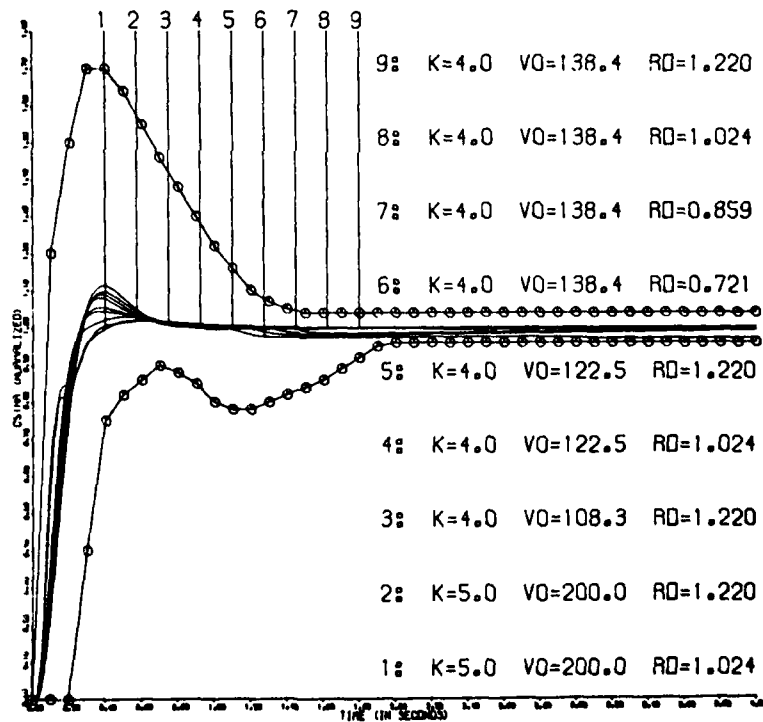
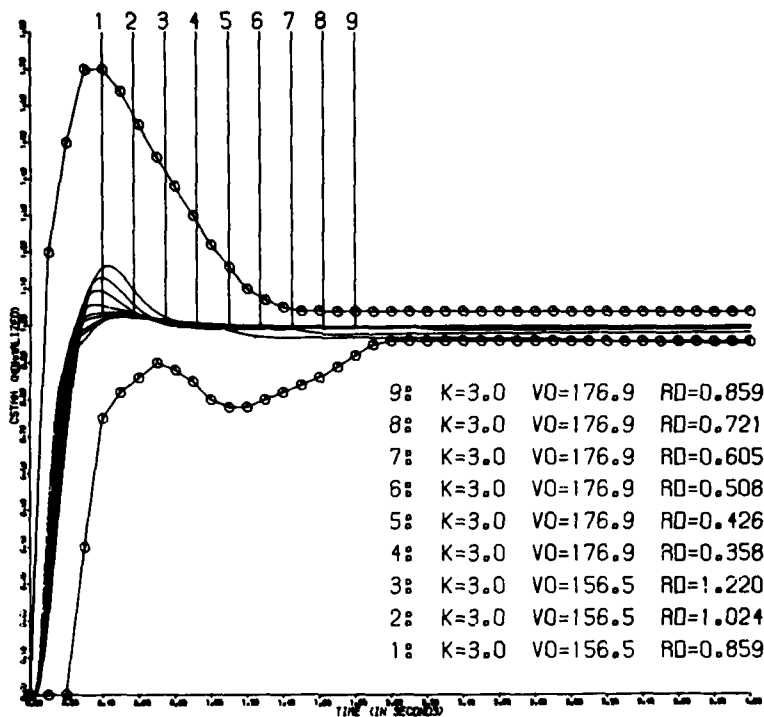
The nonlinear system was simulated and its response found for several hundred command inputs and gust disturbances. Typical (68) responses to c^* step commands are shown in Fig. 4-7 a to h for various combinations of V_0 , ρ and step (k) values. The transient response of $\alpha(t)$, $\dot{\theta}(t)$ etc., depend, of course, on the values of k , ρ , V_0 . Two sets of these are shown in Figs. 4-8 a, b, with Fig. 8a depicting very large $\alpha(t)$ excursion, for which the $C_{ij}(\alpha)$ in Fig. 4-2 are in strongly nonlinear



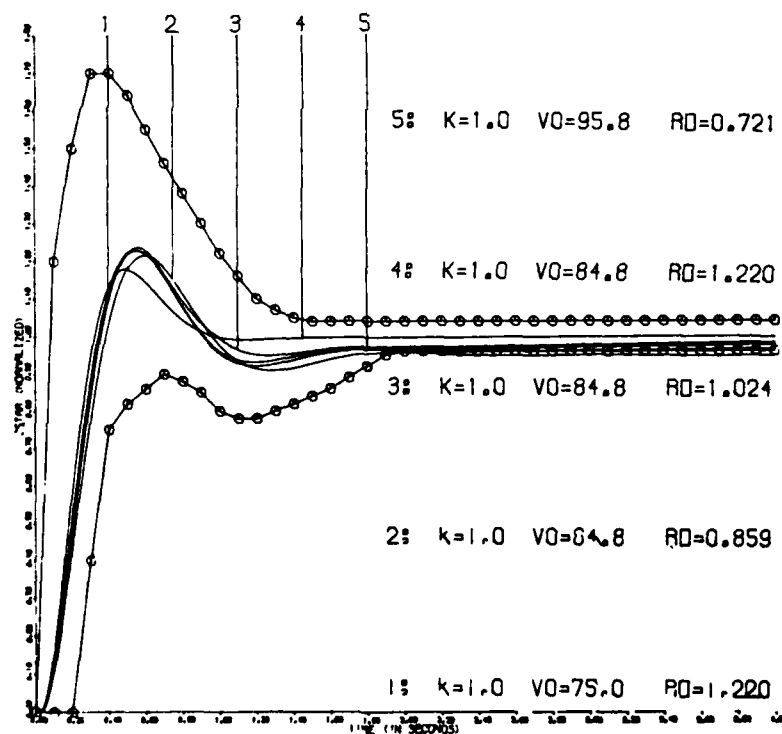
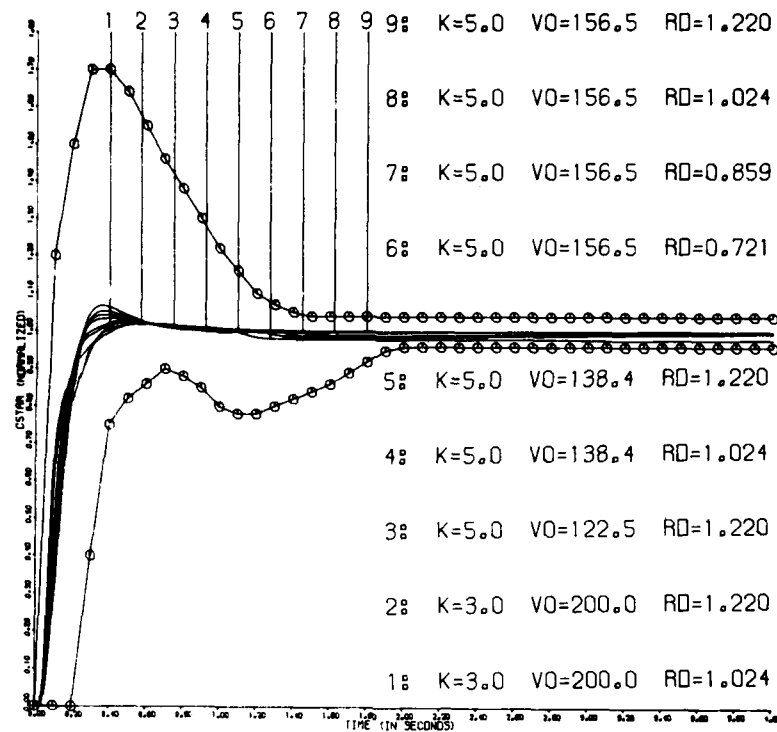
Figures 4-7 a, b. Simulation results. Response to step command of c^* , magnitude K.



Figures 4-7 c, d. Simulation results. Response to step command of c^* , magnitude K.



Figures 4-7 e, f. Simulation results. Response to step command of c^* , magnitude K.



Figures 4-7 g, h. Simulation results. Response to step command of c^* , magnitude K .

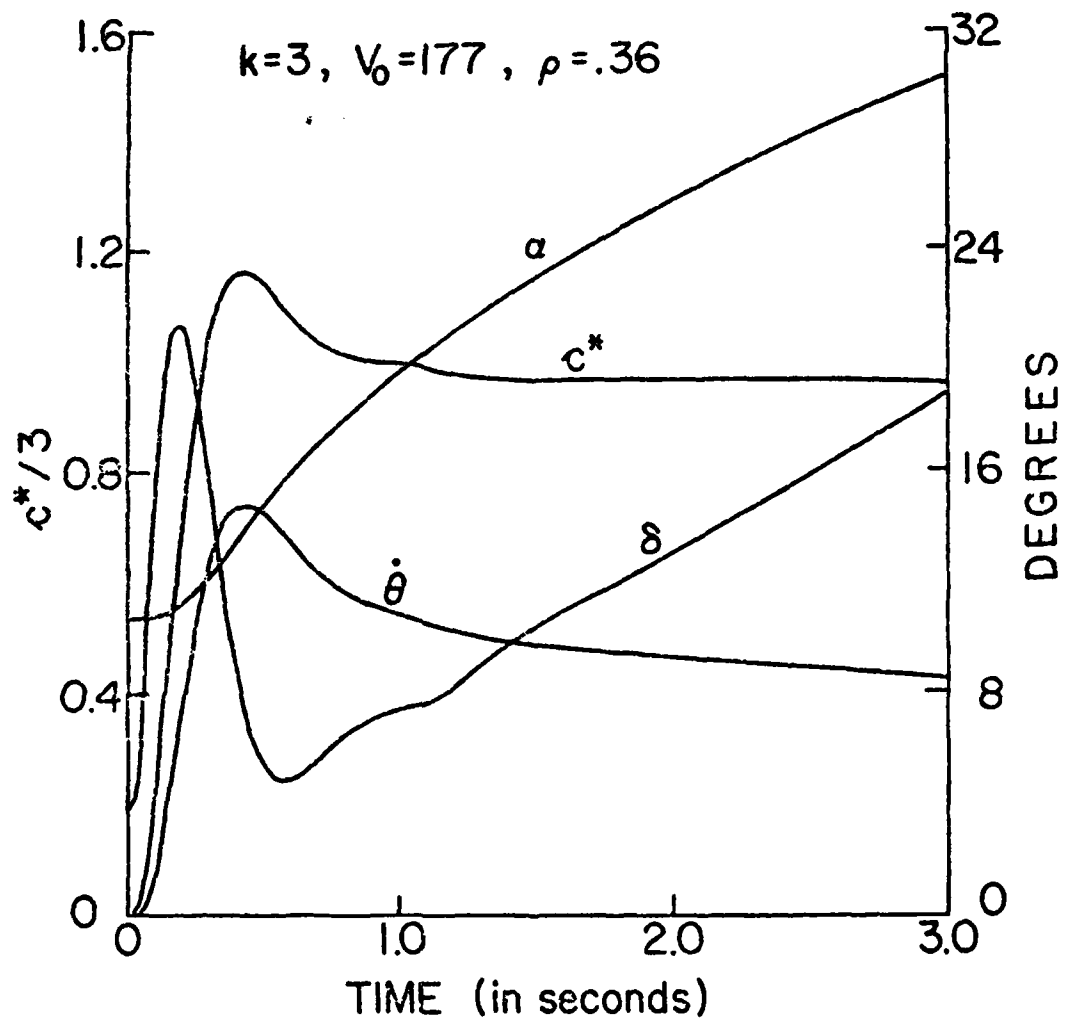


Figure 4-8 a. Responses of $\alpha(t)$, $\dot{\theta}$, δ , c^* .

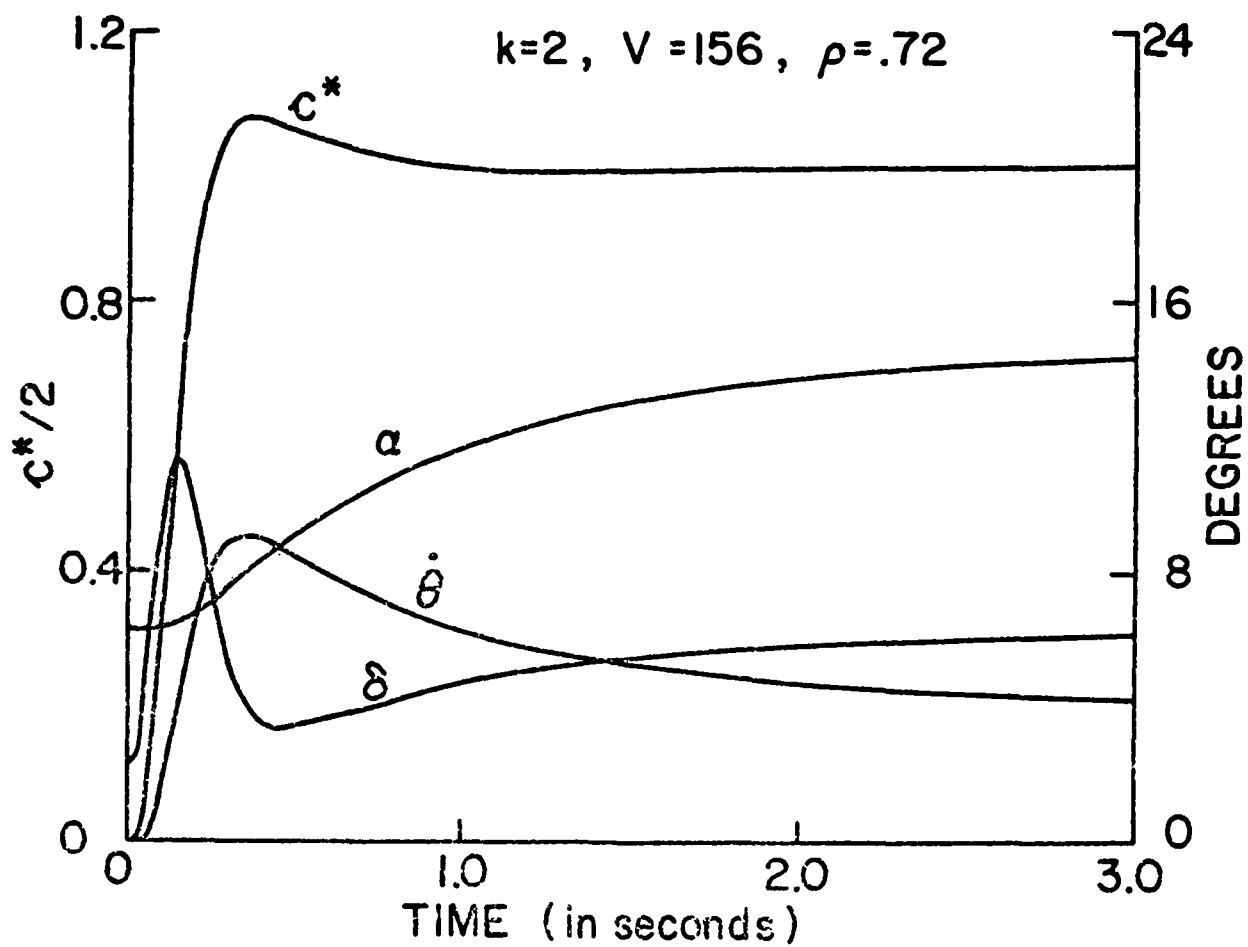


Figure 4-8 b. Responses of $\alpha(t)$, $\dot{\theta}$, δ , c^* .

ranges, These are the inputs for which the system was designed, and for which guarantees can be made. Out of the several hundred cases simulated in a very few cases (Fig. 4-7 h), there was very slight excursion out of the bounds. It is possible to include in the design other inputs and gust disturbances, with specified response tolerances - and then guarantees can be made for these as well. The response to other inputs is nevertheless found here to be also quite satisfactory. This is typical of the design, i.e., the system is not very sharply tuned to the class of inputs used in the design execution. There is reasonable response continuity to other inputs.

Some responses to very large c^* step commands causing hard saturation are shown in Fig. 4-9 a, b. Response to Gust Disturbances. The gust input was modelled by replacing α in (4.3) by $\alpha = \tan^{-1} \frac{u}{V_0} + \alpha_{gust}$. Two kinds of α_{gust} were used. In one α_{gust} is a half-sine wave of amplitude $20/V_0$ radians and half-period $THALF \in [.2, 2] \text{sec}$. Some results are shown in Figs. 4-10 a to c. In (a) the gust begins precisely at the instant of application of simultaneous c^* step commands. The second kind in Fig. 4-11 a-d, is stochastic gaussian with power spectrum $k/(1+\omega^2)V_0^2$ and $(\alpha_{gust})_{rms} = 6/V_0$ radians. Examples of responses to a single square wave c^* command with equal positive and negative values k and total duration $2 THALF$ are shown in Fig. 4-12 a to c.

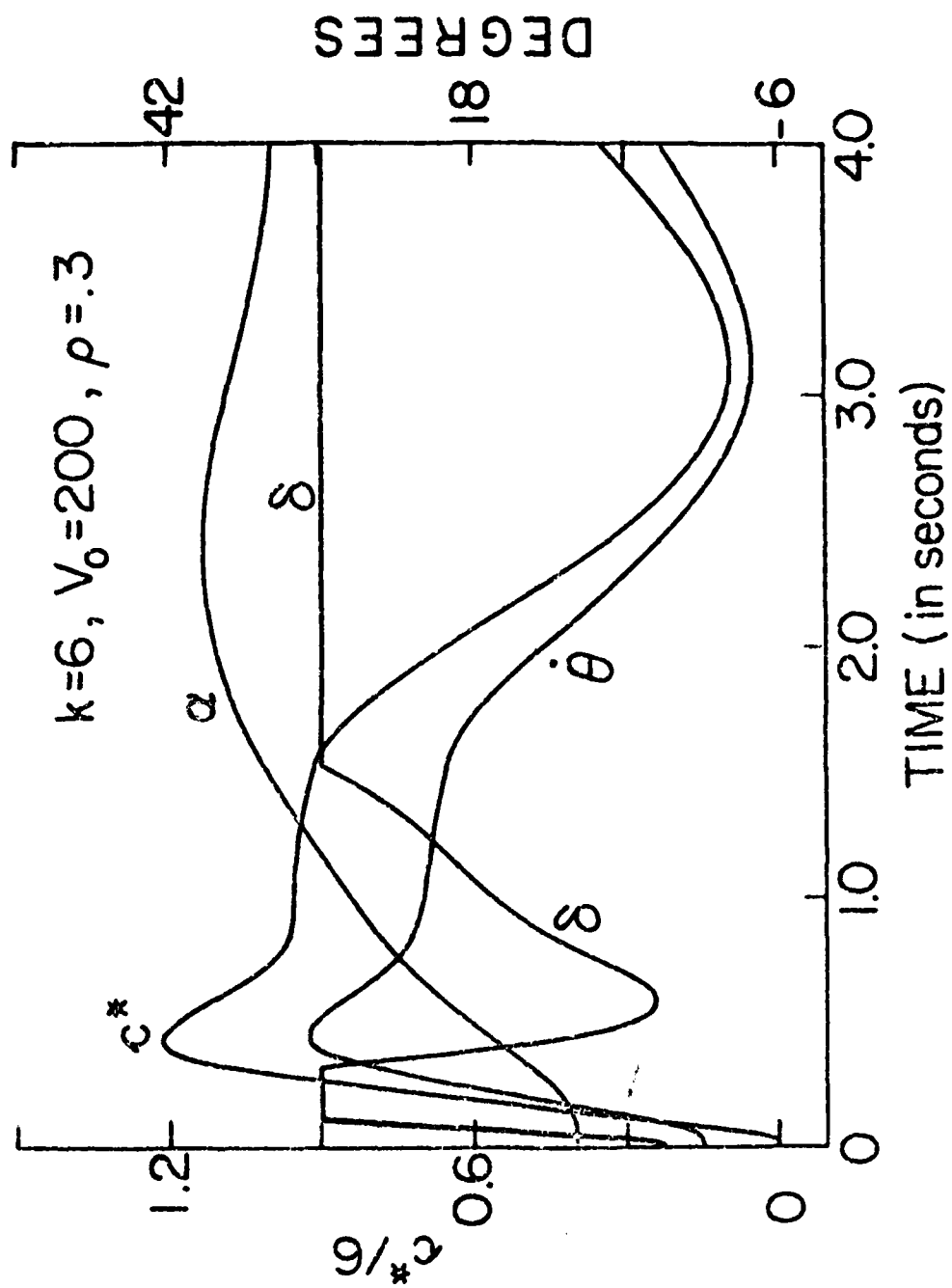


Figure 4-9 a. Responses for input causing hard δ saturation.

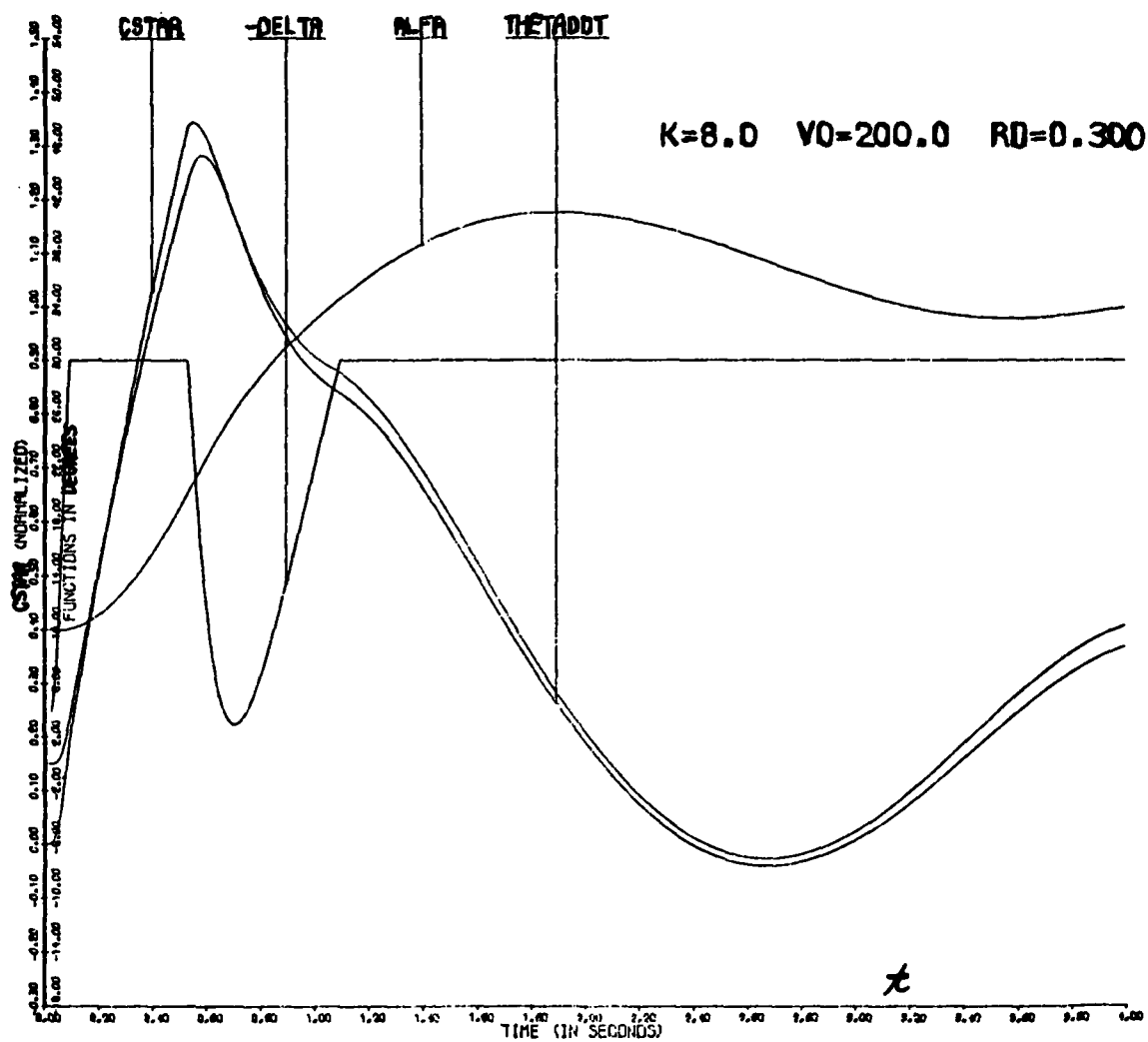


Figure 4-9 b. Responses for input causing hard δ saturation.

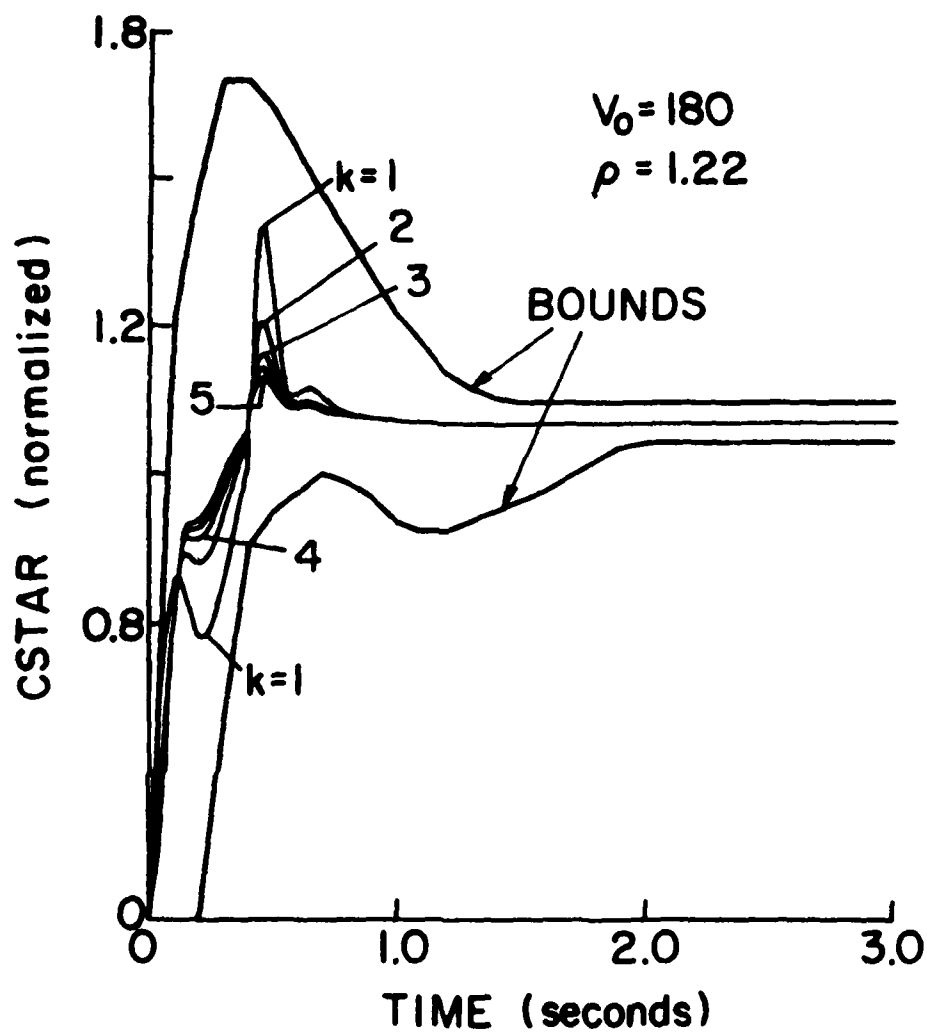


Figure 4-10 a. Responses to gust and simultaneous c^* step command.

RESULTS OF SIMULATION

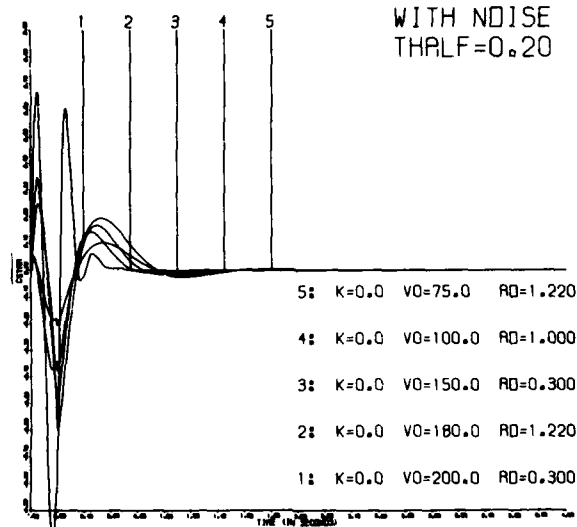


Figure 4-10 b. Responses to gust.

RESULTS OF SIMULATION

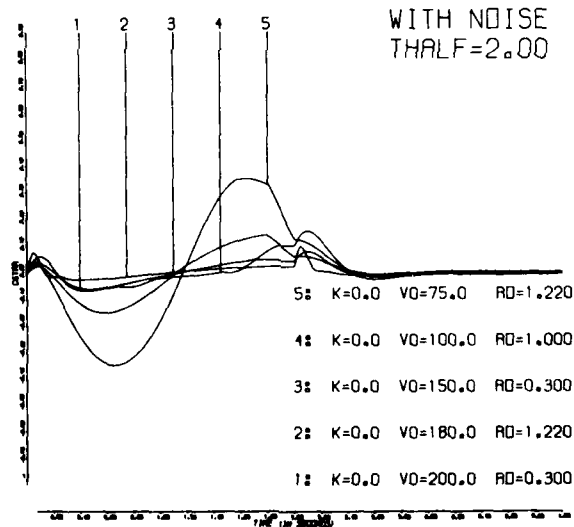


Figure 4-10 c. Responses to gust.

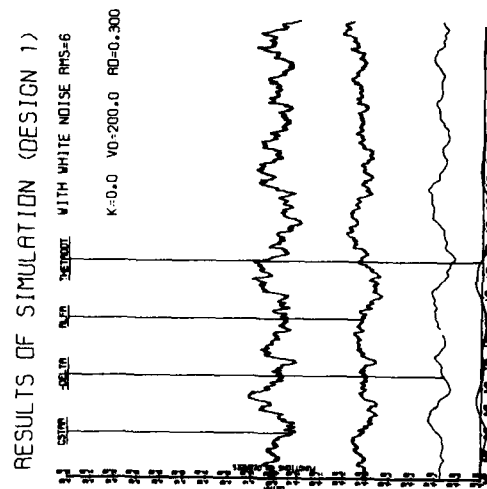
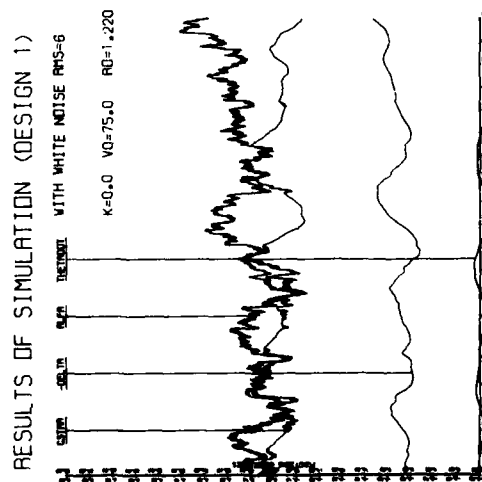
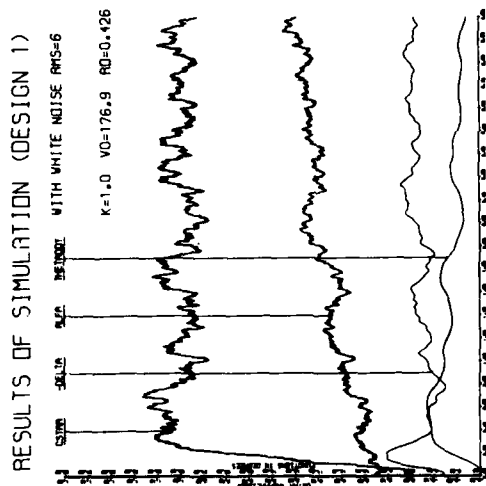
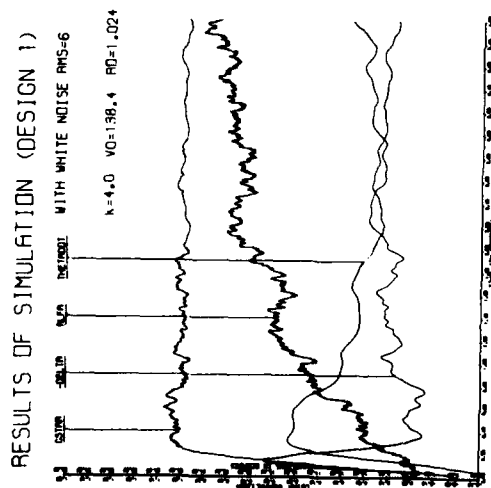
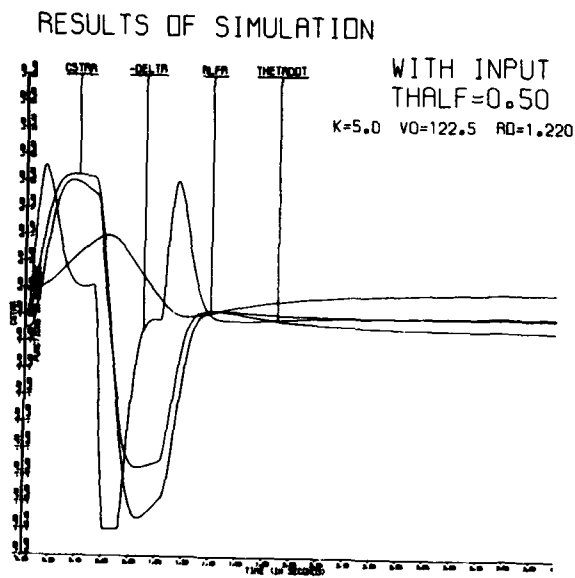
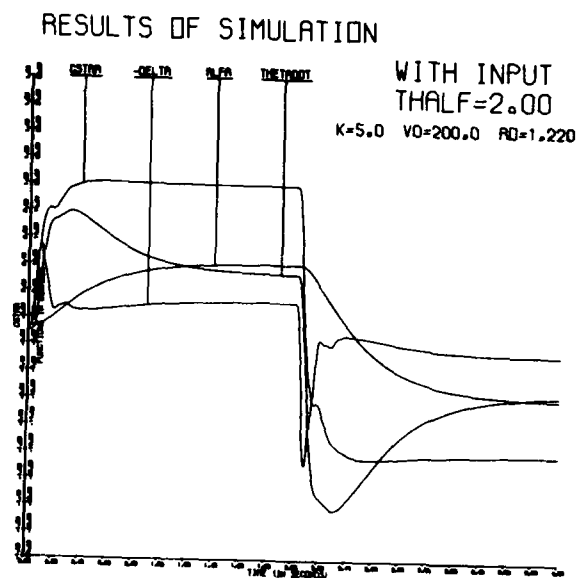


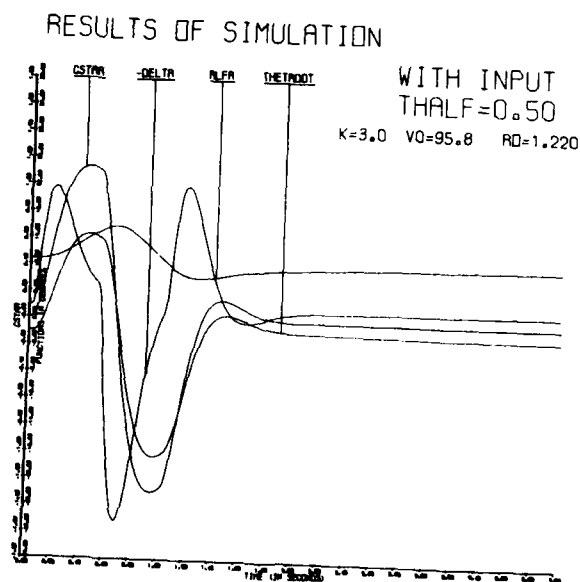
Figure 11a-d. Simulation results: response to stochastic gaussian gusts with power spectrum $\frac{k}{V_0^2(1+\omega^2)}$, $(\alpha_{\text{gust}})_{\text{rms}} = \frac{6}{V_0}$ radius; (a,b) with simultaneous c* step command input $Ku(t)$.



(a)



(b)



(c)

Figure 4-12 a-c. Simulation results: response to a single square wave c^* command with equal positive and negative $\pm K$ values and total duration 2THALF .

4.3 Discussion

A second-order model was used for $T(s)$ with excess of poles over zeros $e_T = 1$, in Step 1. This appears to be incompatible with G, F fifth order and excesses $e_G = 4$, $e_F = 2$, and P (no analytical expression but linearized (4.1-4) give second-order P) with $e_P = 0$. Strict design execution appears to require a $T(s)$ of complexity compatible with $T = FGP/(1+GP)$. Note, however, that in Step 1, the model of $T(s)$ is used only to generate a set which covers the range of a priori specified acceptable outputs. Any $T(s)$ model which achieves this is clearly satisfactory, and the simpler the better. The designer can later choose the complexity of $G(s)$, $F(s)$, with no regard for that of the $T(s)$ model used in Step 1.

The class of applicable nonlinearities has been defined implicitly in Ref. 4, but one very large class can be defined explicitly. Let $D_1 y(t) = D_2 x(t)$ with D_1, D_2 operators which may be nonlinear, uncertain and time-varying, e.g.

$$D_1 y = M(\ddot{y})(\dot{y})^{.5} \operatorname{sgn} \dot{y} + \frac{A+Bte^{-\alpha t}}{E+ Ft} \dot{y}^2 |y|^n + Hy^2$$

$$E \in [1, 5], \quad F \in [.5, 4], \quad A \in [-3, 6], \quad \alpha \in [.5, 1.5]$$

$$B \in [-3, 2], \quad H \in [-4, 1], \quad n \in [.5, 2], \quad M \in [1, 5].$$

The range of M must be of the same sign. All OK y and $D_1 y$ must be bounded for all t in $[0, \infty]$ and $D_1 y$ must exist. Hence y must be twice differentiable except, at most, at a countable number of points. Then $D_1 y \triangleq \psi(t)$ is known and there must exist a unique solution for x in $D_2 x = \psi(t)$. The solution must be bounded for all $t \in [0, \infty]$. Thus, $D_2 x = \psi(t)$ must be "bounded-input, bounded-output" stable. However, $D_1 x(t) = \psi(t)$ may be "unstable" in that a bounded $v(t)$ is allowed to

result in unbounded $z(t)$. It is only necessary that bounded $z(t)$ gives bounded $v(t)$.

It is possible that a simple linearization might do just as well in practice, but this is a matter of chance, whereas this design technique is guaranteed to work if the constraints are satisfied.

The constraint on W that P is mp, is required because only then can one guarantee that any specifications no matter how narrow ($A_2 - A_1$ arbitrarily small but nonzero in Fig. 4-3), may be satisfied for arbitrarily large but bounded parameter uncertainty (but some parameters must not change sign [23]). No such guarantee can be made for nmp P , but the problem is still solvable if the specifications are not too narrow and P is not too large [11] a set.

CHAPTER 5

A SECOND BREAKTHROUGH IN QUANTITATIVE FEEDBACK SYNTHESIS

5.1 The Multiple Input-Output (mio) Problem

A very large number of control problems involve multiple inputs and outputs, with each control input affecting all the output variables to some extent. This is certainly so in many flight control modes. In the $n \times n$ case, there is a matrix of n^2 system response functions to realize. In realistic control, the $n \times n$ plant matrix has significantly uncertain parameters. The real control problem is a quantitative one: to satisfy specified $2n^2$ tolerance sets on the $2n^2$ response functions (n^2 to command inputs and n^2 to disturbance inputs), despite the specified uncertainties in the parameters of the $n \times n$ plant relations.

There is a vast literature on this mio (often denoted as "multivariable") problem. However, nearly all of it deals with assumed perfectly known plants, so the problem treated is securing the desired closed loop response, under the constraint of a feedback structure around the perfectly known plant. Just as in the single input-output case, the quantitative aspects -- the extent of the plant uncertainties and the performance tolerances (i.e., the very reasons for using feedback) -- do not enter as design parameters. Stabilization of the resulting highly multiple-loop system is considered a major undertaking. But note that this is being done for a perfectly known plant matrix. Consider how much more difficult is this stabilization problem when the parameters of the n^2 plant functions have considerable uncertainty -- not 10% or 20%, but hundreds or thousands per cent. Furthermore,

such stabilization is only one part of the problem in genuine quantitative synthesis. Stabilization is insufficient, for one must also guarantee that each of the $2n^2$ closed loop input-output functions satisfy specified tolerances, over the range of plant parameter uncertainty.

Thus, the quantitative lti mlo problem with large uncertainty has long appeared to be intractable, except by cut and try. There has recently appeared, however, an exact synthesis technique for this problem [23; Appendix I of this report]. A highly attractive feature of this technique is that for the $n \times n$ case, it consists of designing n distinct, separate, noninteracting loop transmission functions and n^2 prefilter functions of the F type in Figure 3-1a. Thus, the $n \times n$ problem is broken up into a number of separate single-loop problems. The interaction between them is that of specifications. The tolerances on the output of one of the single-loop problems, appear as "disturbances" in a different one. It may be worthwhile to deliberately tighten the specifications on some of the outputs, and thereby decrease some loop bandwidths needed, without increasing any others. Sometimes there is trade-off, in that such tightening decreases some but increases others. However, these do not affect the basic isolation and noninteraction of the separate single-loop designs. They affect the optimality of the designs in terms of loop-bandwidths needed to do the job.

The above is a very desirable property of the design technique. The stabilization of a feedback system containing a highly interacting, highly uncertain $n \times n$ lti plant becomes one of stabilizing n distinct, separate, noninteracting single loops. But even more than that -- the quantitative synthesis problem is solved. The apriori assigned performance specifications on the $2n^2$ response functions are achieved over the entire range of

parameter uncertainty. There is no need for design iteration after the separate single input-output systems have been designed. This is for minimum-phase plants. In the nonminimum-phase case, the performance tolerances must be compatible with the nonminimum-phase character of the plant, just as in single input-output systems. The research work leading to the above results was performed under AFOSR sponsorship [23], but because of its importance in flight control, is reproduced here as Appendix I. Since then we have gained some experience with the technique and learned how to achieve the trade-offs mentioned above.

5.2 Extension to Nonlinear Uncertain Multiple Input-Output Plants

The nonlinear design philosophy of Chapter 4 can be combined with that of Section 5.1, giving a quantitative synthesis technique for highly uncertain nonlinear $n \times n$ multiple input-output plants. The essential features of both synthesis methods are retained. Because of uncertainty, there is not one set of $n \times n$ nonlinear plant relations, but an infinite class of such sets. This class W is replaced by an infinite class P of $n \times n$ matrices of linear time invariant relations. P is equivalent to W with respect to the sets of acceptable outputs. To do this the nonlinear relations must be solved backwards to find the plant inputs required to give the acceptable outputs. The computer is an essential tool. Once P is available, the problem becomes a quantitative linear time-invariant multiple input-output one, for which the technique of Appendix I may be used. Section 5 of Appendix I presents a somewhat more detailed outline of the procedure.

5.3 Application of Nonlinear and Multivariable Synthesis Techniques to

Flight Control

In many of the important operating modes, the flight control problem is primarily one of regulation and control despite large uncertainty. It is one of achieving desired trajectories as a function of time. It is not one of minimizing some quadratic functional of states and control inputs. In fact, in certain situations one wants to drive the control variables as hard as possible. The justification nevertheless for use of optimal control despite this and despite its ignoring parameter uncertainty and performance specifications, is only that it provides a trial solution. But it is clearly not a synthesis tool developed for the flight control problem. On the other hand, the quantitative synthesis techniques outlined in Chapters 2, 3, 5 and illustrated in Chapter 4 for a detailed nonlinear problem, are very close, almost tailored, to the flight control problem. For the first time in feedback control history, there are available precise rigorous synthesis techniques to cope simultaneously with all the following important factors in the flight control problem:

1. time and frequency domain tolerances on the output variables;
2. large parameter uncertainties;
3. highly nonlinear plant relations;
4. strongly interacting multiple input-output plants;
5. tolerances which are functions of the command inputs, i.e., a desired nonlinear closed-loop system.

REFERENCES

1. Bode, H.W., Network Analysis and Feedback Amplifier Design. Van Nostrand, New York, 1945.
2. Horowitz, I. and Shaked, U., Superiority of transfer function over state-variable methods in linear, time invariant feedback system design, IEEE Trans. on Auto. Control, AC-20, 1975, 84-97.
3. Horowitz, I., A synthesis theory for linear time-varying feedback systems with plant uncertainty, IEEE Trans. on Auto. Control, AC-20, 1975, 454-463.
4. Horowitz, I., Synthesis of feedback systems with non-linear time-varying uncertain plants to satisfy quantitative performance specifications, Proc. IEEE, 64, 1976, 123-130.
5. Horowitz, I., Golubev, B., and Kopelman, T., Flight control design based on nonlinear model with uncertain parameters, to appear in AIAA J. Guidance and Control, Jan.-Feb. 1980.
6. Horowitz, I., Synthesis of Feedback Systems. Academic Press, New York, 1963.
7. Horowitz, I. and Sidi, M., Synthesis of feedback systems with large plant ignorance for prescribed time domain tolerances, Int. J. Control, 16, 1972, 287-309.
8. Krishnan, K.R. and Cruickshank, A., Frequency domain design of feedback systems for specified insensitivity of time-domain response to parameter variation, Int. J. Control, 25, 1977, 609-620.
9. Sidi, M., Synthesis of feedback systems with large plant ignorance for prescribed time-domain tolerance, Ph.D. dissertation, Dept. Applied Math., Weizmann Institute of Science, Rehovot, Israel.
10. Horowitz, I., Optimum loop transfer function in single-loop minimum-phase feedback systems, Int. J. Control, 18, 1973, 97-113.
11. Horowitz, I. and Sidi, M., Optimum Synthesis of non-minimum phase feedback systems with plant uncertainty, Int. J. Control, 27, 1978, 361-386.
12. Rosenbaum, P., Reduction of the cost of feedback in systems with large parameter uncertainty, Ph.D. Thesis, Weizmann Institute of Science, Israel, 1977.
13. Horowitz, I. and Rosenbaum, P., Nonlinear design for cost of feedback reduction in systems with large parameter uncertainty, Int. J. Control, 21, 1975, 977-1001.

14. Horowitz, I., Smay, J. and Shapiro, A., A synthesis theory for self-oscillating adaptive systems (SOAS), Automatica, 10, 1974, 381-392.
15. Horowitz, I., Smay, J. and Shapiro, A., A synthesis theory for the externally excited adaptive system (EEAS), IEEE Trans. AC-19, No. 2, April, 1974.
16. Horowitz, I. and Shapiro, A., A synthesis theory for multiple-loop oscillating adaptive systems, to appear in Int. J. Control, 1979.
17. Krishnan, K.R. and Horowitz, I., Synthesis of a non-linear feedback system with significant plant-ignorance for prescribed system tolerances, Int. J. Control, 19, No. 4, 1974, 689-706.
18. Horowitz, I. and Sidi, M., Synthesis of cascaded multiple-loop feedback systems with large plant parameter ignorance, Automatica, 9, 1973, 589-600.
19. Wang, Te-Shing, Quantitative synthesis of multiple-loop feedback systems with large uncertainty, Ph.D. Thesis, Dept. of Applied Mathematics, Weizmann Institute of Science, Rehovot, Israel, 1979.
20. Horowitz, I., and Wang, T.S., Quantitative synthesis of multiple-loop feedback systems with large uncertainty, to appear in Int. J. System Science, 1980.
21. Wang, B.C., Synthesis of multiple loop feedback systems with plant modification, Ph.D. Thesis, University of Colorado, Boulder, Colorado, 1978.
22. Horowitz, I. and Wang, B.C., Quantitative synthesis of uncertain cascade feedback systems with plant modification, to appear in Int. J. Control, 1980.
23. Horowitz, I., Quantitative synthesis of uncertain multiple input-output feedback systems, to appear in Int. J. Control, 1979 (see Appendix to this report).
24. Toble, H., Elliott, E., and Malcolm, L., A new longitudinal handling qualities criterion, Boeing Co. Commercial Airplane Division, Report TL 693.N3, May 1966.
25. Kisslinger, L., et al., Survivable flight control system, Interim Report 1, McDonnell Douglas, May 1971, p. 12, Table 1.
26. Laacke, F., and Miller, C., Comparison of the basic F4E and the slotted F4E Stall/Near Stall/Spin characteristics, McDonnell Douglas Report MDC A 2181, December 18, 1969.

APPENDIX

QUANTITATIVE SYNTHESIS OF UNCERTAIN MULTIPLE INPUT-OUTPUT FEEDBACK SYSTEM[†]

Isaac Horowitz^{*}

ABSTRACT

There is given an n input, n output plant with a specified range of parameter uncertainty and specified tolerances on the n^2 system response to command functions and the n^2 response to disturbance functions. It is shown how Schauder's fixed point theorem may be used to generate a variety of synthesis techniques, for a large class of such plants. The design guarantees the specifications are satisfied over the range of parameter uncertainty. An attractive property is that design execution is that of successive single-loop designs, with no interaction between them and no iteration necessary. Stability over the range of parameter uncertainty is automatically included.

By an additional use of Schauder's theorem, these same synthesis techniques can be rigorously used for quantitative design in the same sense as above, for $n \times n$ uncertain nonlinear plants, even nonlinear time-varying plants, in response to a finite number of inputs.

^{*} Cohen Professor/^{of} Applied Mathematics, Weizmann Institute of Science, Rehovot, Israel, and Professor of Electrical Engineering, University of Colorado, Boulder. This research was supported in part by the U.S. Air Force Office of Scientific Research, Grant No. AFOSR-76-2946B at the University of Colorado.

[†] Note: The Appendices to this paper are omitted here. They are available in [23].

QUANTITATIVE SYNTHESIS OF UNCERTAIN MULTIPLE INPUT-OUTPUT FEEDBACK SYSTEMS

1. INTRODUCTION

There is great interest in multiple input-output (mio) feedback systems, for obvious reasons. A great deal of significant work (too numerous to list but [1-10] are representative and include bibliographies) has been done, primarily in the realization and properties of the closed-loop input-output relations, under the constraint of a feedback structure around the known, fixed mio "plant." There has been notable work done with uncertain inputs, but again only with fixed, known plants. Of course, plant uncertainty is always implicit, if only because of the usual approximations required to obtain a linear time-invariant model.

In any case, there does not exist as yet any "quantitative synthesis" technique for the mio problem with significant plant uncertainty, even for the linear time-invariant case. By "quantitative synthesis" is meant that there are given quantitative bounds on the plant uncertainty, and quantitative tolerances on the acceptable closed-loop system response. The objective is to find compensation functions which guarantee that the performance tolerances are satisfied over the range of the plant uncertainty. In "quantitative design," one guarantees that the amount of feedback designed into the system is such as to obtain the desired tolerances, over the given uncertainty range. In other designs, the amount of feedback may be more or less than necessary--it is a matter of chance. The practical experienced designer may find the

latter approach sufficient. However, a scientific theory of feedback should certainly include quantitative design techniques.

In this paper it is shown how Schauder's fixed point theorem can be used to generate a variety of precise quantitative mio synthesis techniques suitable for various problem classes. An outstanding feature of each synthesis procedure is that it consists of a succession of direct (no iterations necessary) single-loop design steps. Furthermore, by a second use of Schauder's theorem, the techniques are rigorously applicable to quantitative synthesis of nonlinear uncertain mio feedback systems. This paper concentrates on existence proofs but a 2×2 example is included.

1.1 Preliminary Statement of a Linear Time Invariant MIO Problem

In Fig. 1, $P = [p_{ij}(s)]$ is a $n \times n$ matrix of the plant transfer functions in the form of rational functions, each with an excess $e_{ij} > 0$ of poles over zeros, and with a bounded number of poles. The $p_{ij}(s)$ are functions of q physical parameters, with m an ordered real q -tuple sample of their values. $M = \{m\}$ is the class of all possible parameter combinations. The elements of the $n \times n$ lti compensation rational transfer function matrices $F = [f_{ij}(s)]$, $G = [g_{ij}(s)]$ are to be chosen practical (each with an excess of poles over zero). They must ensure that in response to command inputs the closed-loop transfer function matrix $T = [t_{uv}(s)]$ (of $c = Tr$) in Fig. 1 where c, r are the $n \times 1$ matrices (vectors) of system outputs and inputs, respectively, satisfy conditions of the form

$$0 < A_{uv}(\omega) \leq |t_{uv}(j\omega)| \leq B_{uv}(\omega), \forall m \in M \quad (1)$$

If the $t_{uv}(s)$ have no poles or zeros in the right half-plane (are stable and minimum-phase), then $t_{uv}(s)$ is completely determined by $|t_{uv}(j\omega)|$, so (1) suffices (Bode 1945). It has been shown (Horowitz 1976) that time-domain tolerances of the form

$$u_1^v(t) \leq \frac{d^v \hat{c}(t)}{dt^v} \leq u_2^v(t)$$

$v = 0, 1, \dots, n_1$ any finite number, can be satisfied by means of tolerances like (1) on $|c(j\omega)|$, where $c(s) = \int \hat{c}(t)$. The writer finds it much more convenient to develop the synthesis theory in the frequency domain, and the above proves its sufficiency for time-domain synthesis.

This presentation concentrates on the command response problem, but the same ideas can be used to handle the quantitative disturbance response problem under plant uncertainty, as will be shown in Sec. 6. The constraints on the plant and the specifications are introduced as needed, in order to clarify the reasons for their need.

2. DERIVATION OF SYNTHESIS TECHNIQUE

In Fig. 1, there are available n^2 loop transfer functions in $L = [l_{ij}(s)] = PG$, and $n^2 f_{ij}$ in F for satisfying the tolerances (1) on the $n^2 t_{ij}$. But in the expansion of $T = [t_{ij}(s)] = (I + L)^{-1}LF$, each $t_{ab}(s,m)$ ($m \in M$) is a function of all the $l_{ij}(s,m)$ each uncertain, resulting in very complicated expressions for t_{ab} and making direct quantitative synthesis seemingly impossible--at least so far unsuccessful. The objective here is to convert each $t_{ab}(s,m)$ design problem into an equivalent single-loop problem with uncertainty. This is done for each t_{ab} , by lumping all the other inter-

acting t_{ij} variables into an 'equivalent disturbance', as follows.

In Fig. 1, $c = PG(Fr - c)$, so

$$(P^{-1} + G)c = GFr. \quad (2)$$

Hence, the following restriction on P:

$$(P1): \Delta(s) \triangleq \text{determinant } P(s) \neq 0, \forall s \in M.$$

Let $r_v \neq 0$ and $r_i \equiv 0, i \neq v$, so the resulting $c_j(s) = t_{jv}(s)r_v$. Let

$$P^{-1} = [p_{ij}(s)]. \quad (3)$$

The u th element of (2) is then

$$r_v(s) \sum_{i=1}^n (p_{ui} + g_{ui})t_{iv} = \sum_i g_{ui}f_{iv}.$$

To simplify the presentation, we take $g_{ui} \equiv 0$ for $u \neq i$ (although in practice it may be useful not to do so). Then letting $r_v(s) = 1$, the last equation can be written as

$$t_{uv} = \frac{\frac{1}{p_{uu}} g_{uu} f_{uv} - \frac{d_{uv}}{p_{uu}}}{1 + \frac{g_{uu}}{p_{uu}}} \triangleq \tau_{uv} - \tau_{duv} d_{uv} \quad (4a)$$

$$d_{uv} = \sum_{i \neq u} p_{ui} t_{iv} \quad (4b)$$

This corresponds precisely to the single-loop problem of Fig. 2, with

$p_{uve} = 1/p_{uu}$. Of course, the t_{iv} in d_{uv} of (4b) are not known but the bounds (1) on $|t_{iv}|$ are known, generating a set $D_{uv} = \{d_{uv}\}$. We define the extreme d_{uv}

$$|d_{uve}| = \sup_M \sum_{i \neq u} |p_{ui}| |B_{iv}|, B_{iv} \text{ of (1)} \quad (5)$$

Suppose we can find $g_{uu}(s)$ and $f_{uv}(s)$, such that in the notation of (4,5)

$$0 < |\tau_{uv}| \pm |\tau_{duv}| |d_{uve}| \in [A_{uv}, B_{uv}], \forall m \in M \quad (6)$$

Then the magnitude of the right side of (4a) $\in [A_{uv}, B_{uv}]$ for all $m \in M$ and for all possible combinations of t_{iv} ($i \neq u$) which satisfy (1). Suppose this is so $\forall u, v$ combinations, and the other Schauder conditions of Sec. 2.1 are satisfied. Then Schauder's fixed point theorem can be used to prove that these same n g_{uu} and n^2 f_{iv} are a solution to the synthesis problem (1).

2.1 Application of Schauder's Fixed Point Theorem

This theorem states that a continuous mapping of a convex, compact set of a Banach space into itself, has a fixed point (Kantorovich and Akilov 1964). We define the Banach space to be the n^2 $C[0, \infty]$ product space denoted here by $C(n^2)$, with norm = \sum individual sup norms. $C[0, \infty]$ is the Banach space of real continuous functions $f(\omega)$, $\omega \in [0, \infty]$ with $\|f\| = \sup_{\omega} |f(\omega)|$. The convex compact set in each of the n^2 $C[0, \infty]$ is taken as the acceptable set of $|t_{uv}(j\omega)|$ satisfying (1), denoted by $\{h_e(\omega)\} = H_{uv}$. Additional constraints have to be assigned to the $h_e(\omega)$ in order that each H_{uv} set is compact and convex in $C[0, \infty]$. These constraints have been justified in detail in (Horowitz 1975) and are therefore only summarized here. If each set is convex and compact in $C[0, \infty]$, their n^2 product set denoted by $H(n^2)$ is convex and compact in $C(n^2)$.

Constraints on $H_{uv} = \{h(\omega)\}_{uv}$

1. \exists continuous functions $A_{uv}(\omega)$, $B_{uv}(\omega)$ with properties of (1) as bounds on $h(\omega)$
2. $h'(\omega)$ is uniformly bounded: $\exists K, \exists |h'(\omega)| < K, \forall h, \omega$

AD-A082 424 WEIZMANN INST OF SCIENCE REHOVOTH (ISRAEL) DEPT OF --ETC F/6 1/3
RESEARCH IN ADVANCED FLIGHT CONTROL DESIGN.(U)
JAN 80 I HOROWITZ, B GOLUBEV, T KOPELMAN AFOSR-77-3355

UNCLASSIFIED

AFFDL-TR-79-3120

NL

2
A
20 1/2



END
DATE
FILMED
4 80
DTIC

3. $h(\omega) \rightarrow 0$ as $\omega \rightarrow \infty$ in the form k/ω^e , e a fixed finite number ≥ 3 to allow

at least one excess of pole over zeros for the elements of F, G, P in Fig. 1.

These constraints guarantee (Horowitz 1975) that $h(\omega)$ can be taken as the magnitude of a function $\hat{h}(s)_{s=j\omega}$ which has no zeros or poles in the interior of the right half-plane or on the $j\omega$ axis. $\text{Arg } \hat{h}(j\omega)$ is obtained from $h(\omega)$ by any one of a number of Bode integrals (Bode 1945).

An element of $H(n^2)$ consists of n^2 positive functions on $[0, \infty]$, $h_{ik}(\omega)$.

Using any appropriate Bode integral, find the associated phase function denoted here by $\arg[h_{ik}(\omega)]$, giving the minimum-phase stable function $\hat{h}_{ik}(s)$,

$\hat{h}_{ik}(j\omega) = h_{ik}(\omega) + j \arg[h_{ik}(\omega)]$. For future use, denote this sequence of operations whereby $h(\omega)$ is transformed into $\hat{h}(j\omega)$, as the "Bode transformation" $B(h(\omega))$. Define ϕ on $H(n^2)$ by

$$\phi = (\psi_{11}, \psi_{12}, \dots, \psi_{nn}): H(n^2) \rightarrow H(n^2), \psi_{uv}(h_{11}, h_{12}, \dots, h_{nn})$$

$$= \left| \frac{g_{uu} f_{uv} - \sum_{i \neq u} P_{ui} B(h_{iv}(\omega))}{P_{uu} (1 + \frac{g_{uu}}{P_{uu}})} \right| \quad (7)$$

using for P_{ui}, P_{uu} any specific fixed $m \in M$. (Note the similarity of (7) to (4a,b)).

In Appendix 2, it is shown that g_{uu}, f_{uv} can be found such that ϕ maps $H(n^2)$ into itself. It is also necessary to prove ϕ is continuous, as follows.

ϕ is a continuous mapping

ϕ is continuous if each of its n^2 components is continuous. The first step in each mapping is $B(h_{iv}(\omega)) = \hat{h}_{iv}(j\omega)$. In (Horowitz 1975, Sec. III) it is proven that the step $h_{iv}(\omega) \rightarrow \arg h_{iv}(\omega) \hat{h}_{iv}(\omega)$ is continuous in the $C[0, \infty)$ norm. Hence,

the mappings $h_{iv}(\omega) \rightarrow h_{iv}(\omega) \cos \theta_{iv}(\omega) \triangleq \mathcal{R}_{iv}(\omega)$, $h_{iv}(\omega) \rightarrow h_{iv}(\omega) \sin \theta_{iv}(\omega) \triangleq \mathcal{X}_{iv}(\omega)$ are continuous. The denominator of (7) is a constant on $H(n^2)$, and so are g_{uu} , f_{uv} and the P_{ui} in the numerator. Thus, the numerator has the form

$$\text{Num.} = |K_a + jK_b - \sum_i (C_i + jD_i)(\mathcal{R}_i(\omega) + j\mathcal{X}_i(\omega)), j = \sqrt{-1},$$

all other terms real and only the \mathcal{R}_i , \mathcal{X}_i mappings on $H(n^2)$. Infinitesimal changes in \mathcal{R}_i , \mathcal{X}_i clearly result in similar change in Num., so Num. is continuous on $H(n^2)$ and so is each ψ_{uv} of (7) and hence ϕ . The conditions in Schauder's theorem are satisfied, so ϕ has a fixed point.

This means \exists a set of $h_{ij}(\omega)$ denoted by $h_{ij}^*(\omega)$, \ni

$$h_{uv}^*(\omega) = \left| \frac{g_{uu}f_{uv} - \sum_{i \neq u} P_{ui} \hat{h}_{iv}^*(j\omega)}{P_{uu}(1 + \frac{g_{uu}}{P_{uu}})} \right| \quad (8)$$

$u, v = 1, \dots, n$, where $\hat{h}_{iv}^*(j\omega) = B(h_{iv}^*(\omega))$.

We would now like to deduce from (8), that

$$B(h_{uv}^*(\omega)) = h_{uv}^*(j\omega) = \frac{g_{uu}f_{uv} - \sum_{i \neq u} P_{ui} \hat{h}_{uv}^*(j\omega)}{P_{uu}(1 + \frac{g_{uu}}{P_{uu}})} \quad (9 \quad ?)$$

For, if (9) is true, then by letting $\hat{h}_{uv}^*(j\omega) = t_{uv}(j\omega)$, we have recovered (4) and the $n^2 \hat{h}_{uv}^*(j\omega)$ are a solution to the mio problem for that specific $m \in M$. The solution is unique if every building block in the mio system has a unique output for any given input, which is a very reasonable condition. This makes

it unnecessary to prove that there are no transitions from (8) to an expression similar to (9) but with right half plane poles and/or zeros. Since m is any element of M , this is true for all $m \in M$ (of course with a different set of \hat{h}_{uv}^* for each m).

The step from (8) to (9) is a crucial one and must be justified with great care. Given an analytic function $\phi(s)$, there is an infinitude of $\psi(s)$ such that $|\phi(j\omega)| = |\psi(j\omega)|$, $\omega \in [0, \infty]$, e.g.

$$\psi(s) = \phi(s) \frac{(1 - \tau_1 s)(1 + \tau_2 s)}{(1 + \tau_1 s)(1 - \tau_2 s)}$$

But $\phi(s) \neq \psi(s)$ even though $|\phi(j\omega)| \equiv |\psi(j\omega)|$. But suppose we know from other sources that $\phi_1(s)$ has no right half plane zeros or poles, then given

$|\phi_1(j\omega)| \equiv M(\omega)$ a magnitude function which is Bode transformable, we can conclude that $\phi_1(j\omega) \equiv B(M(\omega)) = \hat{M}(j\omega)$. Hence, to justify (9) we must prove that the expression inside the vertical bars in (8) has no right half-plane zeros or poles. The pole part is easy, because $1 + g_{uu}/P_{uu}$ is obviously designed to have no right half-plane zeros; certainly g_{uu} , f_{uv} won't be assigned any such poles; $\hat{h}_{iv}(s)$ doesn't have any by definition, and P_{ui} is not allowed any such poles--see Sec. 3.1. To prove the zero part, note that from (6) and Rouché's theorem, the number of zeros of the right side of (9) in the right half-plane, equals such number of

$$\frac{g_{uu} f_{uv}}{P_{uu} (1 + \frac{g_{uu}}{P_{uu}})},$$

which is easily made zero in the single-loop synthesis steps (if P_{uu} has no right half-plane poles, a condition necessary for other reasons--see Sec. 3.1). Thus, the expression inside the bars in (8) has no right half-plane poles or zeros, justifying (9). This is a very valuable result. The problem of stabilizing a highly uncertain $n \times n$ mio system is automatically disposed of in the synthesis procedure, which is furthermore one of designing n single-loop transmission functions.

It is worth noting that even if the above proof were not available, it would not be disastrous for this synthesis theory. It would only be necessary to guarantee that at one $m \in M$, the system is stable and minimum-phase. For then, this would be so $\forall m \in M$, because by the continuity of the poles (and zeros) with respect to the parameters, the right side of (8) would have to be infinite (zero) at some ω , in order that for some $m \in M$ the system should be unstable (or have a right half-plane zero). However, the synthesis procedure by definition precludes this. And it is a relatively easy matter to guarantee the desired conditions at one $m \in M$.

3. CONSTRAINTS ON MIO PLANT

The above results hinge on our ability (a) to find g_{uu} and f_{uv} to satisfy (6) $\forall \omega$, all u, v pairs and all $m \in M$ (b) that each equivalent single-loop design is stable and minimum-phase $\forall m \in M$. These lead to constraints on the mio plant, obtained by applying single-loop design theory to achieve (a,b). Appendix 1 gives an existence theorem for single-loop design. The first part of the design (see Appendix A3) gives bounds on the nominal loop transmission which is g_{uu}/P_{uu0} of (4a), where P_{uu0} is the 'nominal' associated with a nominal $m_0 \in M$.

These bounds must be satisfied in order that a specific system transfer function t_{uv} satisfy (1). Here g_{uu}/P_{uu0} is used for n t_{uv} ($v = 1, \dots, n$) functions. It is proven in A3, that a g_{uu}/P_{uu0} can be found which satisfies the conditions for all n t_{uv} functions.

For example, consider t_{u1} at $\omega = \omega_1$ and suppose $A_{u1}(\omega_1) = .9$, $B_{u1}(\omega_1) = 1.1$ in (1). We could split this range $[.9, 1.1]$ into say $[\tau_{u1}, 1.05]$ for τ_{u1} and $.05$ for $\tau_{du1}d_{u1}$ in (4), using d_{u1e} of (5) for d_{u1} . The technique in A3 or better (Horowitz and Sidi 1972), is then used to find a bound on $g_{uu}(j\omega_1)$. Here, we note a tough constraint. Sooner or later in ω , $|g_{uu}(j\omega)|$ must become very small with $1 + g_{uu}/P_{uu} \rightarrow 1$ and then in (4a)

$$t_{uv} \rightarrow \frac{g_{uu}f_{uv} - d_{uv}}{P_{uu}} \quad (10)$$

and in (7), $\psi_{uv} \rightarrow$ the numerator of its right side divided by P_{uu} . Now (4a, 5, 6) in general require that

$$|t_{uv}|_{\max} > 2|\tau_{duv}d_{uve}| \quad (11)$$

But $|t_{uv}|_{\max} = B_{uv}$ and at high frequencies

$$|\tau_{duv}d_{uve}| \rightarrow \frac{\sup_{\substack{M \\ i \neq u}} |P_{ui}| |B_{iv}|}{|P_{uu}|}.$$

To see what this leads to take, for example, $n = 2$ so that the above applied to $v = 1$, $u = 1, 2$ gives

$$B_{11} > \frac{2|P_{12}|B_{21}}{|P_{11}|}, \quad B_{21} > \frac{2|P_{21}|B_{11}}{|P_{22}|},$$

requiring

$$1 > \frac{4|P_{12}P_{21}|}{|P_{11}P_{22}|} \quad \text{as } \omega \rightarrow \infty \quad (12)$$

Thus, a constraint on P is

$$(P_{2a}): \exists \omega_h, \exists \text{ for } \omega > \omega_h, |P_{11}P_{22}| > 4|P_{12}P_{21}| V_{meM}. \quad (13)$$

It is known that as $s \rightarrow \infty$,

$$p_{ij} \rightarrow \frac{k_{ij}}{s^{e_{ij}}},$$

so the above becomes

$$\frac{|k_{11}k_{22}|}{\omega^{e_{11}+e_{22}}} > \frac{4|k_{12}k_{21}|}{\omega^{e_{12}+e_{21}}}.$$

If the uncertainties in the k_{ij} are independent and $e_{11} + e_{22} = e_{12} + e_{21}$, this becomes

$$k_{11\min}k_{22\min} > 4k_{12\max}k_{21\max}. \quad (14)$$

There is an important problem class for which the inequality is less harsh. This is the "basically noninteracting" class, where one ideally desires $t_{ij} \equiv 0$ for $i \neq j$, but because of uncertainty accepts $A_{ij} = 0$, $|t_{ij}| \leq B_{ij}$ for $i \neq j$, in (1). Also, one doesn't care if t_{ij} ($i \neq j$) is nonminimum-phase. Condition (6) then applies only to $u = v$. The f_{uv} ($u \neq v$) are set equal to zero and (13) becomes

$$\exists \omega_h, \exists, |P_{11}P_{22}| > 2|P_{12}P_{21}| m_e M, \omega > \omega_h. \quad (15)$$

It is desirable to ease inequality (13) in the general case. Note that (6) can be satisfied over any finite ω range by making $|1 + g_{uu}/p_{uu}|$ large enough. Thus, as previously indicated, one can split the $[A_{uv}, B_{uv}]$ tolerance so that $|\tau_{uv}| > |\tau_{duv}| |d_{uve}|, \forall m \in M$, e.g. assign $|\tau_{uv}| \in [E - \epsilon, E + \epsilon]$ with $E = (A_{uv} + B_{uv})/2$, $2\epsilon < B_{uv} - A_{uv}$ and the balance $(B_{uv} - A_{uv} - 2\epsilon)/2$ is assigned to $\tau_{duv} d_{uv}$ of (4a). But $|1 + g_{uu}/p_{uu}|$ must then be made large enough to satisfy the resulting requirements, and it can for any finite ω range. The trouble is that g_{uu} must be allowed to \rightarrow zero as $\omega \rightarrow \infty$, leading to (13), etc., if we insist on (6). We could ignore (6) at large ω , say for $\omega > \omega_H$, with ω_H as large as desired but finite, letting $|\tau_{uv}| \ll |\tau_{duv}| |d_{uve}|$ for $\omega > \omega_H$. Then for $\omega > \omega_H$, (11) is replaced by the weaker

$$|t_{uv}|_{\max}^M > |\tau_{duv} d_{uve}| \quad (16)$$

and for $n = 2$, (13) is then replaced by

$$(P_{2b}): \exists \omega_H, \exists \text{ for } \omega > \omega_H, |p_{11} p_{22}| > |p_{12} p_{21}|, \forall m \in M \quad (17a)$$

An important question is whether (17a) is an inherent basic constraint in the presence of uncertainty, no matter what design technique is used, or is due only to this specific design technique. The methods suggested in (Rosenbrock 1974, Owens 1978) to achieve diagonal dominance, may be helpful in satisfying (17a), but they would have to be extended to uncertain plants. Note that in Rosenbrock 1974, Owens 1978), diagonal dominance is desired $\forall \omega \in [0, \infty)$, whereas in (P_{2b}) it is required only for $\omega > \omega_H$.

For the analog of (17a) at $n = 3$, it is found that diagonal row dominance of P^{-1} for $\omega > \omega_H$, is a sufficient condition. The necessary condition can be written as

$$\exists \omega_H, \exists \text{ for } \omega > \omega_H \quad |P_{11}P_{jj}| > |P_{1j}P_{j1}| \quad \text{and}$$

$$|P_{11}P_{33}| > (|P_{12}P_{23}| + |P_{13}P_{22}|)(|P_{22}P_{31}| + |P_{21}P_{32}|) \quad (17b)$$

which can be written as,

$$\begin{aligned} |P_{11}P_{22}P_{33}| &> |P_{11}P_{23}P_{32}| + |P_{12}P_{21}P_{33}| + |P_{12}P_{23}P_{31}| \\ &+ |P_{13}P_{22}P_{31}| + |P_{13}P_{21}P_{32}| \quad \text{for } \omega > \omega_H \end{aligned} \quad (17c)$$

The latter has the following interpretation. Array the matrix P^{-1} in the usual manner, but twice-one under the other as in Fig. 3a. Then the terms on the right side of (17c) consist of the products of the entries crossed by the dashed lines.

However, if ω_H is so used, it is no longer possible to use Rouché's theorem and thereby prove each t_{ij} is minimum-phase. But we can still design so that the nominal t_{ij} are minimum-phase and we know from (6) that $t_{ij}(j\omega) \neq 0$ for $\omega \in [0, \omega_H]$. Therefore, from the continuity of the zeros of t_{ij} with respect to the parameters of the system, if t_{ij} has any right half-plane zeros, they must enter the right half-plane as shown in Fig. 3b. It is unlikely that such a zero which must migrate all the way up to $j\omega_H$, should move back into the significant control bandwidth region A. The point is that if right half-plane zeros are "far-off", they have little effect and the system is "dominantly" minimum-phase.

Rouche's theorem can still be used if we can guarantee that (6) is satisfied for a semicircle consisting of the segment $[-j\omega_H, j\omega_H]$ and the right half-plane half-circumference of the circle of radius ω_H , centered at the origin. Then, there are definitely no right half-plane zeros of t_{ij} in this half-circle, and the system is "dominantly" minimum-phase. This is quite practical in the design technique of (Horowitz and Sidi 1972), discussed in A3.

3.1 Modification of mapping ϕ

Note that for the "dominantly minimum-phase" and the "basically noninteracting" cases, the application of Schauder's theorem in (2.1), Eqs. (7-9), etc., needs modification, because nonminimum-phase $t_{uv}(j\omega)$ cannot be uniquely derived from $|t_{uv}(j\omega)|$. Redefine $h \in H_{uv}$ of 2.1 to consist of an ordered pair: $h(\omega)$ as before and $q(\omega)$, the imaginary part of $\hat{h}_{uv}(j\omega)$ with $h = |\hat{h}_{uv}(j\omega)|$; $h \in H_{uv}$ the same as before but $q(\omega) \in C[0, \infty)$ with $0 \leq |q(\omega)| \leq h(\omega)$. Constraints 2,3 in 2.1 on $h(\omega)$ also apply to $q(\omega)$. Let $(HQ)_{uv} \subset C^2[0, \infty)$ denote the set $\{(h(\omega), q(\omega))\}$ with $|(h, q)| = ||h|| + ||q||$. Obviously, $(HQ)_{uv}$ is compact and convex in $C^2[0, \infty)$. The extension to the n^2 product set is straightforward.

The mappings ψ_{uv} in (7) are redefined. Each ψ_{uv} is a pair of mappings, one the absolute value as before, the second the imaginary part with the absolute bars on the right removed. On the right side of (7), $B(h_{iv}(\omega))$ is replaced by $r_{iv}(\omega) + jq_{iv}(\omega)$, with $h_{iv}^2 = r_{iv}^2 + q_{iv}^2$, $(h_{iv}, q_{iv}) \in (HQ)_{iv}$. It is necessary to prove that ϕ maps each element of $(HQ)_{uv}$ into itself.

The proof follows immediately from that for the minimum-phase case -- this is obvious from (6), the definition of d_{uve} in (5), and Appendices 1,2. The proof that ϕ is continuous is straightforward. Accordingly, the Schauder conditions are satisfied and there exists a fixed point which satisfies the specifications. Such specifications, by themselves, would not be good ones because they permit highly nonminimum-phase $t_{uv}(s)$. However, they are satisfactory if it is known from other sources that t_{uv} is "dominantly minimum-phase".

3.2 Additional Constraints on P

Constraints A1(1)-(3) in the Appendix, must be applied to the $1/P_{uu}$, since in Fig. (2) $p_{uve} = \frac{1}{P_{uu}} = p$ of Appendix. A1.1 requires that there be no change in the excess of poles over zeros of $\frac{1}{P_{uu}} = \frac{\Delta}{\Delta_{uu}}$ where $\Delta = \det. P$ and Δ_{uu} its uu th minor, as m ranges over M . Also, that for at least one $m \in M$, denoted by m_{uo} , P_{uu} has all its poles and zeros in the interior of the left half-plane. The m_{uo} can be different for each u .

A1.2 requires that $1/P_{uu}$ is minimum-phase $\forall m \in M$, and its zeros do not get arbitrarily close to the $j\omega$ axis. Since $1/P_{uu} = \Delta/\Delta_{uu}$, this means Δ must have no right half-plane zeros. Hence the P_{ij} in general have no right half-plane poles. (For those who wish it, P is restricted to be controllable and observable $\forall m \in M$, but these concepts are unnecessary if P is properly formulated in terms of physical uncertain parameters (Horowitz and Shaked 1975)). Since the p_{ij} in $P = [p_{ij}]$ are finite rational functions, the latter part of A1.2 is automatically satisfied.

A1.3 for $n = 2$ is the same as (17), which shows that (17) is a fundamental condition for linear time-invariant design, not an "extra" condition due to our design technique, at least for $n = 2$. However, (13) is an "extra" condition. Note, the extension of single-loop design to disappearing poles and zeros in A_6 may perhaps permit disappearing poles and zeros in the mio plant functions.

4. OTHER DESIGN EQUATIONS

The previous design equations constitute only one of many design techniques derivable from Schauder's fixed point theorem. Only two more will be briefly mentioned here.

Both are based on the use of a nominal diagonal loop transmission matrix. The design obligations on the loop transmission elements are then independent of the way the plant input and output terminals are numbered. If G is made diagonal, such numbering is important and after one arbitrarily numbers the plant input terminals, he should try to number the outputs such that the main effect of input i is on output i . Manipulation of (2) somewhat differently from Sec. 2, gives

$$\begin{aligned}
 t_{11} &= \frac{f_{11} \ell_{11} / \delta_{11} + \sum_{i \neq 1} v_{1i} t_{i1} / \delta_{11}}{1 + \ell_{11} / \delta_{11}} \\
 t_{21} &= \frac{f_{21} \ell_{22} / \delta_{22} + \sum_{i \neq 2} v_{2i} t_{i1} / \delta_{22}, \text{ etc.}}{1 + \ell_{22} / \delta_{22}}
 \end{aligned}
 \quad
 \begin{aligned}
 L_o &= P_o G \\
 P_o &= [P_{ij}]
 \end{aligned}
 \quad (18)$$

where $V = [v_{ij}] = I - P_0(P)^{-1}$, P_0 is the 'nominal' plant matrix and therefore fixed, P is the general uncertain plant matrix, $\delta_{ii} = 1 - v_{ii}$. The ℓ_{ii} are the nominal elements of the loop transmission matrix L . Eqs. (18) lend themselves to single-loop design and use of Schauder's theorem, precisely as did Eqs. (4).

Another interesting set of design equations is obtained by designing to control the changes in t_{ij} , rather than t_{ij} directly. Let $T_0 = [t_{ij0}]$ be the 'nominal' system transfer matrix and $T = [t_{ij}]$ the actual which is uncertain, $\Delta T = [\Delta t_{ij}] = T - T_0$. Then it can be shown that

$$\Delta T = (I + L)^{-1} VT, \quad V = I - P_0 P^{-1} \quad (19)$$

where P_0, P are likewise the 'nominal' and uncertain plant transfer matrices, and $L = P_0 G = [\ell_{ij}]$ is the nominal loop transmission matrix.

If L is taken diagonally, the result is ($n + 2$ for simplicity)

$$\Delta t_{11} = \frac{v_{11}t_{11} + v_{12}t_{21}}{1 + \ell_{11}}, \quad \Delta t_{12} = \frac{v_{11}t_{12} + v_{12}t_{22}}{1 + \ell_{11}} \quad (20)$$

and similar obvious ones for $\Delta t_{21}, \Delta t_{22}$.

The design problem is now completely one of disturbance attenuation, with the disturbances $d_{11} = v_{11}t_{11} + v_{12}t_{21}$, etc., whose range is known. Schauder's theorem is applicable in the same manner as before. Note that V represents the 'normalized' plant variation matrix. Eqs. (20) appear to be much simpler to use for design (once

the Δt_{ij} tolerances are formulated) than (4), and their use needs to be intensively researched. However, both for (18) and (20) the constraints considered in 3., leading to (11-15) must be found, and these may possibly be tougher than before. Also, both a nominal \underline{p} and T must be chosen, which is not good, because the optimum pairing is not apriori known. However, the analogs of (14,17) may be more lenient.

4.1 Bandwidth Minimization

An important criterion for comparison of design techniques is their "cost of feedback," which we take as the bandwidths of the loop transmission functions--because they determine the system sensitivity to sensor noise. Obviously, quantitative synthesis techniques must first be invented before one can turn to their optimization (for without such quantitative techniques comparison is possible at best, by analysis after a specific numerical design has been made). This approach via Schauder's theorem promises to generate a variety of such techniques, and the next step will be optimization.

5. DESIGN EXAMPLE

The 2×2 plant elements are $p_{ij} = k_{ij}/(1+sA_{ij})$ with correlated uncertainties, giving a total of 9 parameter sets in Table 1. The design was performed to handle the convex combination generated by these 9 sets (Figure 6).

TABLE 1

<u>No.</u>	<u>k₁₁</u>	<u>k₂₂</u>	<u>k₁₂</u>	<u>k₂₁</u>	<u>A₁₁</u>	<u>A₂₂</u>	<u>A₁₂</u>	<u>A₂₁</u>
1.	1	2	.5	1	1.	2	2	3
2.	1	2	.5	1	.5	1	1	2
3.	1	2	.5	1	.2	.4	.5	1
4.	4	5	1	2	1.	2	2	3
5.	4	5	1	2	.5	1	1	2
6.	4	5	1	2	.2	.4	.5	1
7.	10	8	2	4	1.	2	2	2
8.	10	8	2	4	.5	1	1	2
9.	10	8	2	4	.2	.4	.5	1

A "basically noninteracting" system is desired, with the off-diagonal transmissions specified in the ω -domain $|t_{12}(j\omega)|, |t_{21}(j\omega)| < 0.1 \forall \omega$. The diagonal t_{11}, t_{22} bounds are identical and were originally in the time-domain in the form of tolerances on the unit step response shown in Fig. 4a, b (which also shows the design results for those of the 9 cases which were reasonably distinguishable). These time-domain bounds were translated into the "equivalent" bounds on $|t_{ii}(j\omega)|$ shown in Fig. 5 (Horowitz and Sidi 1972, Krishnan and Cruickshank 1977).

Familiarity with quantitative single-loop design is assumed here. One can do a problem of this complexity by hand. The sets $\{p_{iie}(j\omega)\}$, called the plant templates, are obtained on the Nichols chart. Some of these templates of $P_{11}^{-1} = \frac{\Delta}{p_{22}}, P_{22}^{-1} = \frac{\Delta}{p_{11}}$

are shown in Fig. 6 at various ω values. The larger the template, the greater uncertainty at that ω value. The tolerances on t_{uu} of (4a) and Fig. 5 were divided between τ_{uu} and τ_{duu}^d as discussed in Sec. 2. Each of these, in conjunction with the templates, leads to bounds on the nominal loop transmission $\ell_{u\omega o} = \frac{g_{uu}}{p_{uu o}}$. Some of these bounds on ℓ_{iio} , due to τ_{11} , are shown as solid lines in Fig. 7, i.e., it is necessary for ℓ_{11o} to lie above the indicated boundary. The tolerances on τ_{duu}^d lead to the dashed line bounds on ℓ_{11o} . No attempt was made to optimize the division of the tolerances between τ_{11} and τ_{d11}^d . The composite bound on ℓ_{11o} must satisfy both. The $\ell_{11o}(j\omega)$ chosen is also shown in Fig. 7. There was no attempt made to optimize the ℓ_{iio} ; the design was made by hand quickly, so the $\ell_{iio}(j\omega)$ are larger than need be, with the tolerances therefore satisfied better than necessary--as seen in Figs. 4a, b. Optimal $\ell_{iio}(j\omega)$ would lie on their boundaries at each ω , so in this example there is considerable overdesign.

Here we took

$$\ell_{11o} = \frac{\Delta_o}{p_{22o}} g_{11} = \frac{10}{s} \frac{(1+.007s)}{(1+.025s)} \left[\frac{1+s}{400} + \frac{s^2}{(400)^2} \right]$$

with

$$\frac{\Delta_o}{p_{22o}} = \frac{.75 (1+3.66s)}{(1+s)(1+3s)} ;$$

$$l_{22o} = \frac{\Delta_o}{p_{11o}} g_{22} = \frac{9}{s} \frac{(1+.02s)}{(1+.1s) \left[1 + \frac{s}{150} + \frac{s^2}{(150)^2} \right]}$$

with

$$\frac{\Delta_o}{p_{11o}} = \frac{1.5 (1+3.66s)}{(1+3s)(1+2s)} .$$

The requirements on f_{11} , f_{22} ($f_{12} = f_{21} = g_{12} = g_{21} = 0$ here) were found using single-loop design technique [15] as briefly explained here in A4, and

$$f_{11} = \frac{1}{1 + .5s} , \quad f_{22} = \frac{1}{1 + .33s}$$

were found satisfactory. The system was simulated on the digital computer with the results shown in Figs. 4a, b. The t_{12} , t_{21} tolerances were easily satisfied by the design.

While this is not a very challenging example of the design technique, nevertheless the uncertainty is very large and one should consider how quick, simple and straightforward was the design procedure, and also consider what alternatives are offered in the mio literature. There are no other techniques available for systematic design to specifications in the presence of significant uncertainty which guarantee design convergence and attainment of design tolerances.

Whatever present popular technique is used, it would be necessary to cut and try and endeavor to understand the relations between the cutting and the results as one continued to cut and try, because these techniques have no provision for significant uncertainty. In the above design, one sweep was known to be sufficient because the plant and the design tolerances (ω -domain) satisfied constraints, P_1 etc.

5. EXTENSION TO NONLINEAR UNCERTAIN MIO PLANTS

Once there is a quantitative design technique for linear time invariant mio uncertain plants, it appears at least conceptually possible to extend it to a significant class of nonlinear, even nonlinear time-varying, uncertain mio plants. The procedure is a generalization of that used (based also on Schauder's theorem) in (Horowitz 1976) for single loop uncertain nonlinear systems. The key feature is the replacement of the nonlinear plant matrix set (a set because of the uncertainty), by a linear time invariant plant set which is precisely equivalent to the original nonlinear set, with respect to the acceptable system output set. The procedure is briefly presented for the case where one wants the system with nonlinear uncertain plant to behave like a linear time-invariant system for a specified class of command input sets.

It is essential that the command input sets represent a good sampling of how the system will actually be used. For example, suppose $n = 3$ and in actual use r_1, r_2 always exist simultaneously (with $r_3 = 0$), and r_3 appears by itself (with $r_1 = r_2 = 0$). Say there are ten typical $r_1(t)$ inputs and for each typical $r_1(t)$ there are five typical $r_2(t)$. This makes a subtotal of 50 input sets, to which is added the number of typical $r_3(t)$ say 10, giving a class $R = \{\bar{r}\}$ of 60 sets, of which 50 have the form $\bar{r} = (r_1, r_2, 0)$ and $\bar{r} = (0, 0, r_3)$ for the balance. Choose $\bar{r}_1 \in R$. The family of acceptable outputs for this input, is known from the tolerances on t_{ij} , giving for that one input vector a family $\mathcal{H} = \{\bar{h}\}$, $\bar{h} = (h_1, h_2, h_3)$. The mio plant is represented by a family (because of parameter uncertainty) \mathcal{W} of nonlinear differential mappings

$\mathcal{W} = \{W\}$, $W = (w_1, w_2, w_3)$; $c_1 = w_1(x_1, x_2, x_3, m)$, . . . , $c_3 = w_3(x_1, x_2, x_3, m)$, where the x_i are the plant inputs, c_i the plant outputs, and m is the plant parameter vector $m \in M$.

Take a sample acceptable output triple $\bar{h} = (h_1, h_2, h_3)$ and find the corresponding plant inputs at some specific $m \in M$ (or in other words, pick a $W \in \mathcal{W}$) and let $c_j = h_j$ and solve the nonlinear equations backwards, giving the input set (x_1, x_2, x_3) . Take the Laplace transforms $\hat{x}_i(s)$ of x_i , $\hat{h}_j(s)$ of h_j giving the vectors $\hat{x}[s] = (\hat{x}_1(s), \hat{x}_2(s), \hat{x}_3(s))$ $\hat{h}[s] = (\hat{h}_1(s), \dots, \hat{h}_3(s))$. Repeat for other \bar{h} samples in the acceptable output set \mathcal{H} , giving two paired families of $\hat{x}[s]$, $\hat{h}[s]$.

Select any combination of three $\hat{x}[s]$, forming a 3×3 matrix \hat{X} and corresponding paired combination of three $\hat{h}[s]$, forming the matrix \hat{H} . Set $\hat{H} = \hat{P}\hat{X}$ and solve for $P = \hat{H}(\hat{X})^{-1}$. P is the linear-time-invariant equivalent of the specific $w \in W$ picked, with respect to the specific trio of acceptable output vectors picked. Repeat over different trios. Repeat the entire operation over different $w \in W$, giving a class $P_1 = \{P\}$ which is the linear-time-invariant equivalent of the W family, with respect to the class of acceptable outputs H for input vector \bar{r}_1 . Repeat the entire operation for $\bar{r}_2, \dots, \bar{r}_{60}$ giving $\{P_i\} = P_{\text{total}}$ which is the linear time equivalent for the nonlinear W , with respect to the tribe of 60 families of acceptable output sets. The equivalence is exact if the conditions for application of Schauder's theorem are satisfied. We now have a linear time-invariant uncertain mio problem, which let us presume we can solve. If and only if we can guarantee the solution of the latter, then the same compensation functions will work for the original nonlinear uncertain mio plant. Hence the importance of quantitative linear time invariant design techniques (over and above their intrinsic importance)--for they enable the precise solution of nonlinear uncertainty problems.

The design effort in the above appears to be enormous but it is conceptually straightforward and easy. An ordinary control engineer can implement it and the digital computer is, of course, an essential

tool. Conceptually too, it appears possible to extend the method to obtain nonlinear relations between inputs and outputs within specified bounds, despite large plant uncertainty, even nonlinear time-varying, as can be done for the single input-output case. The prospect is fascinating. Imagine being able to work with the actual nonlinear equations of a jet engine, or a chemical process, etc., include uncertainties in the modelling, even uncertainty in system order (see Appendix), and designing to achieve outputs within specified tolerances over the given range of uncertainty.

6. DISTURBANCE ATTENUATION

Let x in Fig. 1 be a $n \times 1$ matrix of disturbances. The resulting system output (with $r = 0$) is $c = (I + PG)^{-1} Px \triangleq Zx$, $Z = [z_{ig}]$, the $n \times n$ disturbance response matrix. Bounds on Z are given in the form

$$|z_{uv}(j\omega)| < b_{uv}(\omega), \quad \forall \quad m \in M \quad (21)$$

Rewrite $c = Zx$ in the form $(P^{-1} + G)c = x$. Let $x_i \neq 0$ only for $i = v$, so $c_i = z_{iv}x_v$, and

$$\sum_{i=1}^n (P_{ui} + g_{ui})z_{iv} = \delta_v^u = \begin{pmatrix} 0, & u \neq v \\ 1, & u = v \end{pmatrix},$$

$$(P_{uu} + g_{uu})z_{uv} = \delta_v^u - \sum_{i \neq u} (P_{ui} + g_{ui})z_{iv}$$

$$z_{uv} = \frac{\delta_v^u - \sum_{i \neq u} (P_{ui} + g_{ui})z_{iv}}{P_{uu}(1 + \frac{g_{uu}}{P_{uu}})} \quad (22)$$

Let

$$x_{uve}(\omega) \triangleq \sup_m \sum_{i \neq u} \left| \frac{p_{ui} + g_{ui}}{p_{uu}} \right| b_{iv}(\omega) \quad (23)$$

The $g_{ui}(\omega)$ ($i \neq u$) can be chosen to minimize $x_{uve}(\omega)$, but for simplicity we shall assume them zero. From (22,23)

$$|z_{uv}(\omega)| < \left| \frac{\delta_v^u / p_{uu} + x_{uve}}{(1 + \frac{g_{uu}}{p_{uu}})} \right| \quad (24)$$

If $1/p_{uu}$ satisfies the constraints listed, then it is obviously possible to guarantee $|z_{uv}(\omega)| < \text{any finite number}$, no matter how small, at any finite ω . Also it can be made zero at a finite number of ω values by assigning poles to g_{uu} at these values. Assume that g_{uu} can be chosen to satisfy (21) $\forall \omega \in [0, \infty)$. Then one can set up the conditions for Schauder's theorem, precisely as was done in 2.1. The set $b_{uv}(\omega)$ must have been formulated such that $B(n^2)$, the n^2 product set of the $b_{uv}(\omega)$, is compact convex in $C(n^2)$, analogous to $H(n^2)$ in 2.1. The analog of Φ in (7) must be formulated with the modification of Sec. 3.1, inasmuch as we do not care if the $z_{uv}(s)$ are nonminimum-phase.

Conditions analogous to (12-17) for $n = 2$, are obtained as follows. As $\omega \rightarrow \infty$, $g_{uu}/p_{uu} \rightarrow 0$ so in (24), the right side \rightarrow its numerator. But $|z_{uv}(j\omega)| \leq b_{uv}(\omega)$ of (21). Let $u = 1, v = 2$ and then $u = 2, v = 1$ and obtain the necessary condition (for $g_{12} = g_{21} = 0$),

$$\text{As } \omega \rightarrow \infty, \quad p_{12}p_{21} < p_{11}p_{22}, \quad \forall \text{ } m \in M \quad (25)$$

similar to (17) but here only at ∞ , because there is no concern with the minimum-phase property. Setting $u = v = 1$, and then $u = v = 2$ in (24), we get the conditions

$$\text{As } \omega \rightarrow \infty, b_{11} > \left| \frac{1}{p_{11}} \right| = \left| p_{11} - \frac{p_{12}p_{21}}{p_{22}} \right|, b_{22} > \left| p_{22} - \frac{p_{12}p_{21}}{p_{11}} \right| \quad (26)$$

But in reality as $\omega \rightarrow \infty$, $c \rightarrow Px$ so $Z \rightarrow P$ and $z_{11} \rightarrow p_{11}$, $z_{22} \rightarrow p_{22}$. Hence, assignment of b_{ij} (as $\omega \rightarrow \infty$) to satisfy (25) is no obstacle, because the $b_{uv}(\omega)$ are upper bounds on the $|z_{uv}(j\omega)|$.

BIBLIOGRAPHY

Astrom, K. J., et al., 1977, Automatica, 13, 457-476.

Bode, H. W., 1945, Network Analysis and Feedback Amplifier Design (New York: Van Nostrand).

Davison, E. J., 1976, IEEE Trans. Aut. Control, 21, 35-47.

Horowitz, I., 1963, Synthesis of Feedback Systems (New York: Academic Press) Secs 7.9, 3.9, 6.14; 1975, IEEE Trans. Aut. Control, 20, 454-464; 1976, Proc. IEEE, 123-130.

Horowitz, I., and Shaked, U., 1975, IEEE Trans. Aut. Control, 20, 84-97.

Horowitz, I. and Sidi, M., 1972, Int. J. Control, 16, 287-309; 1978, Int. J. Control, 27, 361-386.

Kantorovich, L. V., and Akilov, G. P., 1964, Functional Analysis in Normed Spaced (New York: Pergamon Press).

Krishnan, K., and Cruickshank, A., 1977, Int. J. Control, 25, 609-620.

MacFarlane, A. G. J., 1973, Automatica 9, 273-277.

Owens, D. H., 1978, Int. J. Control, 27, 603-608.

Porter, B., and D'Azzo, J., 1978, Int. J. Control, 27, 487-492.

Porter, B. and Tsingias, A., 1978, Int. J. Control, 639-650.

Rosenbrock, H. H., 1974, Computer-Aided Control System Design (New York: Academic Press).

Wang, S. H., and Davison, E. J., 1973, IEEE Trans. Aut. Control, 18, 220-225.

Wonham, W. M., 1974, Multivariable Control Systems: A Geometric Approach (Springer Verlag).

Wonham, W. M., and Morse, A. S., 1972, Automatica, 8, 93-100.

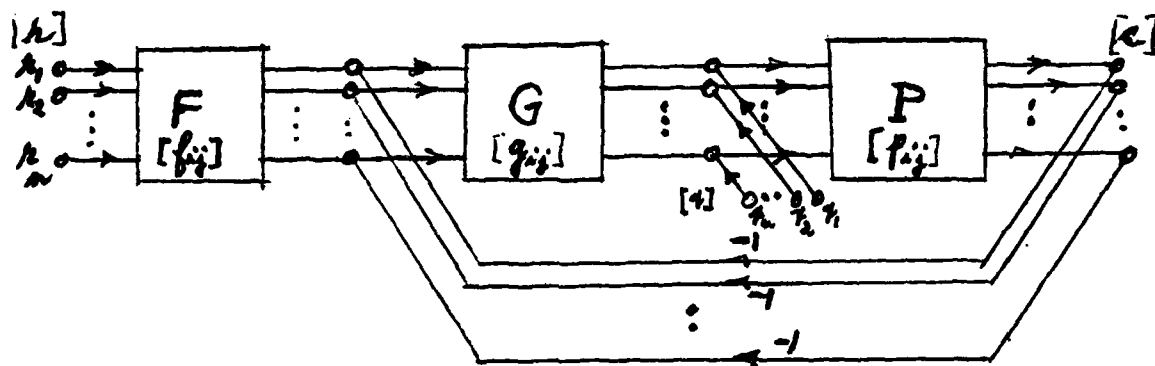


Fig. 1 Multiple input-output two matrix degree-of-freedom feedback structure $c = Tr$, $T = [t_{ij}]$, $c = [c_1 \dots c_n]'$, $r = [r_1 \dots r_n]'$.

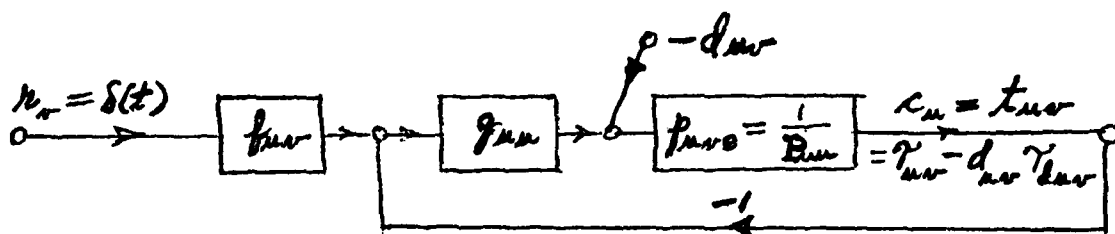


Fig. 2 Single-loop structure equivalent, for synthesis of t_{uv} ;

$$d_{uv} = \sum_{i \neq u} p_{ui} t_{iv}, \quad P^{-1} = [p_{ij}], \quad P = [p_{ij}]$$

$$\tau_{uv} = \frac{f_{uv} g_{uu} p_{uve}}{1 + g_{uu} p_{uve}}, \quad \tau_{duv} = \frac{p_{uve}}{1 + g_{uu} p_{uve}}.$$

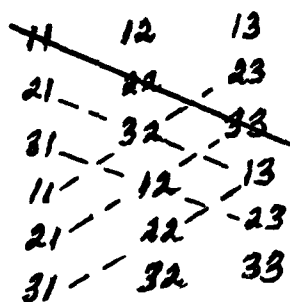


FIG. 3a

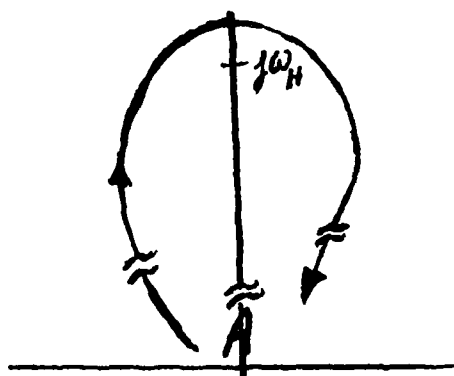
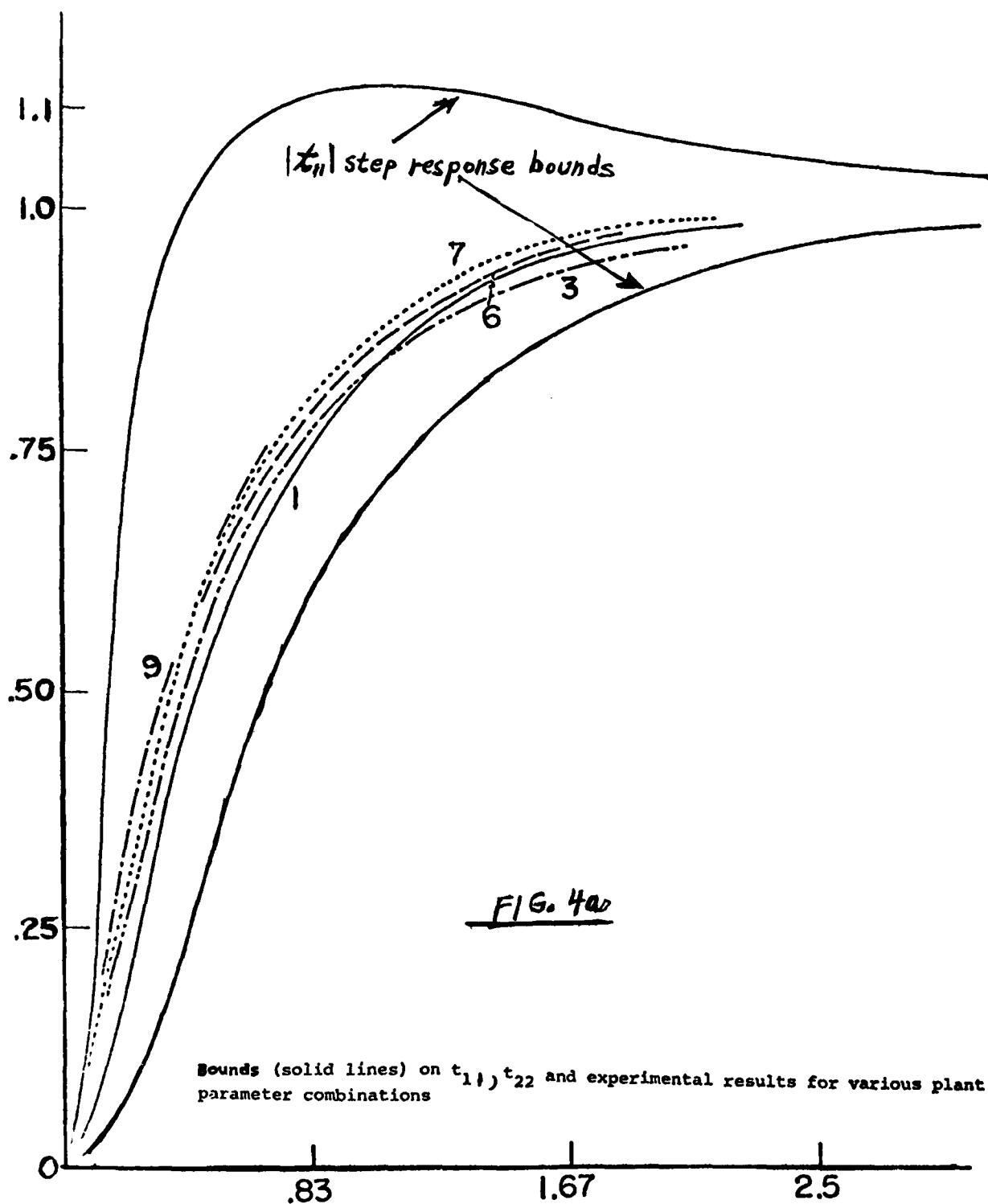


Fig. 3b To reach A in right half-plane, a zero must cross $j\omega$ axis above $j\omega_H$.



Bouds (solid lines) on t_{11} , t_{22} and experimental results for various plant parameter combinations

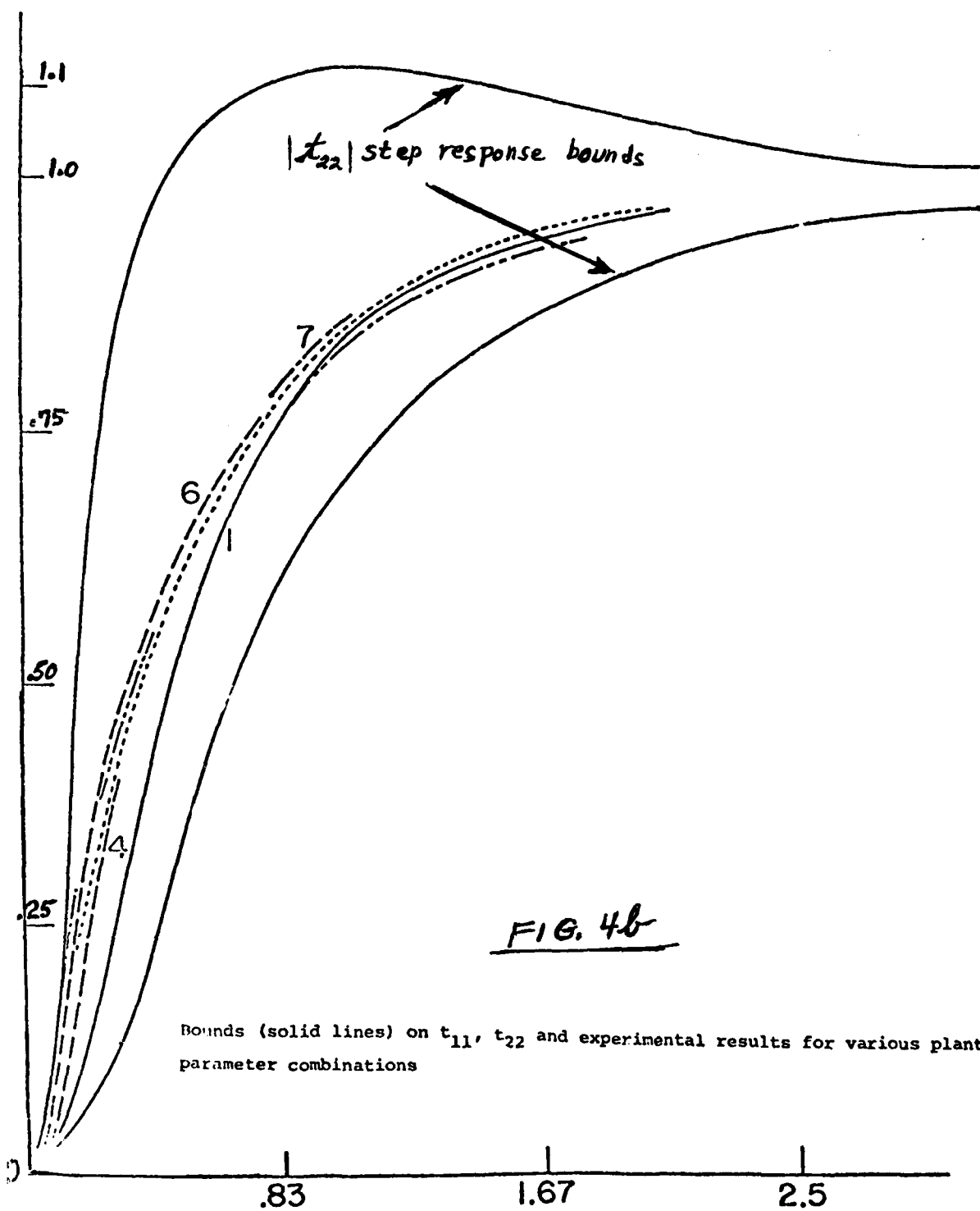


FIG. 4b

Bounds (solid lines) on t_{11} , t_{22} and experimental results for various plant parameter combinations

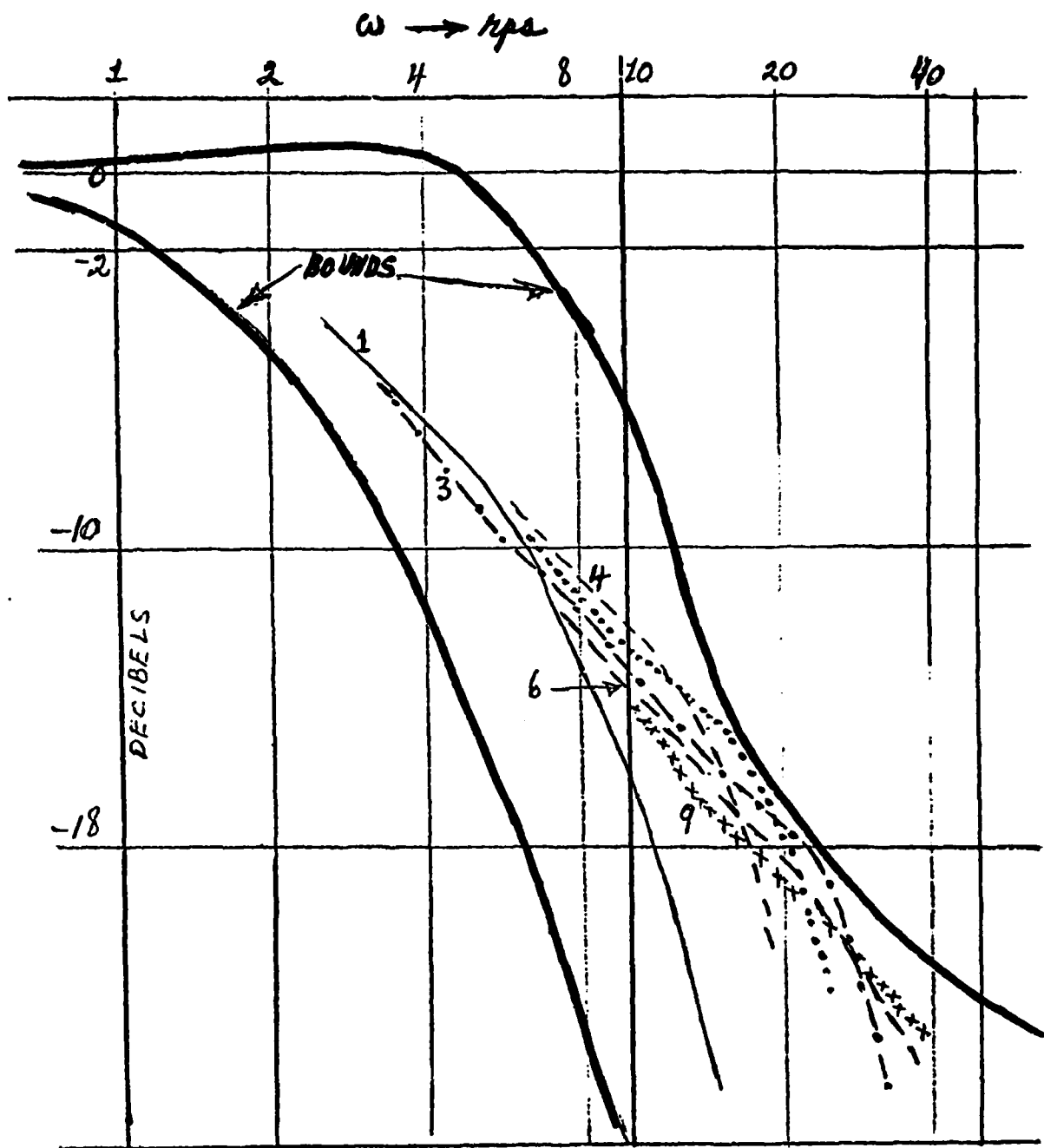


Fig. 5. "Equivalent" frequency domain bounds and experimental results for various plant parameter sets

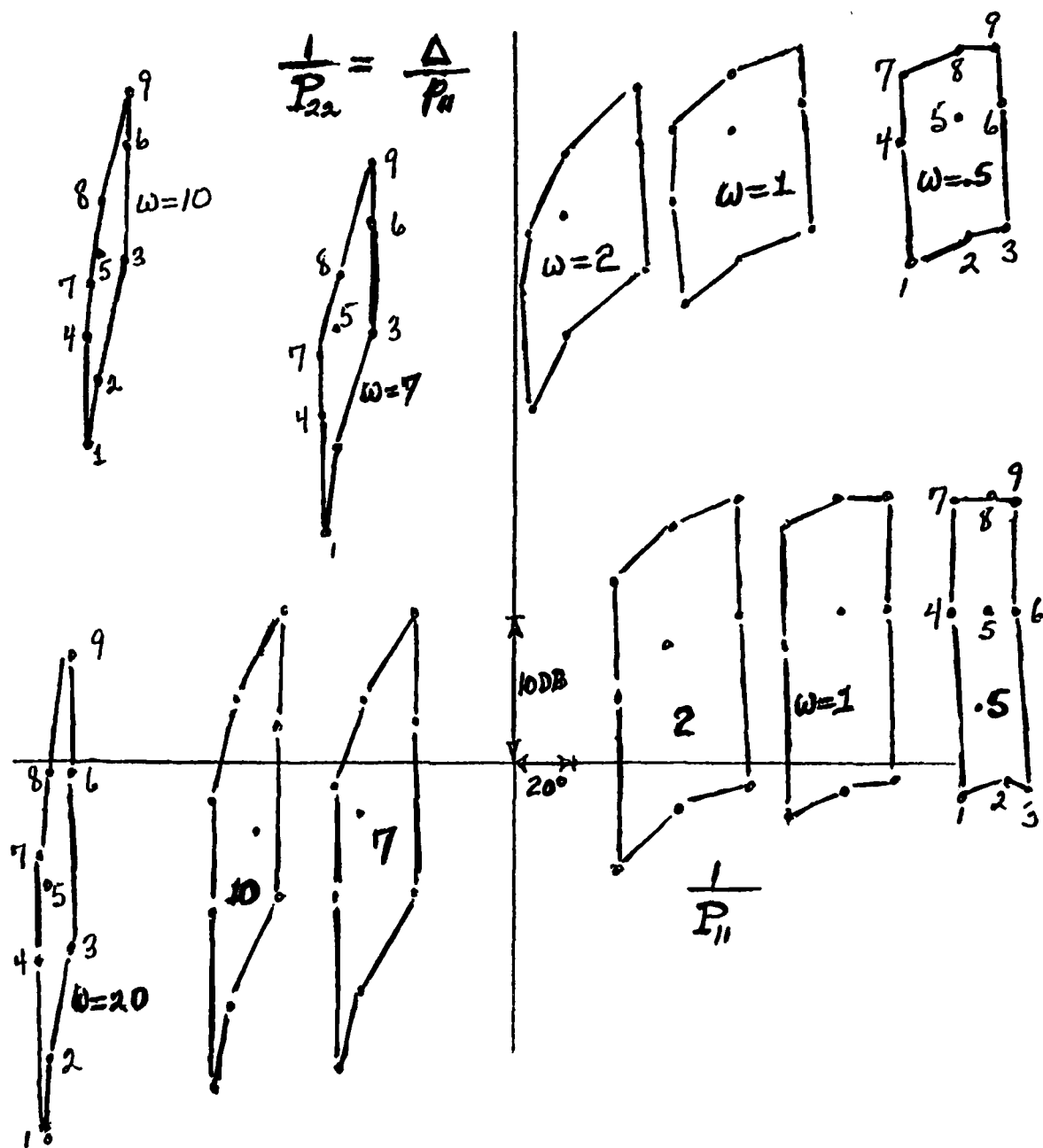


Fig. 6. Templates of $P_{22}^{-1} = \Delta/p_{11}$, $P_{11}^{-1} = \Delta/p_{22}$ at various frequencies, on Nichols Chart

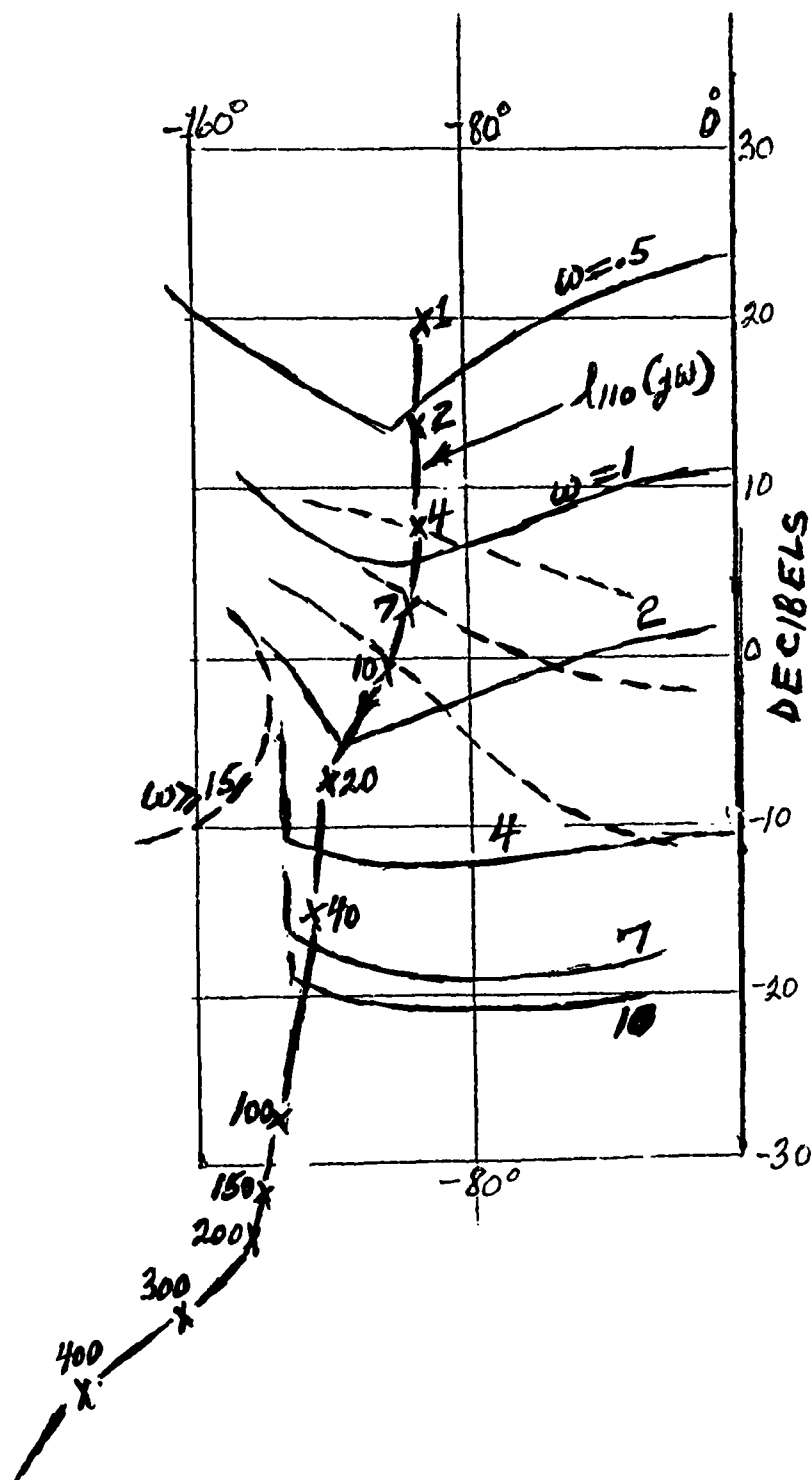


Fig. 7. Bounds on $l_{110}(jw)$. Solid lines are due to $|T_n|$, broken lines due to $|T_n d_{12e}|$